A LABORATORY STUDY OF THE ROLE OF GEOTECHNICAL FABRIC AS A REINFORCING MEDIUM IN A SOIL-FABRIC SYSTEM

By

JACK D. LAWMASTER

Bachelor of Science in Civil Engineering

Oklahoma State University

Stillwater, Oklahoma

1978

Submitted to the Faculty of the Graduate College
of the Oklahoma State University
in partial fulfillment of the requirements
for the Degree of
MASTER OF SCIENCE
December, 1980

Dedicated

To

Jan, my wife.

A LABORATORY STUDY OF THE ROLE OF GEOTECHNICAL FABRIC AS A REINFORCING MEDIUM IN A SOIL-FABRIC SYSTEM

Thesis Approved:

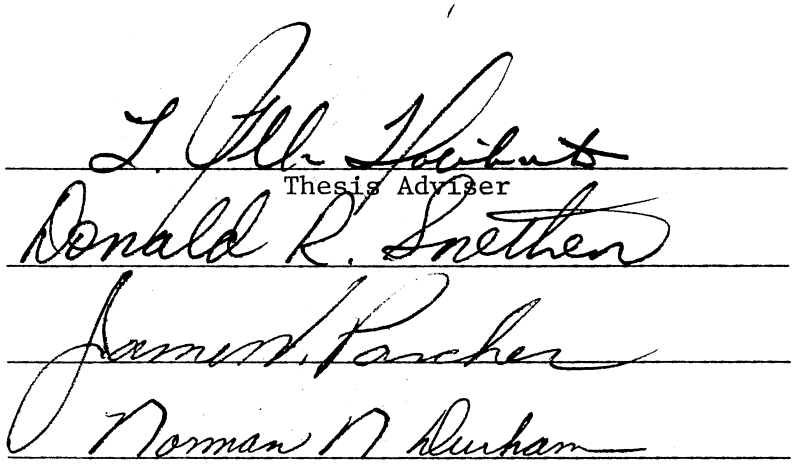

Thesis Adviser

Dean of the Graduate College

PREFACE

This report discusses conclusions reached after analyzing data collected from research conducted for the United States Air Force Office of Scientific Research under grant AFOSR-79-0087. The author is grateful for the opportunity to participate in this research.

Companion research was conducted by graduate student, Mr. J. K. King. Portions of preliminary testing were conducted by Mr. King and undergraduate student, Mr. Page Maxson. Clerical work involved in preparation of this report, was performed by Ms. Barbara Vick with the assistance of Ms. Linda Jackman.

The author wishes to express his gratitude to all of the above mentioned people for their assistance in conducting the research and/or preparing the report.

The author wishes to extend his appreciation to committee members Dr. J. V. Parcher, and Dr. D. R. Snethen for their assistance and careful review of the manuscript. The author is especially grateful to Dr. T. A. Haliburton, his major adviser, for his guidance and assistance, not only during the project, but since January, 1978. Without Dr. Haliburton's sincere concern as a professor, a professional, and a friend, this author would never have attempted to earn the degree of Master of Science, let alone have reached his goal.

A very special thanks goes to my family: to my parents for their patience and support, to my wife, Jan, for her confidence and love, and to my daughter, Janie, for making it all worthwhile.

TABLE OF CONTENTS

LIST OF FIGURES

Figure Page

Figure Page

LIST OF TABLES

CHAPTER I

INTRODUCTION

Geotextile Use in Civil Engineering

Geotextile is a term used to describe a wide variety of artificial-fiber textile products used in civil engineering construction. Other names for geotextile are geotechnical fabric, geofabric, filter cloth, and civil engineering fabric. Approximately 50 geotextiles are commercially available in the United States. There are many different types of geotextiles, but each may be generally classified as a woven or nonwoven fabric. Woven fabrics are fabrics manufactured on a weaving loom, while nonwoven fabrics possess characteristics which are directly related to specific manufacturing processes. Heat bonded, chemically bonded, and needle-punched fabrics are the three principal types of nonwoven fabrics. Geotextiles may be further classified by weight, tensile strength, modulus, creep tendency, permeability, and resistance to corrosion and bacterial action. Fabrics not treated for resistance will generally undergo deterioration after 30 to 60 days of exposure to ultraviolet radiation from sunlight. Fabric costs range from approximately $0.30/sq yd to over $6.00/sq yd. Lightweight fabrics are generally less expensive than heavy fabrics, and nonwoven fabrics are less expensive than woven materials. Fabric weights range from less than 3 oz per sq yd to more than 26 oz per sq yd.

Geotextiles have been used in the construction industry for more than 20 years in hydraulic structures, roads, earth structures, and railway construction; however, their application has been limited because of the lack of proper laboratory investigations and field tests to define proper construction uses of fabric. Despite the success of geotextiles, their use is often overlooked or viewed as "too risky" when in fact it is a viable and cost effective design alternative. The concept of risk in engineering designs incorporating fabric is unfortunate, but even more unfortunate is the fact that this concept is often valid. Many projects which incorporate fabric have failed when they should have been successful. Whether these failures resulted from poor construction procedures or poor design, they served to retard acceptance of fabric use in civil engineering projects. Failures have also made the construction industry more hesitant to accept fabric manufacturers' literature as fact, especially when the literature is normally accompanied by a disclaimer of liability, should the fabric not function as stated.

The results of previous analytical studies, laboratory tests, and field tests led to the definition of four specific functions performed by geotextiles in soil fabric systems. The first three functions which are widely agreed upon are filtration, separation, and reinforcement. The most recent function defined is that of drainage in the plane of the fabric.

Statement of Problem

This report deals with the function of fabric as reinforcement in soil-fabric systems. The present state-of-the-art in fabric reinforcement is limited and changing rapidly. This rapid change may be attributed

to the growing interest of government agencies and the consequential funding of fabric research, as well as research which surfaces due to the competitive nature of geotextile manufacturers.

To understand most previous investigations of the fabric reinforcement function, it is necessary to review the historical use of fabric as soil reinforcement. Initial use of fabric in construction was as a filter through which water could pass without buildup of excess pore water pressure. The filter function was first applied in slope erosion control and wave protection but soon spread to road construction.

Fabric replaced more expensive and time consuming graded filters which normally separated the subgrade from the overlying base or subbase materials. An added benefit of filter fabric which was observed was that the fabric not only allowed water to pass through, but also retained cohesive and cohesionless fines from entering the base or subbase materials which if allowed would be detrimental to the pavement system. This function was appropriately called separation.

After separation had been defined as a fabric function, fabric was used in temporary applications such as construction roads and haul roads. Here the fabric was unrolled over a very soft subgrade to prevent the aggregate from being contaminated when dumped and compacted. It was soon noticed that the roads would initially rut but after the road was graded, subsequent rutting was much less. This was attributed to the fact that the fabric would develop tensile forces during initial rutting and thus resist future rutting. This function which the fabric performed is called reinforcement.

It should be noted, however, that the fabric was placed to perform separation and the reinforcement which occurred was only consequential.

Also with few exceptions laboratory and field tests which have investigated the reinforcement functions of fabrics have placed the fabric in a position satisfactory for separation and then measured the reinforcement potential of the fabric. It is not surprising that such results have shown that fabric has no reinforcement effect until excessive deformation has occurred.

Scope of Research

It is the purpose of this research to investigate geotextile potential for soil reinforcement as a primary fabric function. By placing the fabric in the soil-fabric system at a position which allows the fabric to interfere with the normal shear failure mechanism, it will be shown that fabric can be used as reinforcement without first forcing the reinforced soil system to undergo excessive deformation.

CHAPTER II

LITERATURE SURVEY

Introduction

Current literature pertaining to the reinforcing function of geotextiles may be divided into four categories: field testing and evaluation, laboratory research, design procedures, and mathematical models. Many civil engineers believe that mathematical models should be used to describe the behavior of soil-fabric systems. It is the author's opinion that mathematical models are best used when combined with laboratory test results (1), or field test results (2).

Mathematical models, such as Giroud and Noiray's (3), which are based only on theory are not considered relevant to the literature survey at this time. The rationale for this is that mechanisms of fabric performance are not well defined and may only be postulated, in the absence of field or laboratory testing.

To achieve a better understanding of geotextile behavior, field tests should be instrumented so that stresses and strains within the soil-fabric system can be measured. The U.S. Army Corps of Engineers installed such instrumentation in their Pinto Pass Project in Mobile, Alabama,and data obtained increased the understanding of fabric behavior (4).

Field tests, though useful, are often expensive to conduct. For this reason, laboratory tests are needed to define fabric functions and

identify the mechanisms by which fabrics perform in a soil-fabric system.

Design procedures are considered beyond the scope of this project, and, therefore, discussion is limited to the evaluation of field testing and laboratory research. To avoid repetition in the presentation of various authors' opinions and in order to eliminate literature which does not contribute to the overall effectiveness of the literature survey, discussions of only four pertinent articles are presented in this report.

Pertinent Literature

Sorlie (5)

In 1973, the Norwegian Road Research Laboratory (NRRL) initiated a plate bearing test program to investigate the use of fabric to increase the bearing capacity of weak subgrades. The only fabric used for these tests was Fibertex S170, a nonwoven. In all tests, a loading plate with a diameter of 30 cm was used. Two subgrades consisted of different types of clay and one consisted of bark. Six tests were conducted on each subgrade: three tests with fabric and three without fabric. The fabric was placed between the base and subgrade,and the base consisted of gravel in various thicknesses, from 15 cm to 38 cm. For the tests without fabric, a plastic foil was inserted between the gravel and subgrade in order to provide a separation mechanism. The strength of this foil was less than 10 percent of the strength of the Fibertex S170.

Subsequent to completion of the test series, the data were analyzed. No effect from the fabric was observed with respect to increasing the bearing capacity of the subgrade. It was noted, however, that the fabric reduced deformations after failure pressure was reached.

Kinney and Barenberg (6)

The Waterways Experiment Station, WES, conducted traffic tests on three pavement system sections in which a soft clay subgrade was overlain by 14 inches of granular base. Two of these sections contained a fabric layer between the base and subgrade while the third section, used as a control section, contained no fabric. A loaded truck was repeatedly driven in the same wheelpaths over each section and rutting data were recorded.

These data were then furnished to Kinney and Barenberg to evaluate. Their report attempts to qualitatively explain the mechanisms by which the fabrics function and quantitatively present the test results.

Kinney and Barenberg concluded that fabrics perform two major functions in soil-fabric systems. The first function is separation of subgrade and base materials and the second is redistribution of stresses within the system. Furthermore, they concluded that stress redistribution is achieved through three basic mechanisms as follows:

1. Normal stress is carried by the fabric when tension is induced,
2. Lateral restraint of the soil exists at the fabric interface,
3. The fabric acts in the same manner as reinforcing steel in concrete, and so the pavement system can carry some moment.

Kenney and Barenberg also concluded that fabrics with higher tensile strengths performed the stress distribution more effectively than weaker fabrics. In fact, weaker fabrics had only minor effects on the stress distribution. In addition, pretensioned fabrics were found to achieve tension forces sooner, which reduced overall deformations in the system.

Holtz (1)

In his investigation into the nature of soil-fabric interaction, Holtz performed several triaxial compression tests on fabric reinforced and non-reinforced sand specimens. This work was conducted for the National Science Foundation under Grant No. ENG 74-17810 from March 15, 1975 to May 31, 1978. The report was filed August 25, 1978.

The sand used is described as "dry subangular sand." The specimens were prepared by tamping and were 158 mm high and 72 mm in diameter. Reinforcement was performed by concurrently placing fabric layers at the top, bottom, and third points of the sample. All tests were performed under a constant confining pressure of 41.4 KPa and an undisclosed constant strain rate.

Figure 1 shows the stress-strain relationships for the specimens as presented by Holtz. Prior to failure of the specimens, bulging was observed to occur between the fabric layers, but no tearing or other damage to the fabric was noted.

In summary, Holtz concluded that the fabric reinforcement greatly increased the strength of the samples and this increase was dependent on the fabric properties and soil-fabric interaction. Holtz further stated that the fabric apparently restricted lateral movement of adjacent sand particles, and this restraint is (at least in part) responsible for the strength increase.

Bender and Barenberg (7)

In research conducted for the Celanese Fibers Marketing Company, Bender and Barenberg evaluated Mirafi 140 in a soil-fabric-aggregate (SFA)

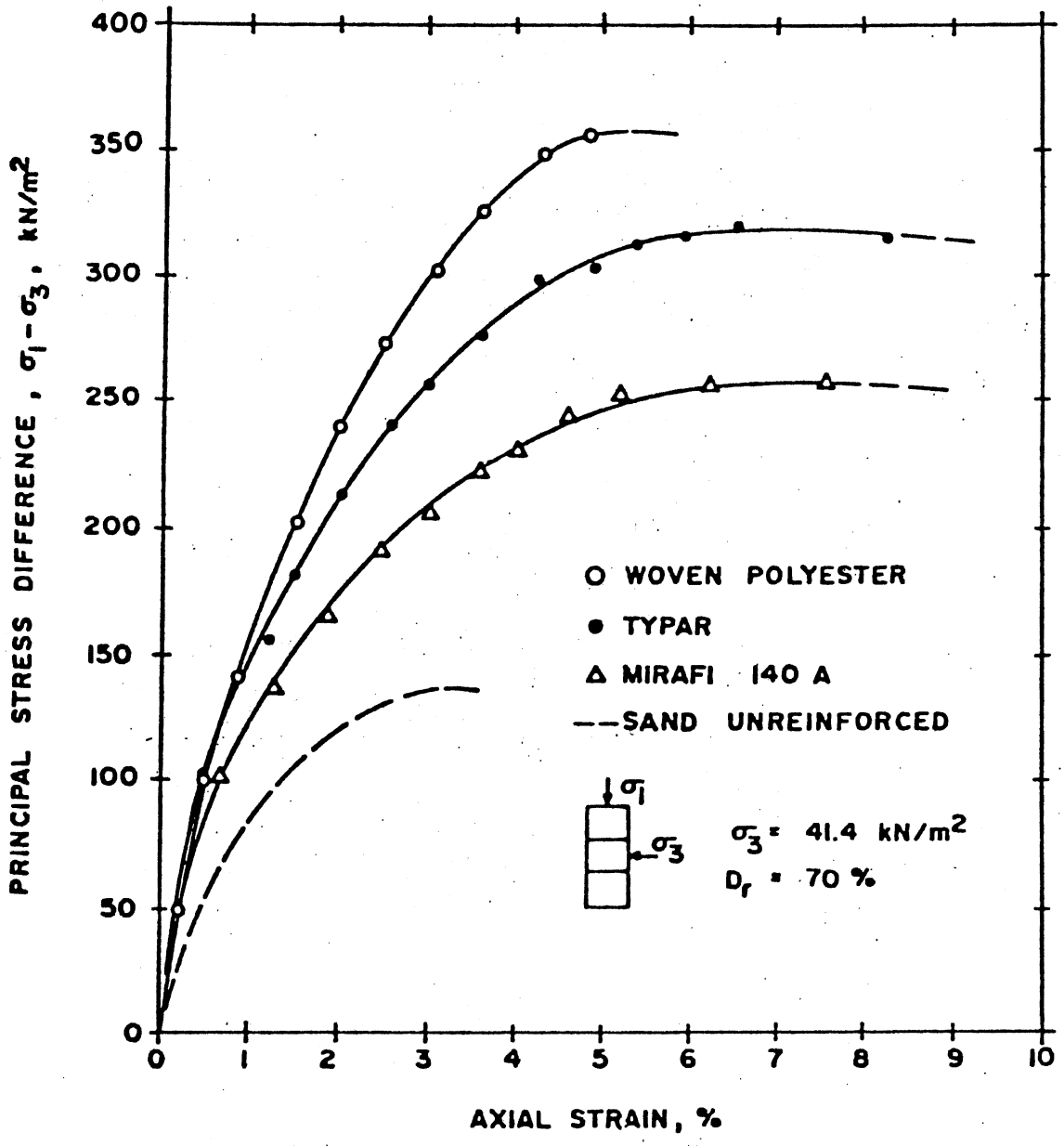

Figure 1. Stress-Strain Relationships for Fabric-Reinforced and Unreinforced Triaxial Specimens of Lafayette Concrete Sand. Unreinforced Test Interpolated From Two Tests at 20.7 and 103.5 kN/m^2. [From Holtz, (1)]

system. The soil used for the system was a low plasticity clay and the aggregate was crushed limestone.

After running repeated plate load tests and static load to failure tests, Bender and Barenberg concluded that the fabric benefited the SFA system through the following four mechanisms:

1. Separation of the soil and aggregate systems,
2. Confinement and reinforcement of the aggregate layer,
3. Confinement of the soil, and
4. Provision of a filter medium to facilitate drainage.

With regard to the reinforcement of the aggregate layer, Bender and Barenberg concluded that the fabric layer absorbs some tensile forces in the system as reinforcing steel does in concrete. These tensile forces in the fabric then tend to restrain the upheaval of the soil contained in the slip planes of the failure zone, and this phenomenon in turn increases the load bearing capacity of the soil.

In their concluding remarks, Bender and Barenberg state "The use of . . . fabrics in the construction of road systems can have a significant effect on the behavior and performance of these systems, especially on systems normally having large deformations" (p. 20).

Summary

After reviewing the above literature and numerous other published and non-published articles, several important items of interest were noted and are discussed below.

In the four papers presented above and all others reviewed, with the exception of Holtz's triaxial results, all authors concluded that no measurable strength gain was available from the soil-fabric system until

the fabric had undergone excessive deformation. However, all tests, except for Holtz's triaxial tests, had been conducted with the fabric in a position suitable for performing the separation function as in a temporary haul road, and not specifically for reinforcement.

The four papers of this literature survey together presented all fabric reinforcement mechanisms, believed by most authorities to be responsible for the strength gain in the soil-fabric systems. These mechanisms are:

1. Normal stress is carried by tension in the fabric,

2. The system can carry some moment because the fabric behaves as reinforceing steel does in concrete, and

3. Lateral restraint of the soil exists at the soil-fabric interface.

CHAPTER III

MATERIAL, EQUIPMENT, AND PROCEDURES

Fabrics Evaluated in Testing Program

A total of 17 synthetic fiber geotechnical fabrics were evaluated in the initial phase of the testing program. These fabrics consisted of 10 woven fabrics and seven nonwoven fabrics, and were obtained directly from fabric manufacturers. Selection of these 17 fabrics was based on correspondence with fabric manufacturers, fabric literature, and results from previous testing (8).

Table I identifies the fabrics by trade name, manufacturer and/or distributor, and fabric description. The fabric trade name was that given each fabric by the manufacturer. The fabric descriptions are those of the author and are based partly upon manufacturers' information.

After preliminary testing, four fabrics were chosen for further evaluation. The fabrics chosen were Bidim C-34, Typar 3401, Celanese 600X, and Nicolon 66475. This selection provided for the testing of two woven fabrics and two nonwoven fabrics. One woven and one nonwoven possessed low tensile strengths and the remaining two fabrics had high tensile strengths.

Testing Program

In order to select the four fabrics used in the load bearing tests,

TABLE I

FABRICS USED IN INITIAL TESTING

Fabric Trade Name	Fabric Manufacturer or Distributor	Fabric Description
Mount Vernon Mills Fabric	Advance Construction Specialties	Woven Nylon Monofilament
Celanese 500X/Mirafi 500X	Celanese Corporation	Woven Polypropylene Monofilament
Celanese 600X/Mirafi 600X	Celanese Corporation	Woven Polypropylene Monofilament
Diamond 8	Collins & Aikman Corporation	Woven Nylon Monofilament
Special 400	Collins & Aikman Corporation	Woven Nylon Monofilament
Retain 72	Collins & Aikman Corporation	Woven Nylon Monofilament
Stitchbond 1375	Collins & Aikman Corporation	Nonwoven Stitchbonded Polyester Monofilament
Fibretex 150	Crown Zellerbach	Nonwoven Needle-punched Spunbonded Polypropylene Monofilament
Fibretex 200	Crown Zellerbach	Nonwoven Needle-punched Spunbonded Polypropylene Monofilament
Fibretex 300	Crown Zellerbach	Nonwoven Neddle-punched Spunbonded Polypropylene Monofilament
Fibretex 400	Crown Zellerbach	Nonwoven Needle-punched Spunbonded Polypropylene Monofilament
Corning Fiberglass Fabric	Dow-Corning Corporation	Woven Fiberglass Monofilament
Typar 3401	E. I. DuPont de Nemours & Co., Inc.	Nonwoven Spunbonded Polypropylene Monofilament

TABLE I (Continued)

Fabric Trade Name	Fabric Manufacturer or Distributor	Fabric Description
Bidim C-34	Monsanto Textiles Co.	Nonwoven Mechanically Entangled Continuous Polyester Filament
Nicolon 66475/Geolon 66475	Nicolon Corporation	Woven Polypropylene Multifilament Strands
Stabilenka 200	Nicolon Corporation	Woven Fiberglass Monofilament
Style 5793	Westpoint Pepperell	Woven Polyester Multifilament Strands

uniaxial tension testing and direct shear testing was performed on all fabrics obtained for the study.

Data determined from uniaxial tension tests included ultimate tensile strength and stress-strain modulus. Direct shear tests were used to measure soil-fabric frictional resistance.

After the four fabrics were selected for further evaluation, creep tests and load bearing tests were conducted. The purpose of the creep tests were to measure time-dependent elongation under static load conditions. The load bearing tests produced stress-strain characteristics of the soil-fabric systems.

Details of Uniaxial Tension Testing

All 17 fabrics were tested in uniaxial tension by procedures developed for the U. S. Army Corps of Engineers (8). In this test, fabric 6 in. wide is placed in tension grips, with an initial gage length of 12 in. between grips. The fabric is then loaded at a constant strain rate of 1 percent/min to failure and the load and deformation are recorded during the test. Failure of the specimen is denoted by tearing or rupture of the fabric accompanied by a reduction of load, or by 50 percent elongation of the fabric where no load reduction occurs. Data provided by the test are then used to determine the stress-strain characteristics and the ultimate tensile stress of the fabric.

For more detailed uniaxial tension testing procedures, the reader is referred to Reference 8.

Details of Direct Shear Testing

Direct shear tests were conducted for all 17 fabrics in the study.

Normal loads of 1.0, 2.0, and 4.0 tsf were individually applied to each soil-fabric sample and direct shear was induced along the soil-fabric interface at a rate of 0.025 in./min. In order to ensure repeatability of tests, Ottawa 20-30 sand which conformed to ASTM C-190 was used as the soil medium. The sand was flooded and vibrated to achieve a dense condition.

For more detailed direct shear testing procedures, the reader is directed to Reference 8.

Details of Creep Testing

The four geotechnical fabrics chosen for load bearing testing were also subjected to creep testing. Fabric strips 1.0 in. wide were placed in grips designed for the test (8), in a manner to minimize slippage and with a gage length of 6.0 in. between grips. Each fabric was initially subjected to a static load equivalent to the stress developed at 2 percent strain during the uniaxial tension test. Elongation of the fabric was measured and recorded at various time intervals until the fabric resisted further creep. At that time, a static load equivalent to the stress developed at 6 percent strain was applied and the elongation over time was again monitored. After creep had reached negligible proportions, a final load equivalent to the stress at 10 percent strain was applied and the process was reiterated.

For a more detailed discussion of the creep testing equipment and procedures, the reader is directed to Reference 8.

Details of Load Bearing Testing

Figure 2 shows a simplified drawing of the load testing apparatus,

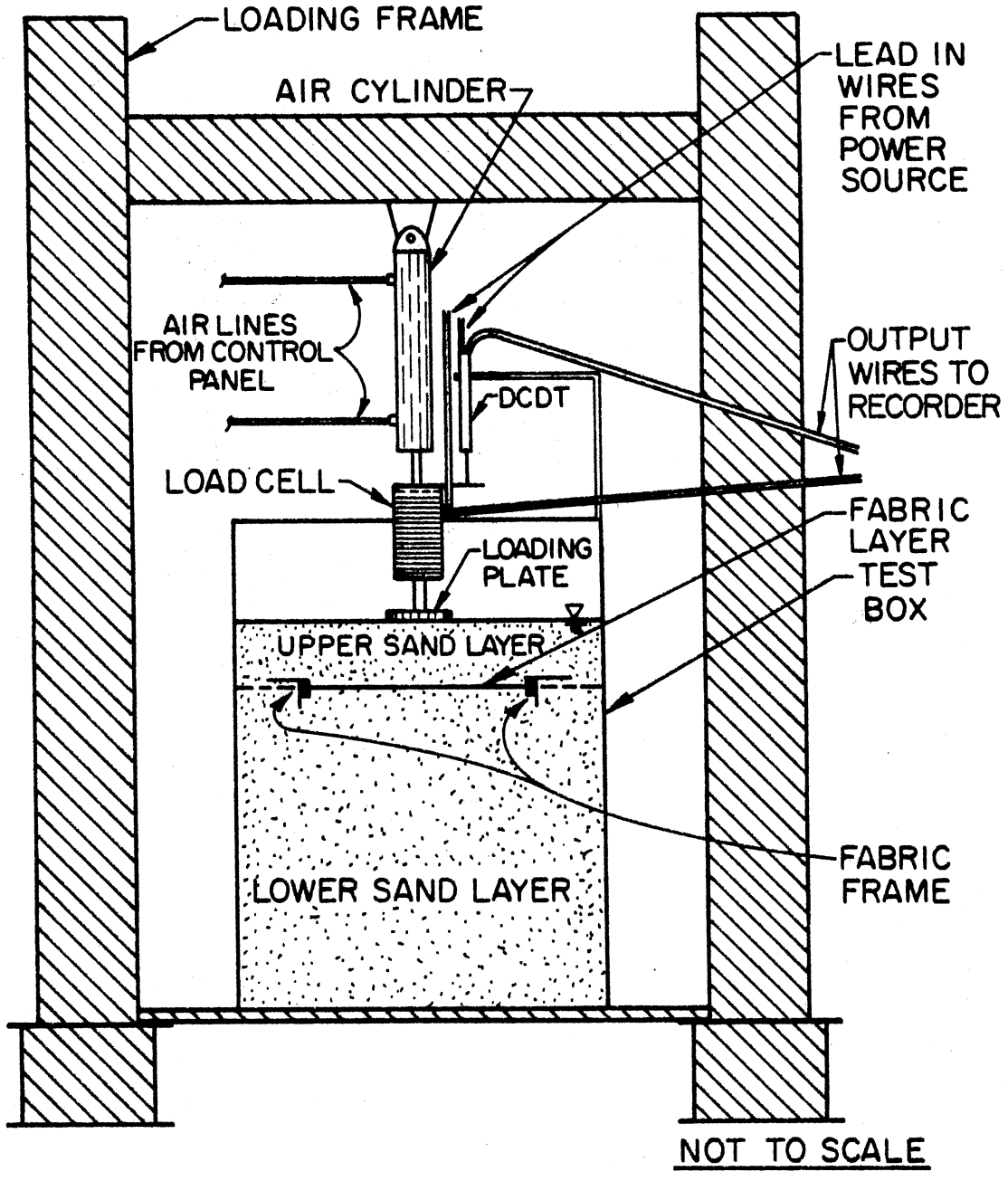

Figure 2. Schematic of Load Testing Apparatus

and Figure 3 is a schematic of the control panel used for applying the load and controlling the frequency and duration of load application. A photograph of the load testing apparatus is shown in Figure 4.

Load was applied to the loading plate with a Schrader air cylinder equipped with a 2.0 in. piston and a 12 in. stroke. The applied load was monitored with a Baldwin-Lima-Hamilton Model U1 strain gage load cell of 2000 lb capacity. The resulting vertical displacement of the loading plate was simultaneously monitored by a Hewlett-Packard Model 3000 Direct Current Displacement Transducer (DCDT). Loads and corresponding displacements were continuously recorded on a Sargent-Welch Model DSRG-2 dual pen strip chart recorder.

As previously stated, the magnitude and duration of loading was controlled by the apparatus shown schematically in Figure 3. The air pressure was controlled using Wilkerson air regulators and gauges. AAA Model S03 solenoid valves were used for directing the air flow through the various lines. The key part of the control panel was the MicroMaster Model WP 6001 MicroProcessor Controller (MPC) manufactured by Western Pacific. The programmable capabilities of the MPC enabled the actuation of the solenoid valves at regular and precise intervals to ensure multiple test accuracy.

In order to accurately determine the effects using fabric reinforcement in a soil system, it was first necessary to select a soil which would allow for repeatability of load bearing tests. Since numerous tests were to be performed, it was desirable to use a soil which would require a minimum of preparation and could be densified into a homogeneous soil mass. For these reasons, Ottawa 20-30 (ASTM C-190) sand was selected. It was also decided that tests would be most likely repeatable

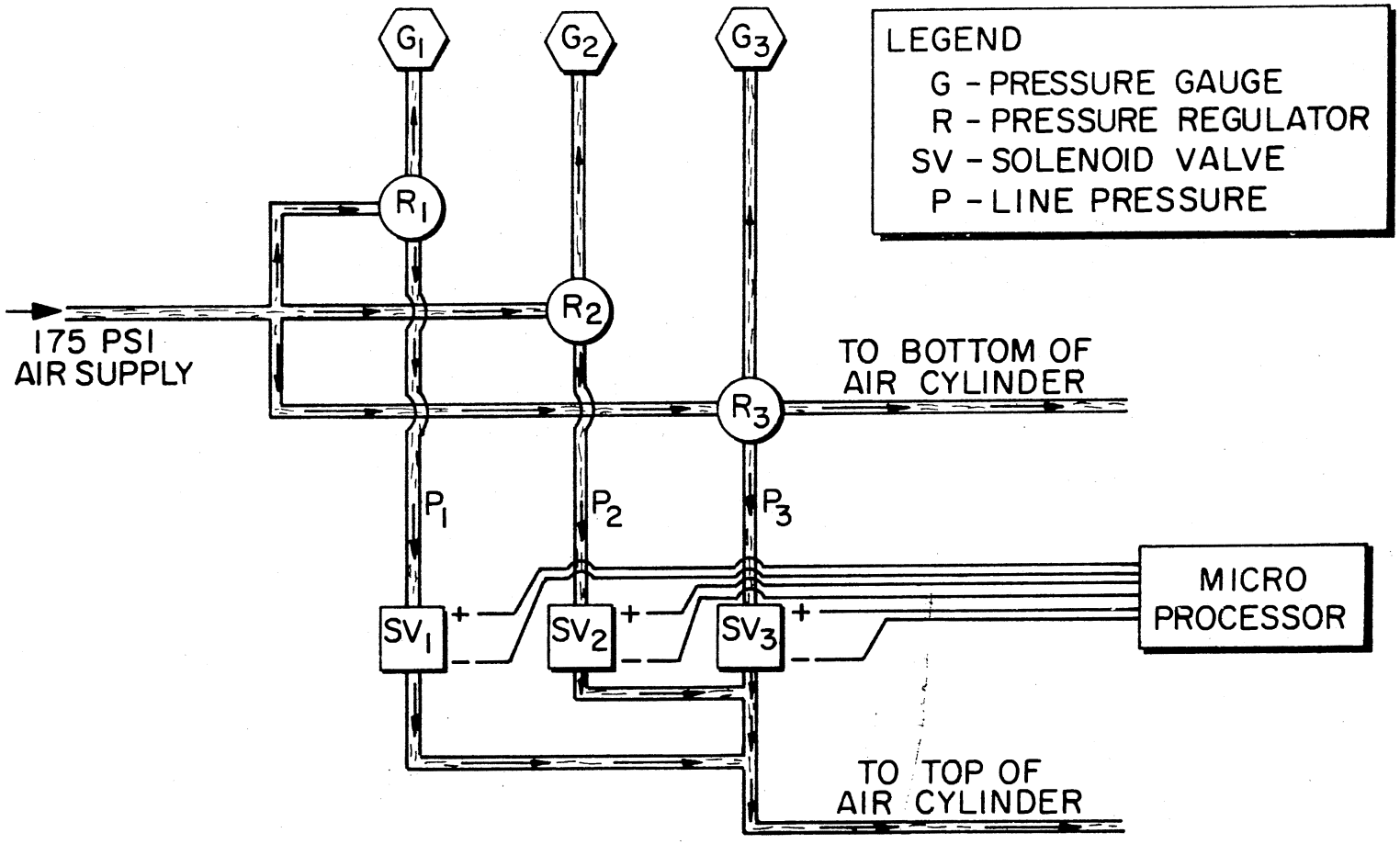

Figure 3. Control Panel Schematic Showing Direction of Airflow en Route to the Air Cylinder

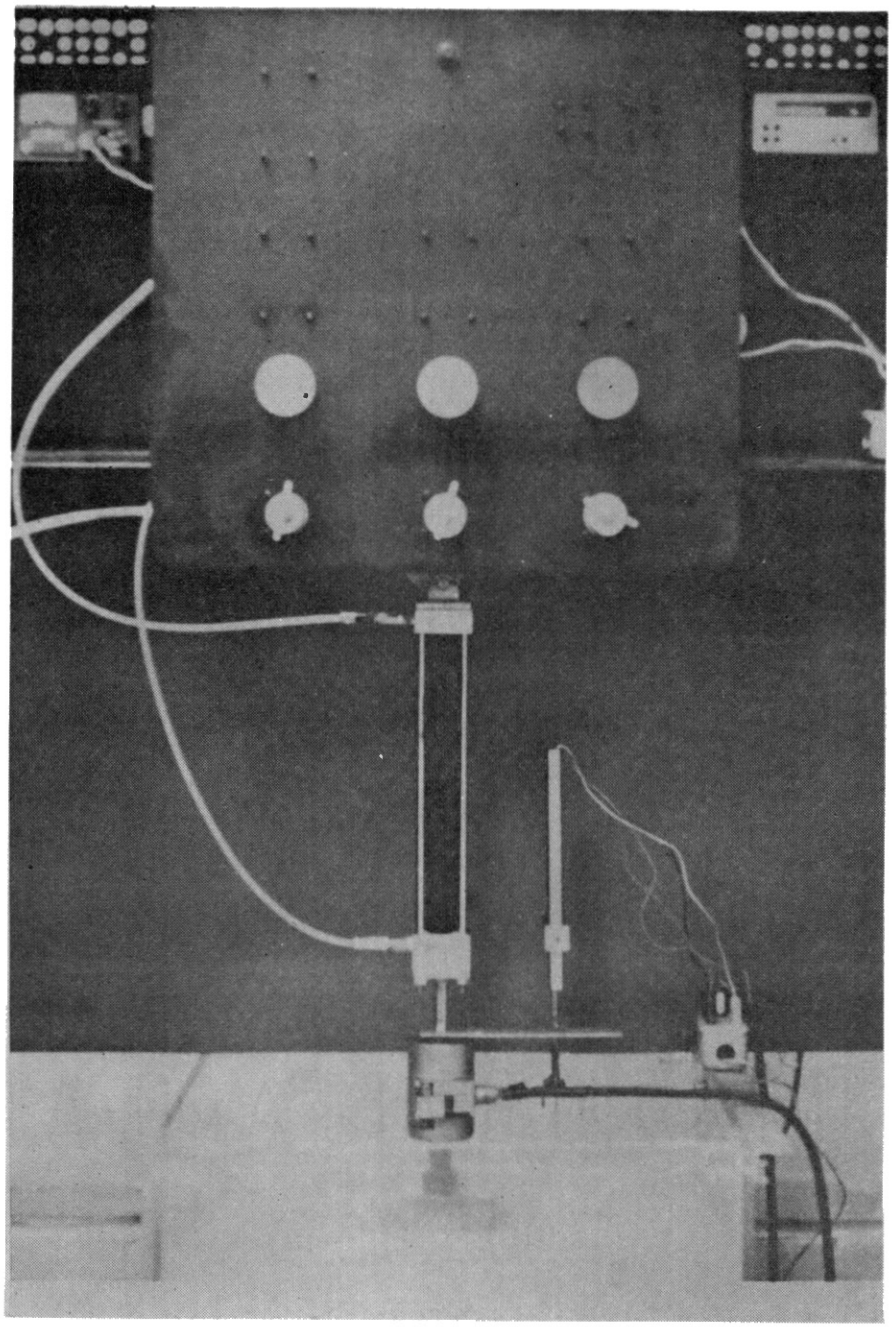

Figure 4. Photograph of Load Testing Apparatus

if the sand was prepared and tested in a flooded condition, with the water table at the surface of the sand.

Testing was conducted with no fabric reinforcement, with fabric reinforcement in the "no slack-no tension" state, and with pretensioned fabric. The frame used in the fabric tests is shown in Figure 5 with fabric installed.

The frame has the capability of holding fabric 12.0 in. by 12.0 in. to 13.2 in. x 13.2 in. between grips, allowing for up to 10 percent biaxial strain for the pretensioned tests. However, a biaxial strain of 2 percent was used for all pretensioned fabric tests as this is considered to be a reasonable value to simulate a practical degree of field pretensioning.

Prior to placement of the fabric and frame, the lower sand layer was vibrated with a WYCO 990-M concrete vibrator to a depth of 14.5± in. Figure 6 shows the pattern and sequence of vibration. Location 5 was directly beneath the center of the loading plate, and vibration lasted for 15 seconds at each location. Following vibration, the sand was rodded with a 3/8-in.-dia bar to achieve a uniform dense condition, and the sand was "struck off" level using the device shown in Figure 7. The fabric and frame were then installed as shown in Figure 8 and the upper sand layer was placed in the desired thickness. Rodding of the upper sand layer was then performed and the sand was struck off level once again. The water level was maintained at the surface of the sand at all times during preparation.

Following preparation of the test box, the loading plate was lowered to the surface and a seating load of 1 psi was applied over the area of the plate, to eliminate any slack in the system. The load was then

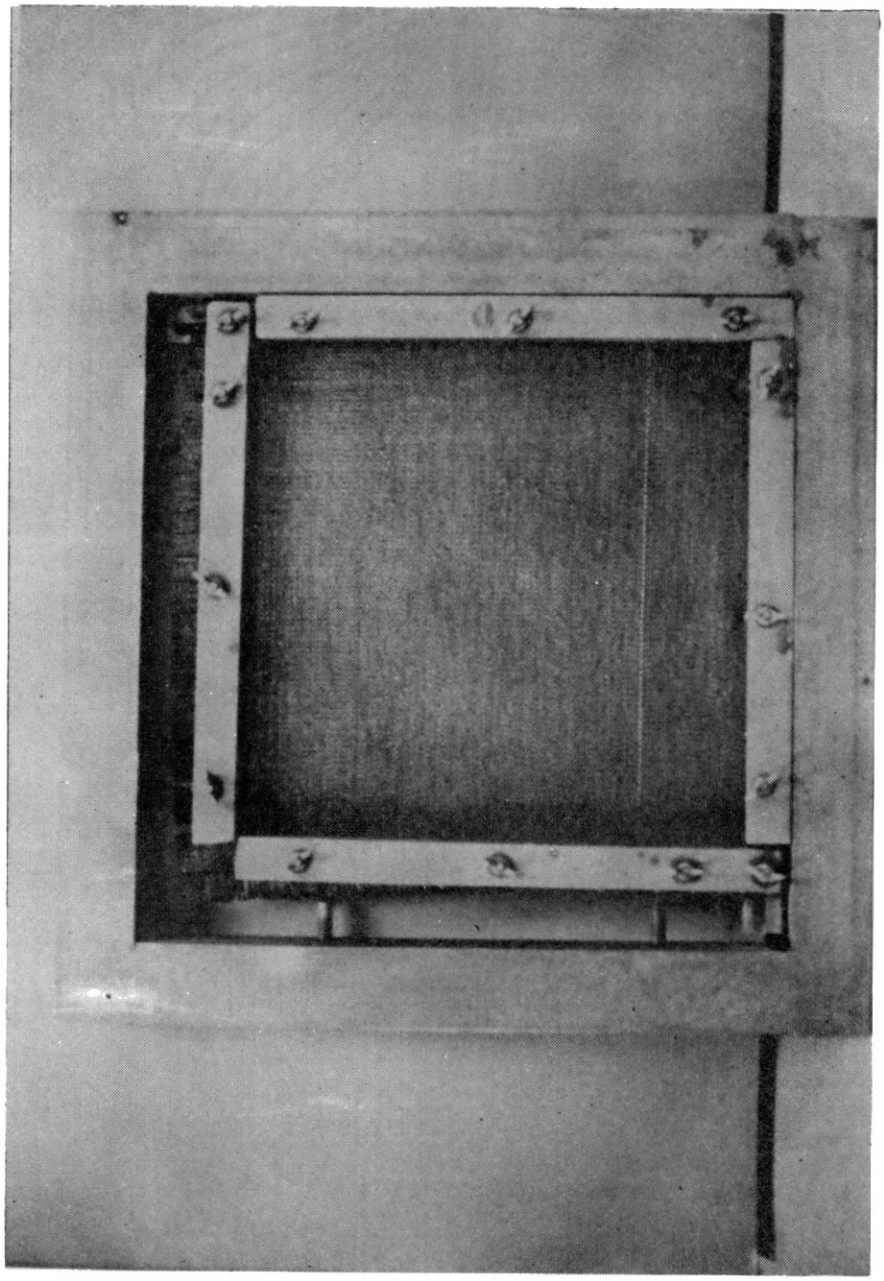

Figure 5. Photograph of Fabric Clamp with Fabric Installed

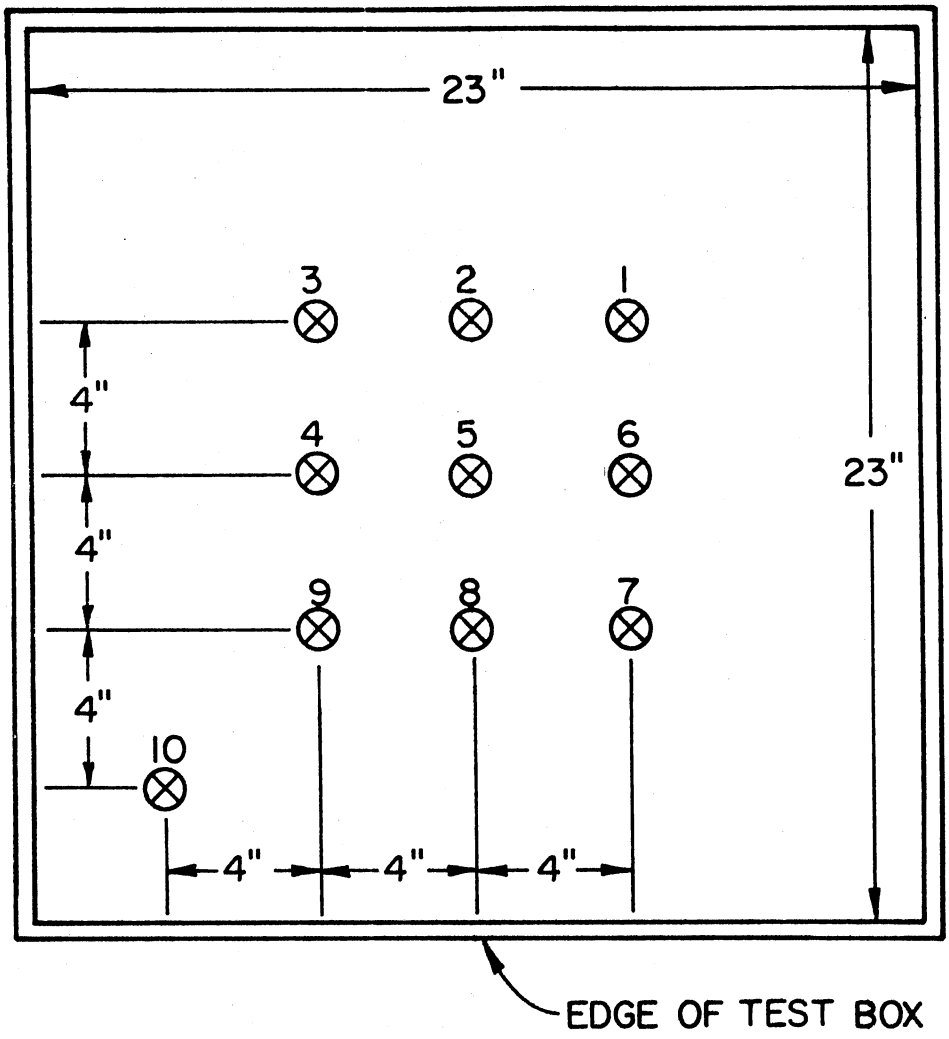

Figure 6. Pattern and Sequence for Vibrating Sand in Order to Achieve Repeatable Testing Conditions

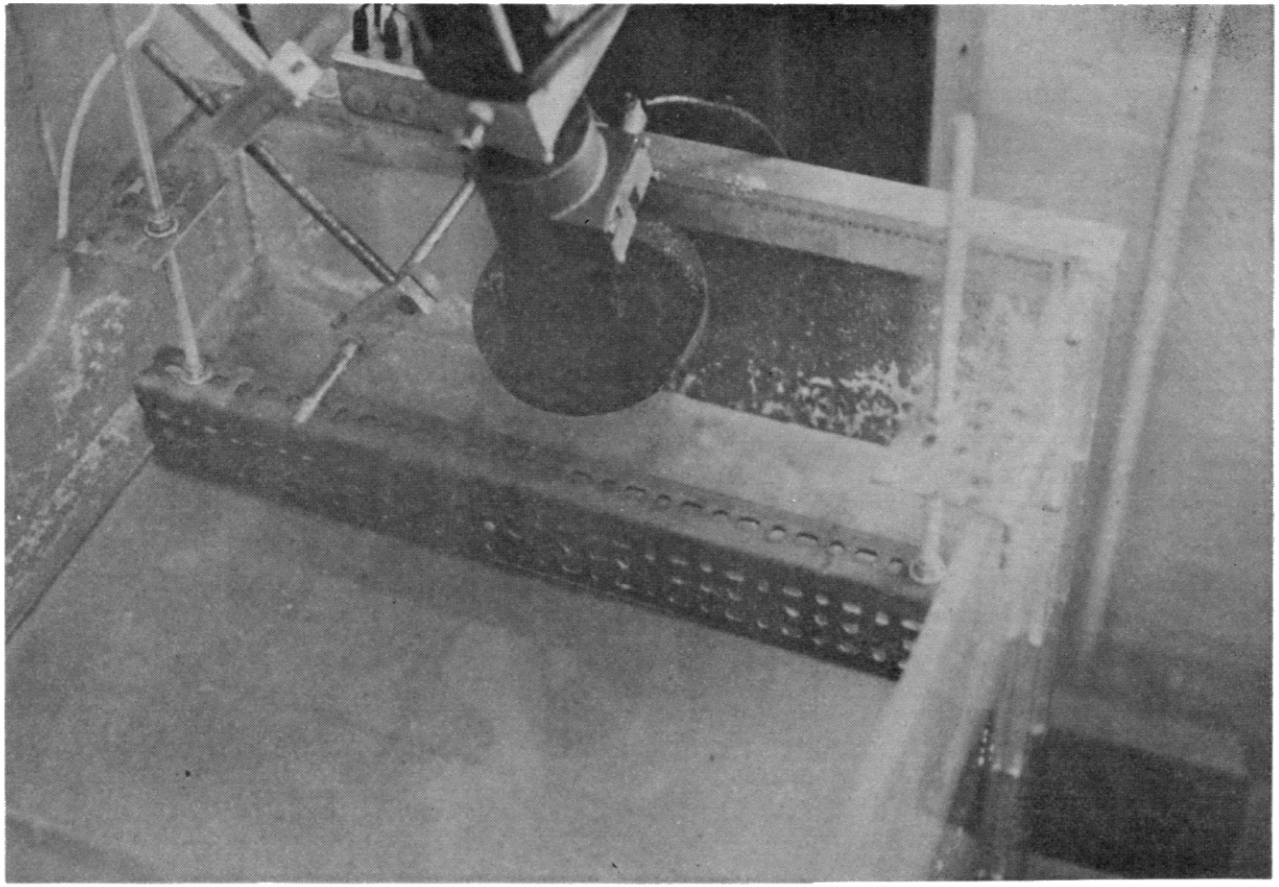

Figure 7. Photograph of Tool Used for Leveling Sand Surface

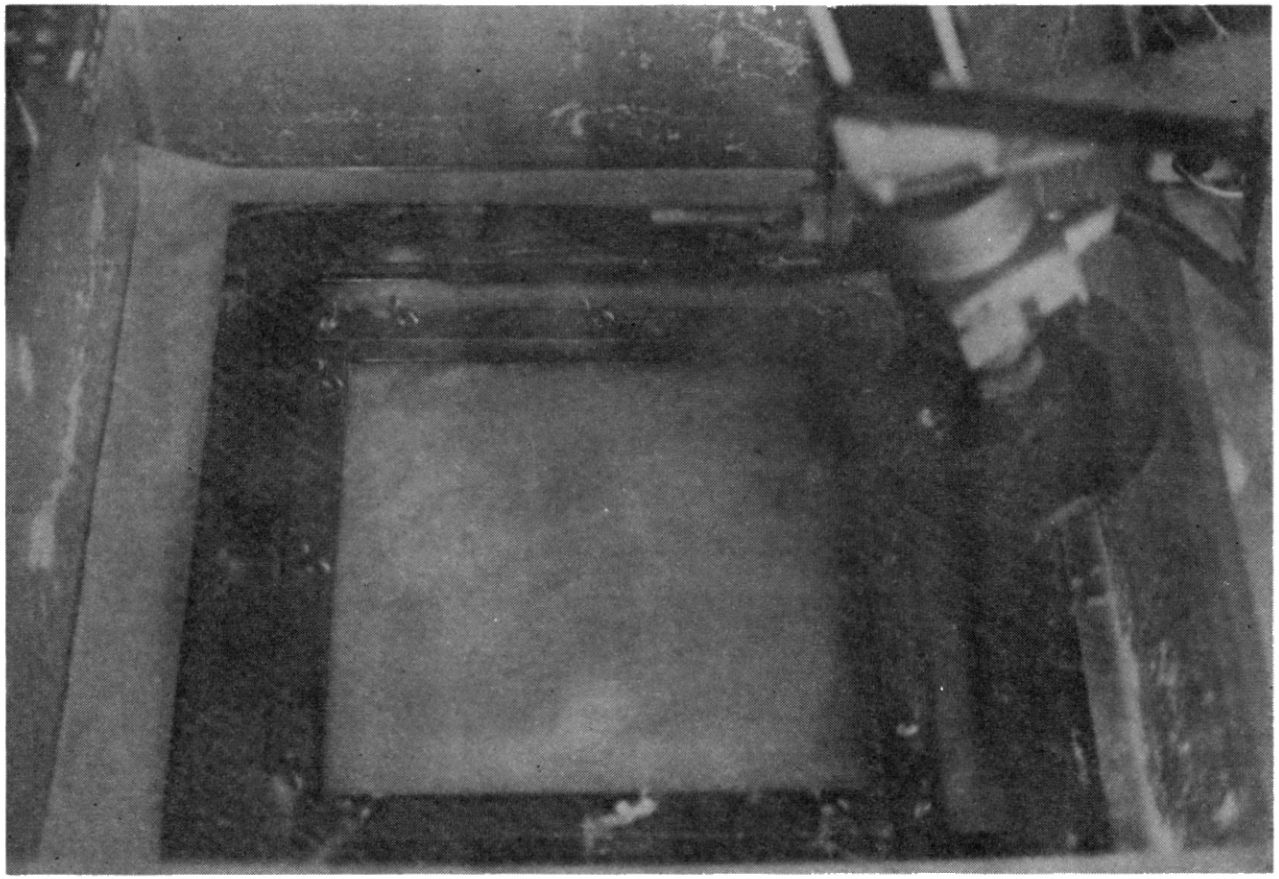

Figure 8. Photograph of Installed Fabric and Frame Prior to Placing Top Layer of Sand

returned to zero and the test was run with loads being applied in increments of 1.5± psi to the air cylinder and each load had a duration of 10.0 seconds. The test was terminated when the peak air supply pressure of 175± psi was reached.

Load bearing tests were also performed on sand without fabric reinforcement so that "before and after" comparisons could be made. For all cases, tests without fabric were run using the same procedure used in each fabric test, with the exception that the fabric and fabric frame were not put into place following the initial vibration and rodding of the lower sand layer.

CHAPTER IV

RESULTS AND DISCUSSION

All 17 geotextiles were initially tested in uniaxial tension and direct shear. Four geotextiles were then selected for testing with the load bearing test apparatus. Creep tests were also conducted on the four fabrics for the purpose of observing time dependent elongation of the fabric during application of a constant load.

Tension Testing

At least three uniaxial tension tests were run on 6 in. wide by 12 in. long strips of each fabric type in order to obtain at least two (and usually three) closely comparable sets of stress-strain data. All geotextiles except the Corning Fiberglass Fabric were subjected to testing in the warp and fill directions. The warp direction has been defined as being ". . . parallel to the finished edge, or parallel to the direction the fabric was extruded from the loom or other manufacturing device." (8). The fill direction is the direction 90 degrees to the warp direction. While many authorities test nonwovens in only one direction and do not differentiate between warp and fill, results have shown appreciable differences in the strength of the fabric in the two directions (8). Several attempts were made to test the Corning Fiberglass Fabric in uniaxial tension, but excessive slippage in the grips prevented accurate testing. A series of photographs of a test run on the Corning Fiberglass

Fabric warp direction are included in Appendix A of this report and slippage may be observed in the photographs.

Appendix A contains photographs of all seventeen fabrics as they were tested. Test results for a specific fabric are also presented in Appendix A immediately following the photograph series of that test.

Figure 9 shows stress-strain data plotted for the warp directions of the four fabrics used in the load bearing testing portion of the project. Nicolon 66475 and Celanese 600X are woven fabrics, and Typar 3401 and Bidim C-34 are nonwoven. It may be seen that the Nicolon fabric is a strong woven fabric and in comparison, the Celanese 600X is relatively weak woven fabric. In comparison to the woven fabrics, both Typar 3401 and Bidim C-34 possess low tensile strengths. However, in the field of nonwovens, the Typar fabric is relatively strong and the Bidim C-34 is comparably weak. This strength reference is made in regard to the initial tensile modulus of the fabric (9).

Strength characteristics of the fabrics were a major factor in their selection for additional testing, but were not the sole justification for their use. Typar 3401 and Bidim C-34, while meeting the desired "strong and weak" strength characteristics respectively, also are two of the most widely used civil engineering fabrics. Nicolon 66475 has a very high tensile strength at low strains and so is the most likely fabric to function for almost any project. Celanese 600X is a fabric which is similar to several other fabrics now on the market, and results for these fabrics may likely be comparable to results obtained for Celanese 600X.

Direct Shear Testing

All fabrics were tested in direct shear to determine their relative

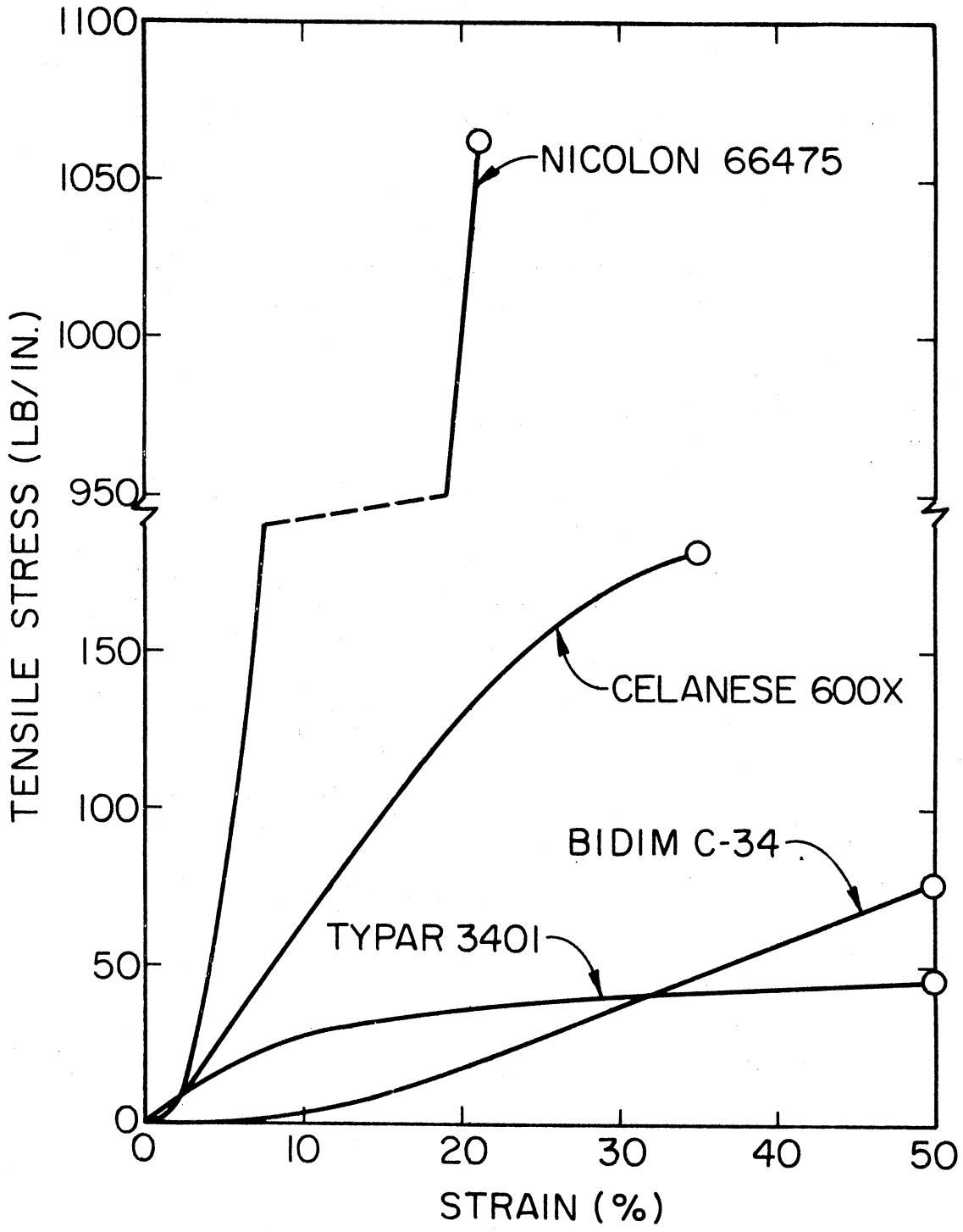

Figure 9. Stress-Strain Data for Fabrics Used in Load Bearing Testing. Results are for Uniaxial Tension Testing in the Warp Direction Only.

frictional resistance, measured in terms of the soil-fabric friction angle ϕ_{SF}. Tests were conducted with Ottawa 20-30 sand compacted to a dense state. The soil friction angle ϕ, for the dense sand, was also determined. Soil-fabric shear testing was conducted only in the warp direction as this is the direction in which maximum stresses should be transmitted when a construction project is properly designed.

Soil-fabric friction test data are summarized in Table II. The value given for each fabric is an average value for tests conducted with normal loads of 1, 2, and 4 tsf. Values of ϕ_{SF} for a fabric were found to vary by as much as 8 degrees between tests with different normal loads. This may or may not be important in design considerations, but if the soil-fabric frictional resistance value is determined with a normal load approximating that which will be found in the field, accurate ϕ_{SF} values should be obtained.

Results of the direct shear testing were indirectly considered in selecting the four fabrics used in the load bearing tests. Data were evaluated to make sure no fabric was selected which had an inferior soil-fabric friction angle. Conversely, if a fabric had been found to have an exceptionally high ϕ_{SF} value, it could have been evaluated further.

Creep Testing

The four fabrics selected for load bearing testing were tested for creep behavior in the warp direction. Using the procedure discussed in Chapter III, data were obtained for each fabric so that creep tendencies could be observed and comparisions of the four fabrics could be made. Results of the testing are presented graphically in Figure 10.

It may be noted that both Bidim C-34 and Nicolon 66475 experienced initial creep upon load application and quickly leveled off in magnitude.

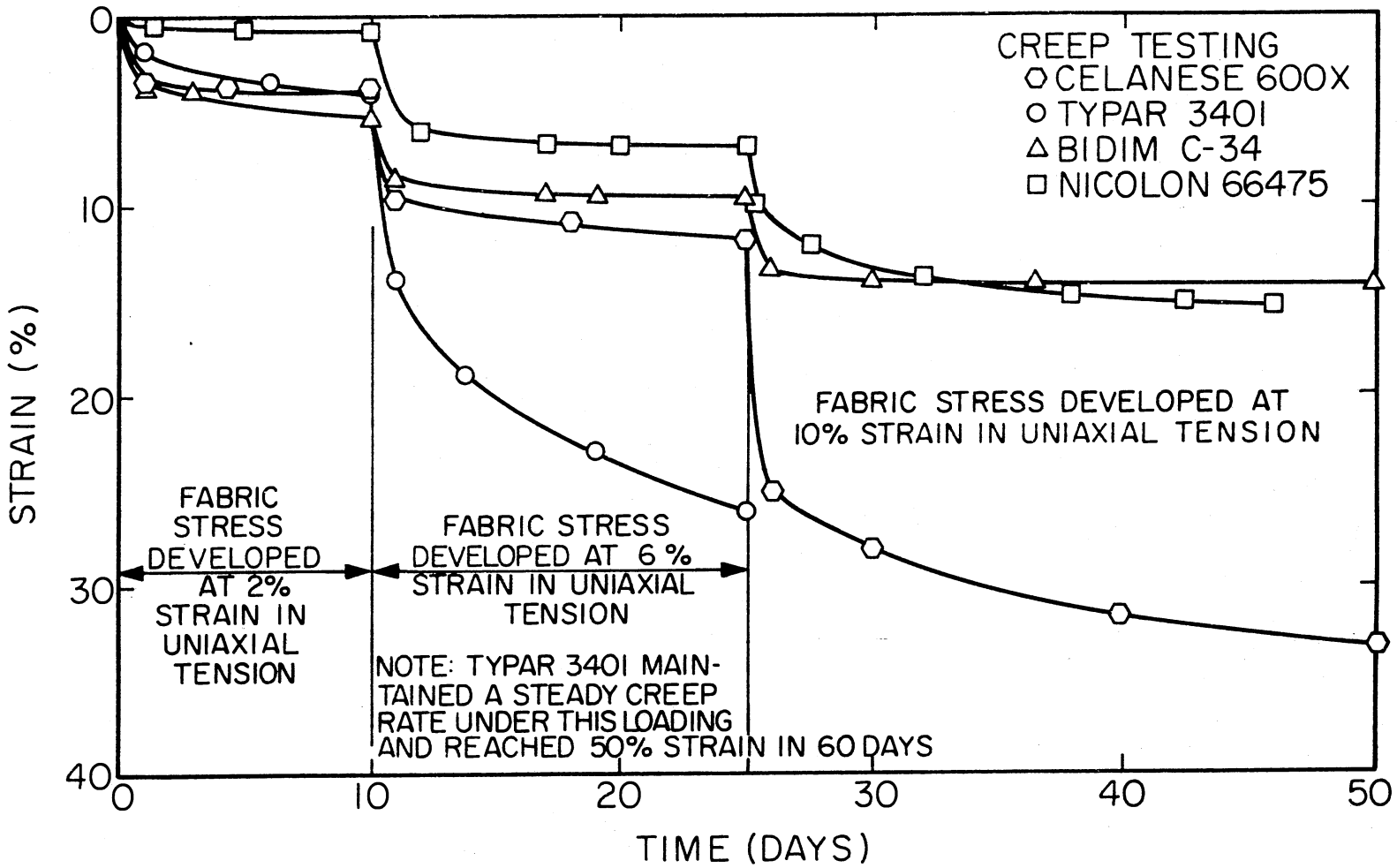

Figure 10. Creep Testing Results for Fabrics Used in Load Bearing Testing. Results are for Warp Direction Testing Only.

TABLE II

SOIL-FABRIC FRICTION VALUES
FABRIC WARP DIRECTION

Fabric Trade Name	Average ϕ_{SF}[1] (Degrees)
Celanese 500X	22
Celanese 600X	36
Diamond 8	40
Special 400	36
Retain 72	42
Stitchbond 1375	41
Fibretex 150	30
Fibretex 200	36
Fibretex 300	34
Fibretex 400	39
Typar 3401	32
Bidim C-34	31
Nicolon 66475	40
Style 5793	40
Corning Fiberglass Fabric	30
Stabilenla 200	40
Mount Vernon Mills Fabric	41

[1] ϕ for soil alone was found to equal 54^{o}, which includes interlock effects.

It is of importance to mention here that although the clamps, which held the fabric during testing, were designed so that slippage would be minimal, some slippage did occur with the woven fabrics. Where possible, slippage effects were taken into account, but in any case, the results for the woven fabrics are representative of "worst case" creep.

Neither nonwoven was tested with a load heavy enough to cause slippage, and consequently both graphs represent accurate test results. Whereas, both Nicolon 66475 and Bidim C-34 leveled off at approximately 15 percent strain at the end of the test, Celanese 600X had reached approximately 35 percent strain by the test's end. Typar 3401 reached 50 percent strain when subjected to a fabric stress equivalent to that obtained at 6 percent during the uniaxial tension test.

While the results have no direct bearing on the load bearing test results, it is obvious that creep tendencies of fabrics may be critical when the fabric is subjected to duration or cyclic loading.

Another interesting point may be made from these test results. As shown in Table I, Celanese 600X is a woven polypropylene monofilament, Nicolon 66475 is a woven polypropylene multifilaments, Typar 3401 is a nonwoven spunbounded polypropylene monofilament, and Bidim C-34 is a nonwoven mechanically entangled continuous polyester filament. These fabric descriptions when combined with the creep results show a definite need for creep testing. One woven fabric behaved differently than the other, and both nonwovens showed different creep tendencies. Also, the fact that both wovens and the Typar 3401 were all composed of polypropylene had no notable influence on the creep results. These observations demonstrate why no estimate of fabric creep tendencies should be made based upon manufacturing process or fabric chemical composition.

Load Bearing Tests

The load bearing test program was composed of an initial testing phase and secondary testing. A total of 63 tests were run during the initial testing, and after the data were analyzed, 18 tests were run during secondary testing. All tests were conducted in the manner outlined in Chapter III.

Initial Testing

In initial testing, a series of tests was run for each plate size-embedment depth combination. A test series consisted of three tests each for the following three conditions:

1. Each fabric with no pretensioning,
2. Typar 3401 and Celanese 600X in the pretensioned state, and
3. The no fabric system.

Each series then consisted of 21 load bearing tests, and there were three different plate size-embedment depth combinations. These were: 6 in. plate-3 in. embedment depth, 4 in. plate-2 in. embedment depth, and 4 in. plate-4 in. embedment depth. Test results are presented graphically for each test condition in Appendix B. Results for each plate size-embedment depth combination are separated into tests without fabric pretensioning and tests with 2 percent pretensioning and are presented graphically in Figures 11 through 16.

The purpose of the fabric-layered load bearing tests was to compare effects which variation of fabric properties had on the soil-fabric system. It may be seen from Figures 11 and 12 that Bidim C-34, in general, had the most desirable effect on the soil-fabric modulus and Typar 3401

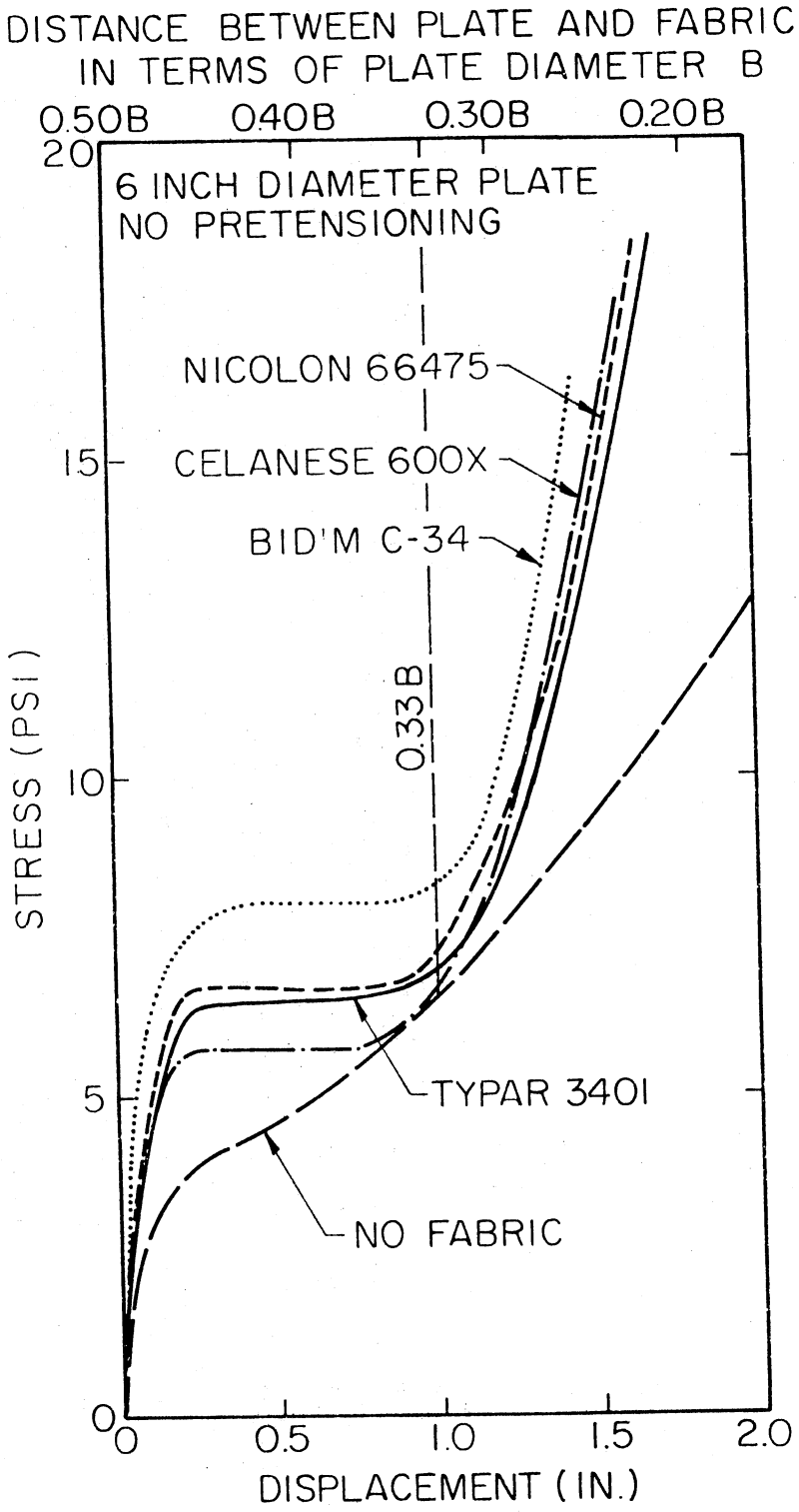

Figure 11. Load Bearing Test Results for Fabrics Loaded with a Plate of Diameter B Equal to 6 in. at an Initial Embedment Depth of 3 in. (0.50B)-No Pretensioning

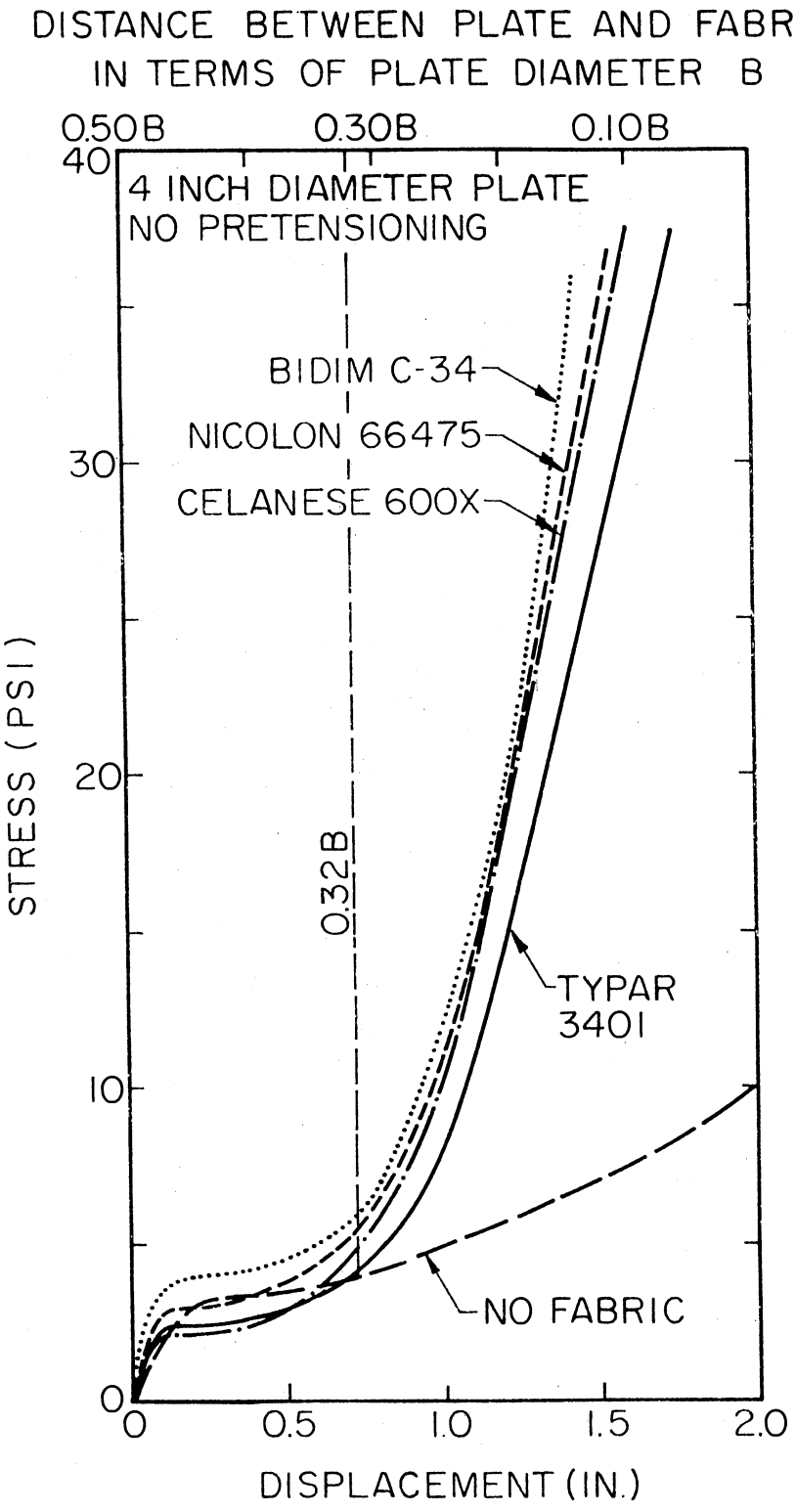

Figure 12. Load Bearing Test Results for Fabrics Loaded with a Plate of Diameter B Equal to 4 in. at an Initial Embedment Depth of 2 in. (0.50B)- No Pretensioning

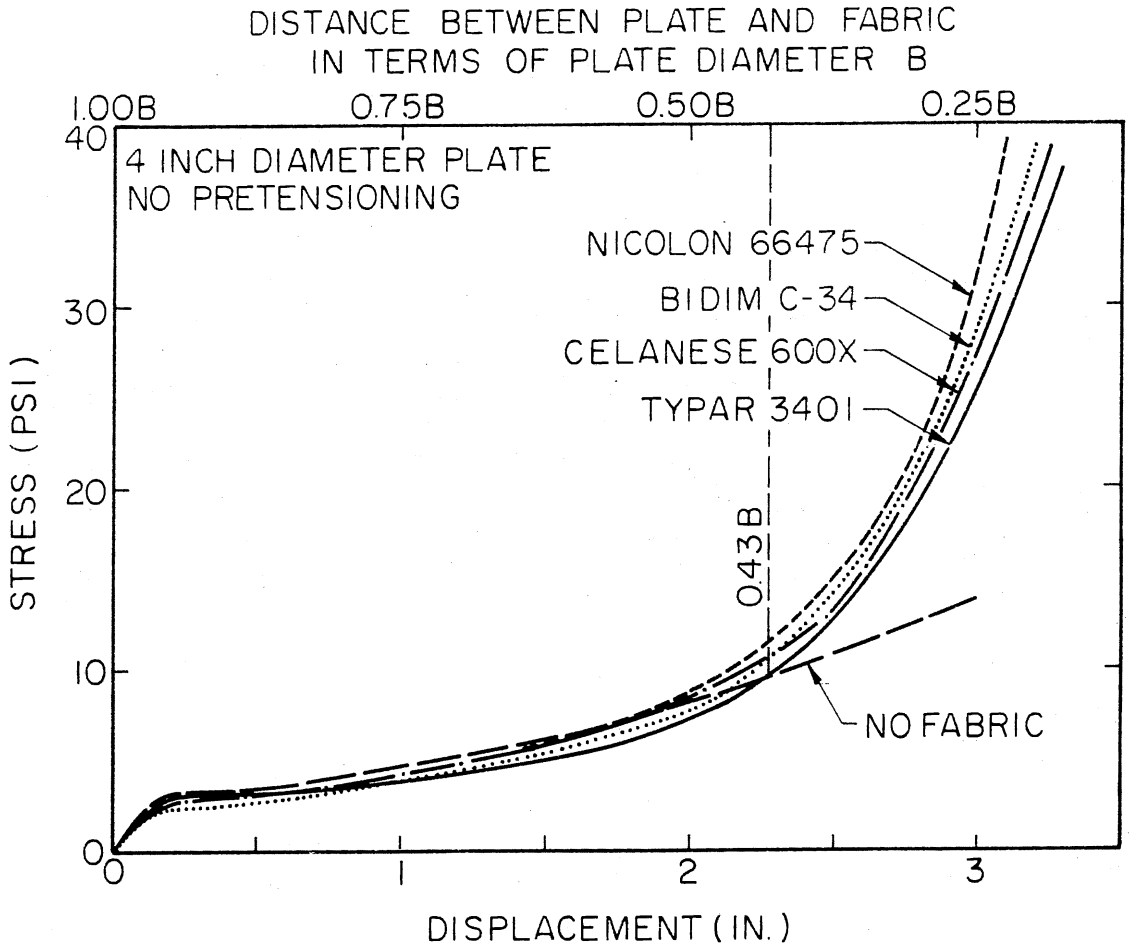

Figure 13. Load Bearing Test Results for Fabrics Loaded with a Plate of Diameter B Equal to 4 in. at an Initial Embedment Depth of 4 in. (1.00B)-No Pretensioning

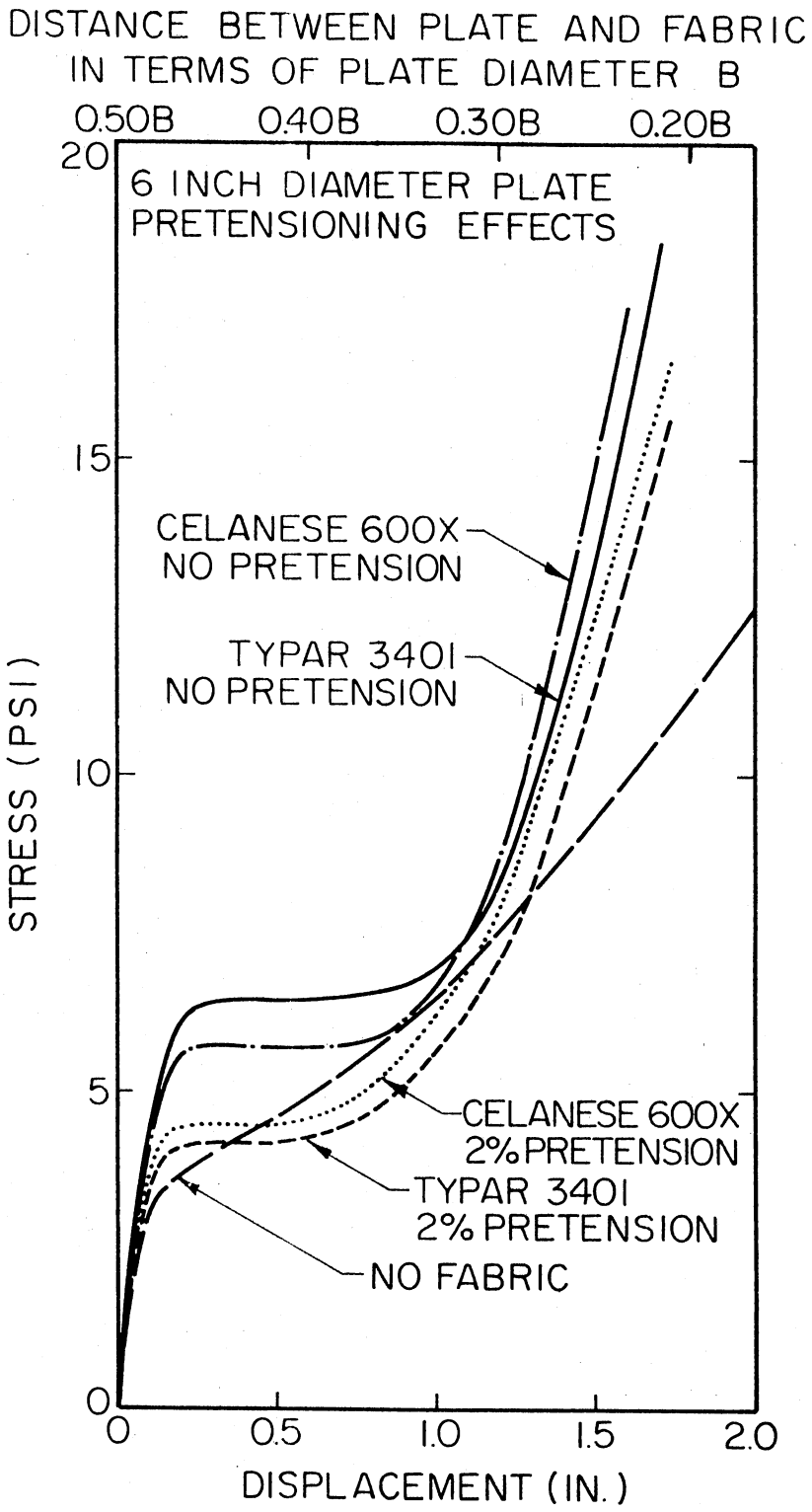

Figure 14. Load Bearing Test Results for Fabrics Loaded with a Plate of Diameter B Equal to 6 in. at an Initial Embedment Depth of 3 in. (0.50B)-Pretensioning Effects

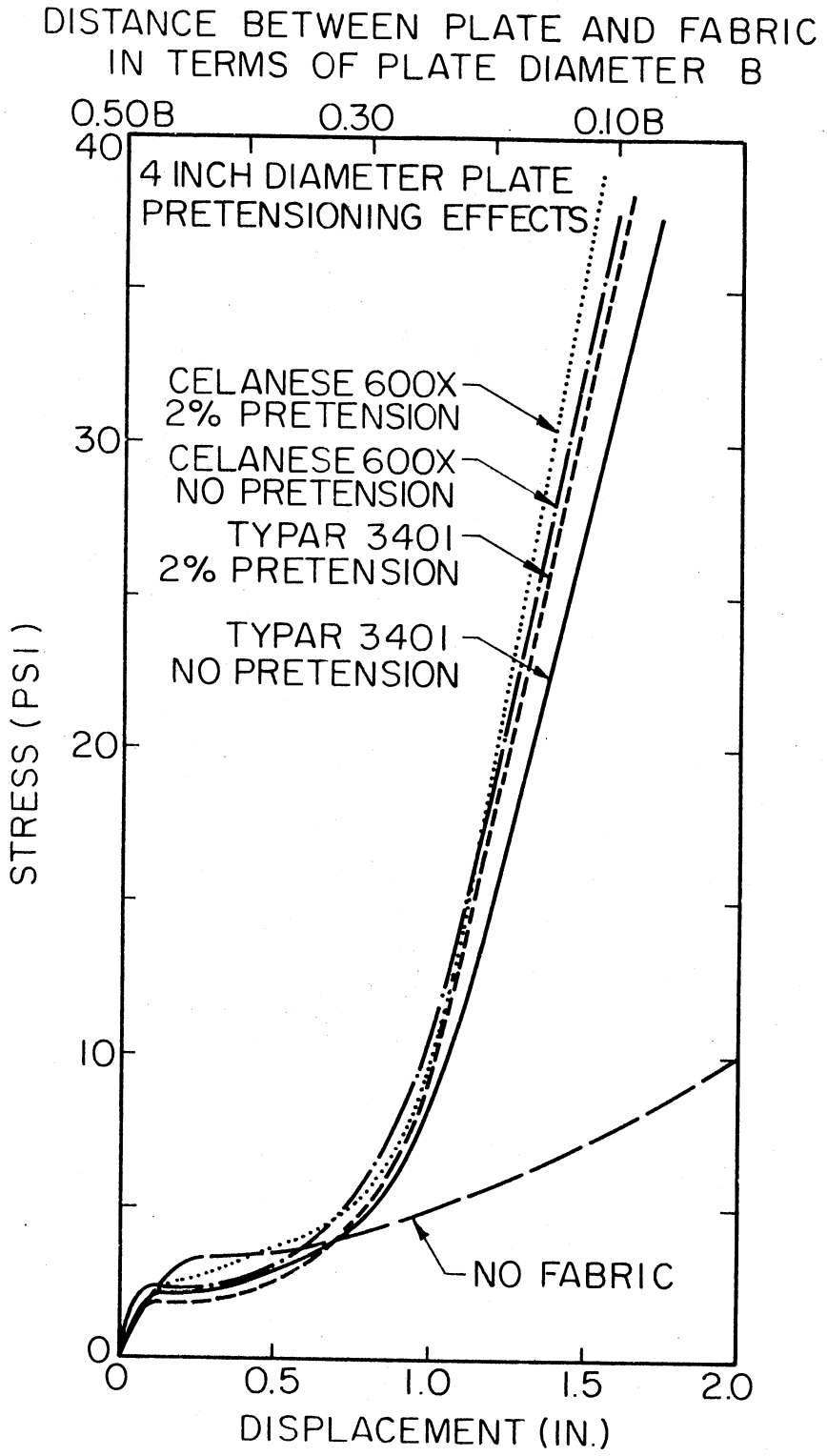

Figure 15. Load Bearing Test Results for Fabrics Loaded with a Plate of Diameter B Equal to 4 in. at an Initial Embedment Depth of 2 in. (0.50B)-Pretensioning Effects

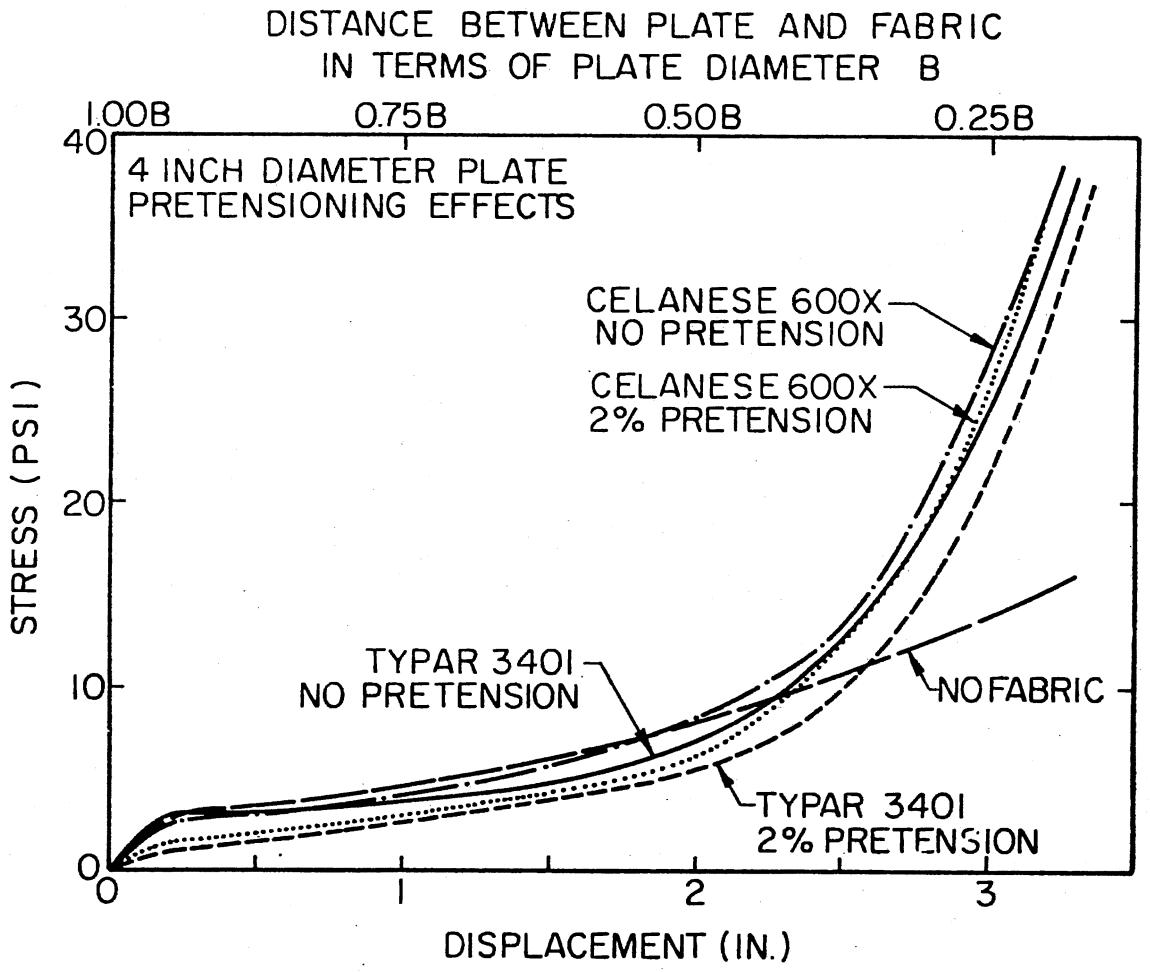

Figure 16. Load Bearing Test Results for Fabrics Loaded with a Plate of Diameter B Equal to 4 in. at an Initial Embedment Depth of 4 in. (1.00B)-Pretensioning Effects

and Celanese 600X the worst effects. Nicolon 66475 data fell between the two nonwoven fabrics.

The fact that Bidim C-34 possesses the lowest tensile strength and lowest value of soil-fabric friction seemingly shows that these specific parameters have no discernable effects on reinforcing the soil-fabric system. It is doubtful that the creep tendencies of the fabric had an influence on the system, as it was loaded for only a short time period. Admittedly, Bidim C-34 and Nicolon 66475 had lower creep rates than did the Typar and Celanese fabrics and this would seem to indicate some relation between creep and soil-fabric system strength, but it can be shown that this is not the case. While the Bidim and Nicolon fabrics had comparable creep rates, Figures 11 and 12 show a higher strength gain was achieved with the Bidim C-34 layered system. Also, Celanese 600X had a lesser initial creep rate than did Typar 3401, but Figure 11 shows that Celanese 600X contributed less to the system initially, and Figure 12 shows both fabrics initially comparable.

Figure 13 shows no difference initially between the "no-fabric" system and any of the four fabric-layered systems. When the loading plate was within a distance of 0.43B (B is the plate diameter) of the fabric layer, a strength gain had begun to occur in all four fabric-layered systems, but no appreciable differences were noted in the spread of data.

Effects of pretensioning may be observed in Figures 14, 15, and 16. Effects alternated from making the soil-fabric system slightly weaker to making it slightly stronger than the system which did not have pretensioned fabric. These slight variations probably result from spread in data and do not represent any significant pretensioning effects. Results do,

however, confirm the conclusion that fabric tensile strength has little effect on the initial strength of the soil-fabric system.

Upon studying test results shown in Figures 11, 12, and 13, it was noted that the initial embedment depth of the fabric had a marked effect on the deformation characteristics of the soil-fabric system. In Figure 13, the initial embedment depth was 4 in., which was equal to the plate diameter B. These results show no initial strength gain over the no-fabric system. Also, approximately 2.3 in. of displacement occurred in the system before any strength gain was observed. At this time, the load bearing plate and the fabric layer were separated by a distance of 0.43B, and the plate had been displaced a distance of 0.57B.

Figures 11 and 12 show that for a plate diameter of B and a fabric layer embedment depth of B/2, the initial soil modulus and bearing capacity were increased with respect to the no-fabric system. Plate displacement required to reach the secondary strength gain was approximately equal to 0.17B and this was a definite improvement over the displacement of 0.57B required when the initial fabric embedment depth was 1.0B. These observations prompted the secondary testing phase of the load bearing tests.

Secondary Testing

A total of 18 load bearing tests were run during secondary testing. Only Typar 3401 and Celanese 600X were tested and two plate size-embedment depth combinations were used. Results of the tests are shown in Figures 17 and 18. Three important observations may be noted: (1) the soil-fabric system strength, in all ranges of displacement, exceeds that of the soil system with no fabric, (2) the initial modulus and

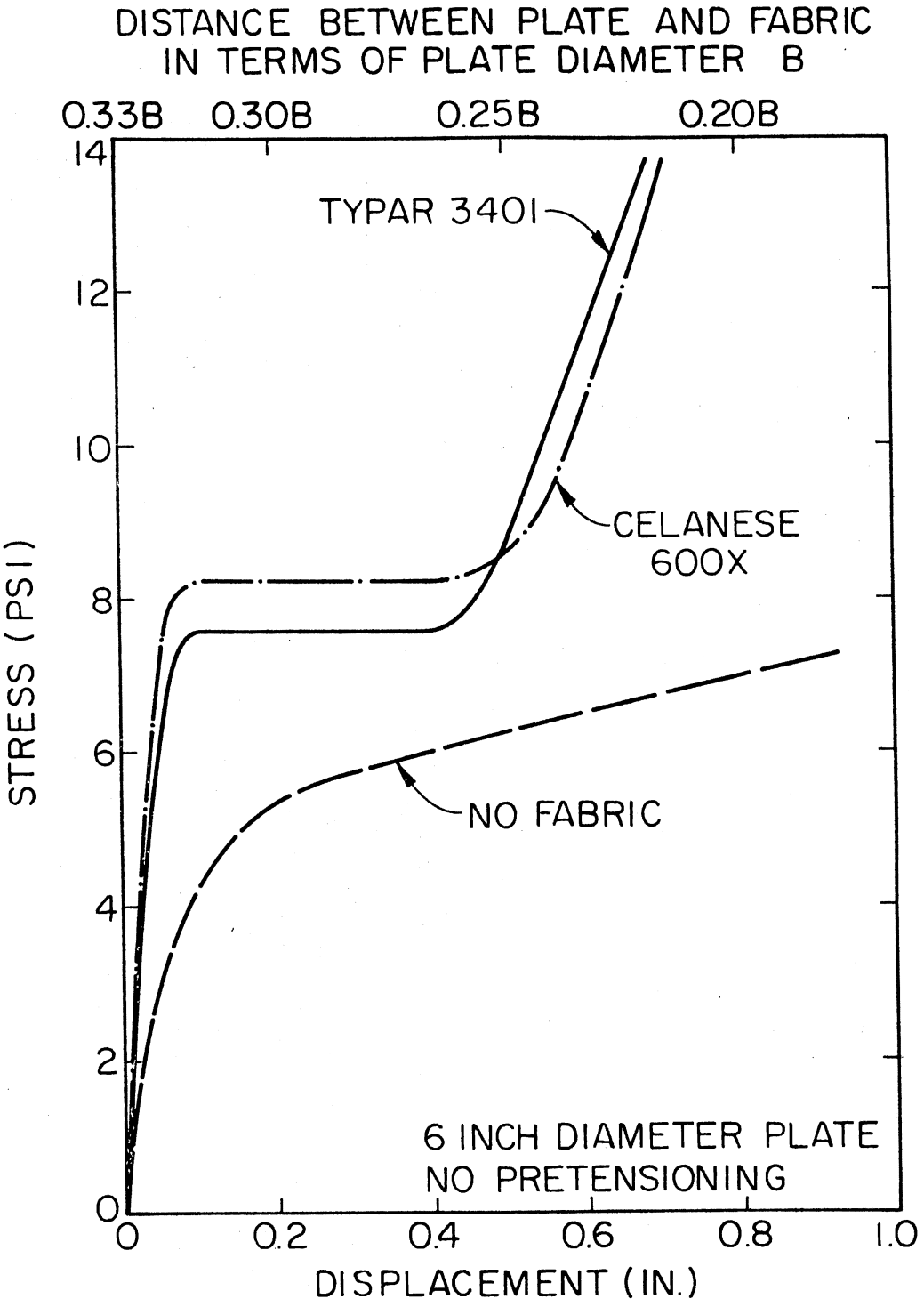

Figure 17. Load Bearing Test Results for Fabrics Loaded with a Plate of Diameter B Equal to 6 in. at an Initial Embedment Depth of 2 in. (0.33B)-No Pretensioning

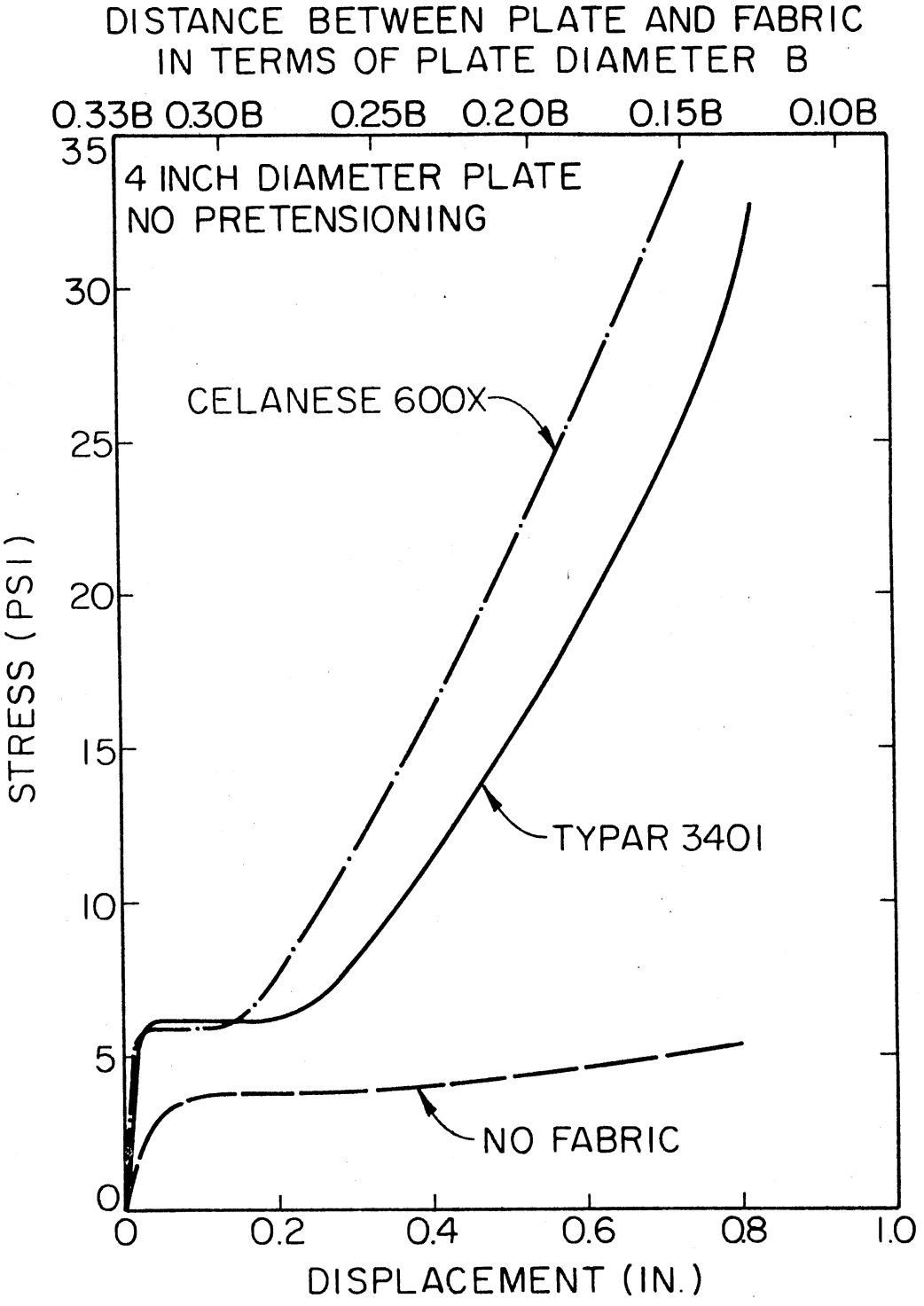

Figure 18. Load Bearing Test Results for Fabrics Loaded with a Plate of Diameter B Equal to 4 in. at an Initial Embedment Depth of 1.33 in. (0.33B)-No Pretensioning

bearing capacity is greater at this embedment depth than at deeper depths, and (3) the total displacement which occurred prior to the second strength gain was less than 0.10B.

Results of secondary testing, while showing desirable effects from reducing fabric embedment depth, also appear to demonstrate the effect which plate size has on the failure characteristics of the system. No differences from plate size variations were noted during the initial testing phase, but in Figures 17 and 18 it can be seen that the 4 in. diameter plate had a plate displacement of approximately 0.04B before reaching a second strength gain, while the 6 in. diameter plate required approximately twice the displacement or 0.08B. This difference may be too small to have any practical significance, but it should be noted in light of future testing.

General Discussion

A detailed discussion of uniaxial tension testing, direct shear testing, and creep testing has been previously published (8) and reiteration of this discussion is unnecessary and outside the scope of this report. One point with respect to direct shear testing should be added. As mentioned previously, values of the soil-fabric friction angle ϕ_{SF} for the same fabric but under varied loads of 1, 2, and 4 tsf have been found to vary by as much as 8 degrees. For most fabrics this is not true, but for any design in which ϕ_{SF} is a critical design parameter, values of normal loads approximating those which will be found in the field, and actual soil from the project site should be used in determining ϕ_{SF}.

While it is not necessary to discuss the actual uniaxial tension testing, direct shear testing, and creep testing, the effect which these

test results have on the soil-fabric system should be clarified. As stated previously, tensile strength, soil-fabric friction, and creep tendencies had no apparent effect on the load bearing test results. Had the applied load been increased or held for a longer duration or had cyclic loading been applied, these fabric parameters might have been interpreted as having a definite bearing on the performance of the soil-fabric system.

Figure 19 shows the typical appearance of Typar 3401 after being subjected to load bearing tests in which the fabric was installed at depths of B/3 and B/2. No fabric damage was noted for Typar 3401 at an embedment depth of 1.0B or for any other fabric at any depth. Fabrics susceptible to this type of damage may perform poorly under cyclic loading and if so, should not be used for reinforcement.

It has been determined that the depth of fabric embedment has a definite role in dictating the behavior of the soil fabric system. Footing size was also shown to possibly have an influence on the system behavior.

While this report is intended to be an investigation into the behavior of fabrics and not to develop a testing procedure, it seems that a viable procedure is nonetheless a product of this report. For a known area of contact pressure and a known ultimate load, a series of load bearing tests can be run on a soil-fabric system and the optimum embedment depth and type of fabric can be determined.

It has been shown that, for the system tested, certain physical properties of fabrics have no obvious effects on the behavior of a soil-fabric system. Variation of embedment depth has, on the other hand, been shown to be a major factor in the soil-fabric system behavior. What has not been discussed is why the soil-fabric system behaves as it does; that is,

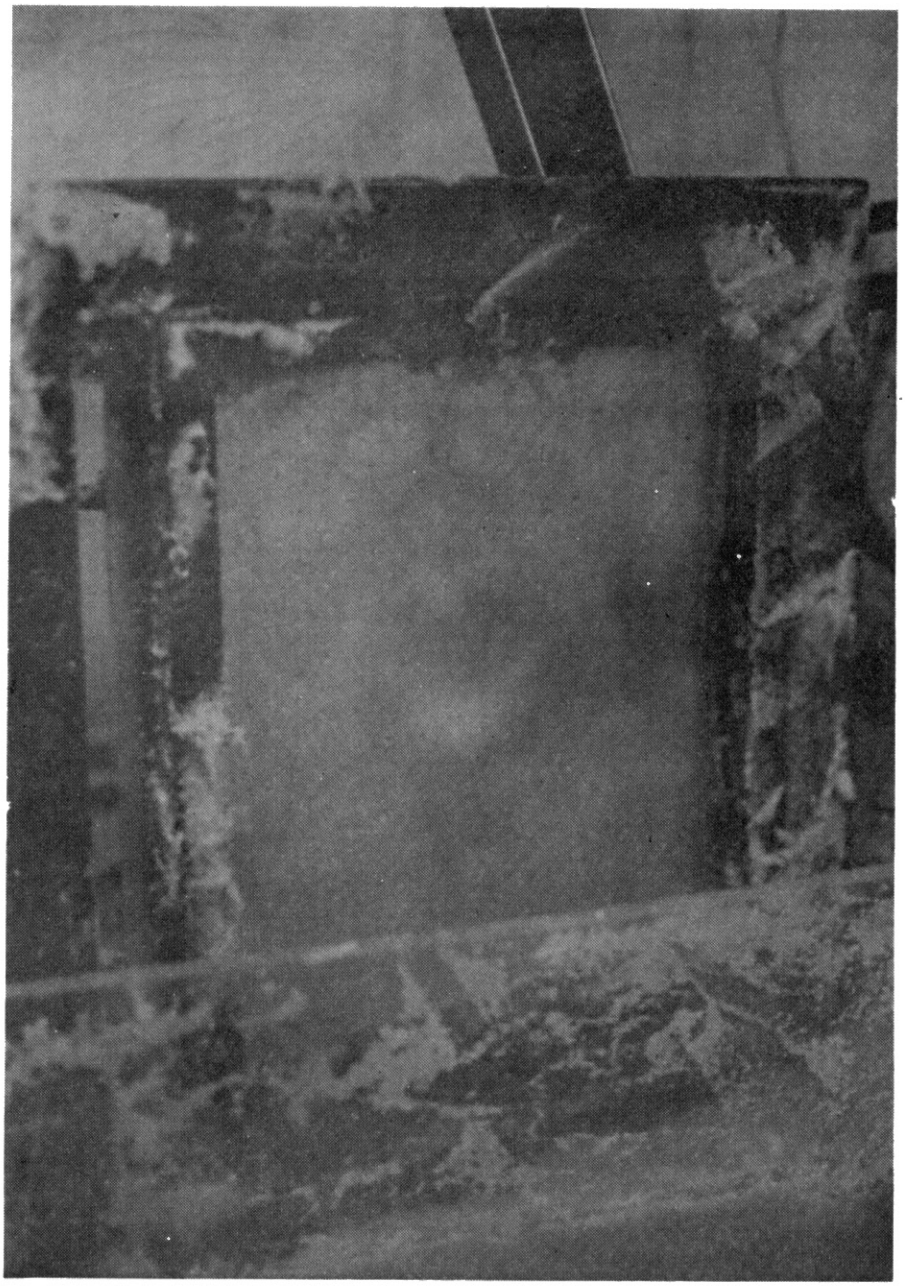

Figure 19. Photograph of Typical Damage to Typar 3401 as a Result of Load Bearing Tests at an Initial Embedment Depth 0.33B

what are the mechanisms by which the fabric functions in the "reinforced" soil-fabric system?

In the past, only theories based on laboratory and/or field tests have been used to describe the fabric mechanisms involved in soil "reinforcement." The following explanation presented by the author is also a theory based upon laboratory tests, and as such is obviously subject to argument.

Discussion of Fabric Reinforcement Theory

Terzaghi's theory of a general shear bearing failure depicts failure in a log spiral fashion with a central wedge which remains stationary with respect to the loaded area (see Figure 20a). In a homogeneous soil mass, this central wedge has geometric proportions which are dependant upon properties of the soil and footing characteristics. One way of looking at this is to say that while there are many possible failure surfaces within the system, this specific log spiral and central wedge type failure represents "the weakest link in the chain." Removal or reinforcement of the weakest link then should result in reinforcement of the total system.

In order for a fabric layer to provide <u>initial</u> reinforcement, it must then alter the shape of the failure surface. Present theory states that a fabric layer can cause reinforcement in only two ways; first by soil-fabric friction inducing lateral restraint and second by creation of tensile forces which provide for carrying of normal stresses and/or moment.

The mechanism of lateral restraint is not a simple concept to visualize. In the absence of civil engineering fabric within a soil system,

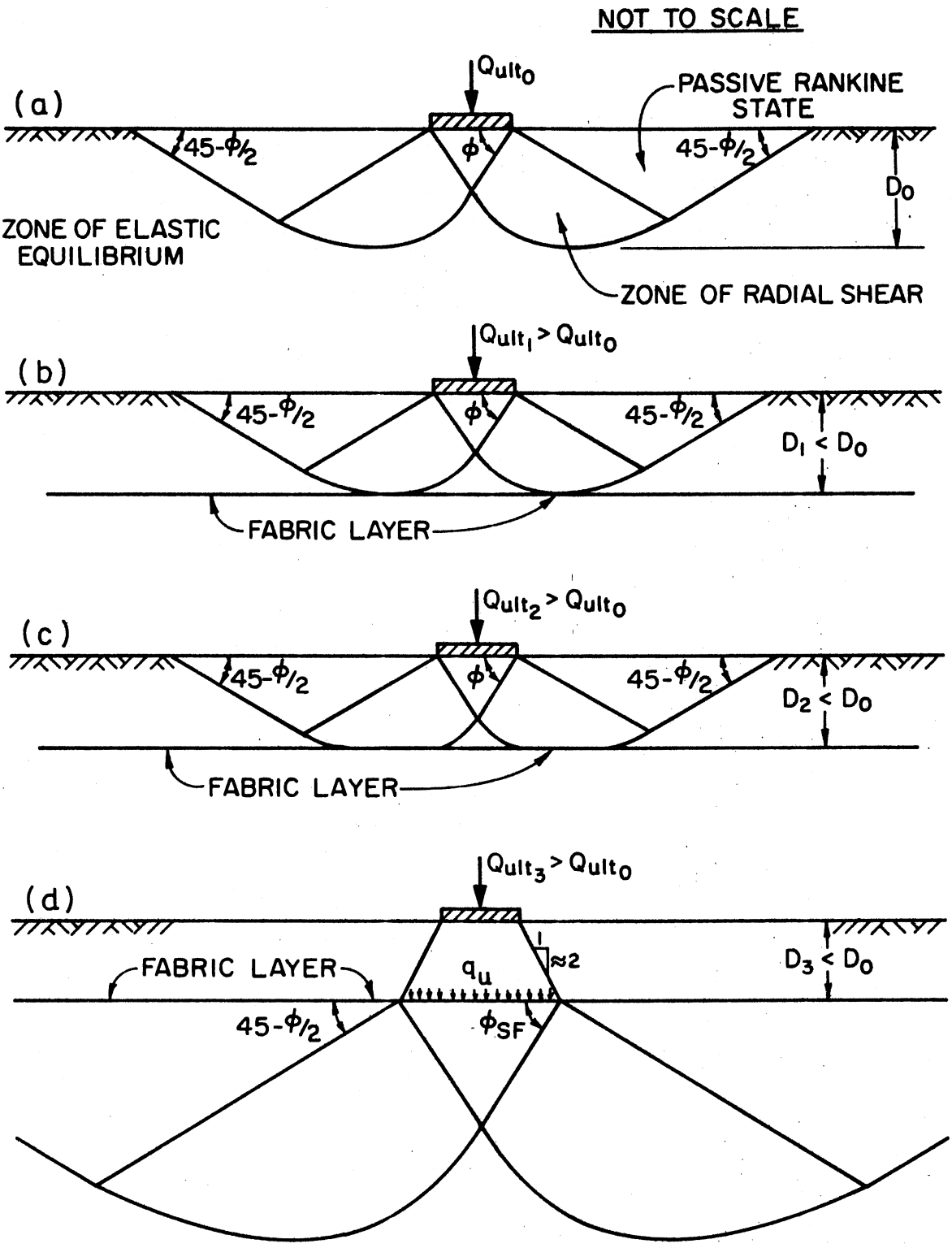

Figure 20. Typical General Shear Bearing Failures. (a) Terzaghi's Conceptual of General Shear Failure Beneath a Strip Footing. (b), (c), and (d) Possible Types of General Shear Failure for a Soil-Fabric System.

tensile stresses developed from applied loading will cause development of tensile strains which tend to maximize at or near the shear failure surface within the soil mass. Resistance to lateral restraint is only available through shearing resistance of the soil and may be calculated by multiplying the overburden pressure at the shear surface by the tangent of the frictional resistance value (ϕ) of the soil mass. A fabric layer installed in a position where tensile strains occur will restrain the soil mass, thus absorbing some tensile stresses which would normally be transmitted to the soil beneath and above the fabric.

Load bearing test results, shown in Figures 11 and 12, indicate that Bidim C-34 had slightly higher initial deformation moduli than the other three fabrics. Bidim C-34 also possessed the lowest initial elastic modulus, as shown in Figure 9, and the lowest soil-fabric frictional resistance. Since lateral restraint is directly related to soil-fabric friction and fabric tensile strength, this would infer the existence of an alternative reinforcement mechanism which causes the initial increase in the deformation modulus.

Membrane-type support occurs only after fabric has undergone sufficient deformation to cause the development of tensile stresses within the fabric. Vertical components of the tensile stresses then carry part of the applied load, and consequently the load is distributed over a larger area of the subgrade. This mechanism, while being responsible for reinforcement effects which occur with large deformations of soil-fabric systems, cannot be responsible for the increase in the initial deformation modulus, which occurred at small displacements.

With these conclusions in mind an explanation must be given which

explains the fabric reinforcement effects shown to exist by load bearing test results presented in Figures 11 through 18.

It is the author's theory that placement of the fabric within the zone of failure forces the shear path to change shape. Figure 21 shows what happens when the neutral wedge maintains its initial dimensions but the log spiral shear surface changes shape. The curve P represents relative passive resistances to shear failure, of each assumed log spiral failure surface. By drawing vertical lines from curve P to an intersection with line AA', failure patterns corresponding to a known resistance may be determined. For an unreinforced soil, a failure surface corresponding to the lowest resistance value shown on curve P will be assumed, and is represented in Figure 21 by the solid log spiral.

It is obvious that when fabric is placed within the region of shear failure, the normal shear failure pattern cannot be assumed. If the fabric layer is placed within this region but below the neutral wedge, four possible modes of failure exist, and three of these modes are shown in Figure 20. Figure 20b shows a pattern in which the log spiral shear surface is raised above the fabric. Figure 20c depicts a sliding failure along the fabric, and a pattern assumed for bearing failure below the fabric is shown in Figure 20d. The fourth mode of failure which may occur within a soil-fabric system is one in which the fabric tears or slips, however, with a proper design this should never occur and did not occur during load bearing testing.

For the four modes discussed above, the neutral wedge maintains original dimensions prior to incipient shear failure. Regardless of which alternative mode of failure occurs, it is obvious that the net result will be an increase in the initial deformation modulus of the soil.

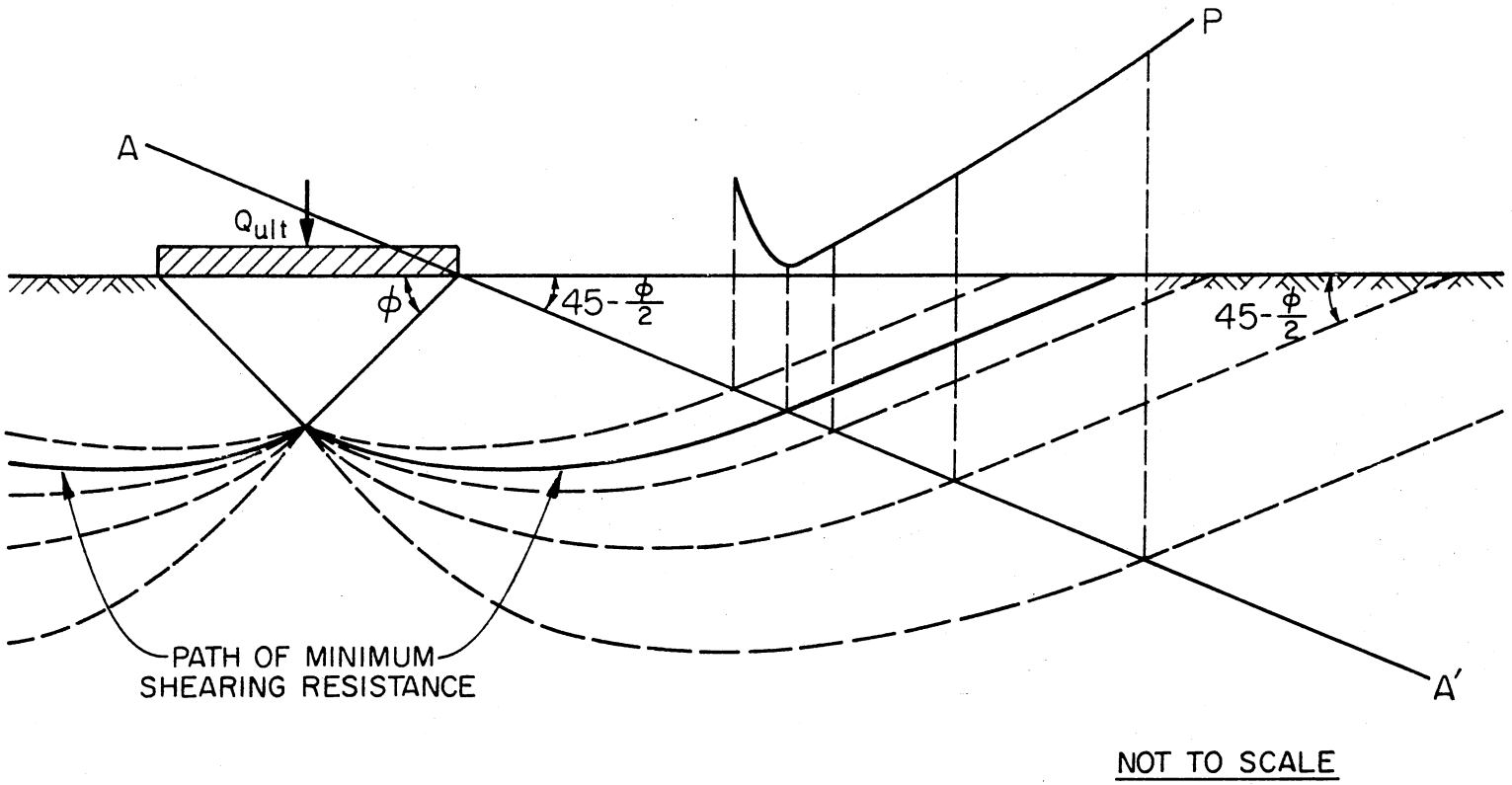

Figure 21. Effects of Changing Log Spiral Shear Failure Patterns, on the Ultimate Bearing Capacity of the System

Once the fabric is raised to a position such that it passes through the neutral wedge the forces still exist for a conventional shear failure which would normally occur in the region above and below the fabric, but this will be prevented by the fabric. (The damage to the Typar 3401 shown in Figure 19, was probably caused by forces transmitted by the neutral wedge.) The shear failure then must assume an entirely different shape than Terzaghi's conceptual view, unless shear failure occurs below the fabric. The pattern assumed by resulting shear failure cannot be visualized at this point but results from Figures 11 through 18 indicate that substantial reinforcement effects occur.

If adequate anchorage of fabric can be obtained such that no slippage will occur with the fabric in a relatively shallow position, the fabric can be placed in a position which may be termed "depth of maximum system reinforcement." From the deepest embedment depth that will result in fabric reinforcement, to the depth of maximum system reinforcement the soil will fail above the fabric. At the depth of maximum system reinforcement shear failure will be as likely to occur below the fabric as above it and at depths less than this shear failure will occur below the fabric.

Shear failure beneath the fabric will occur by distributing the load to the fabric layer and causing a general bearing shear failure such as that shown in Figure 20d, followed by development of membrane-type fabric support. This will likely occur when a failure such as that shown in Figure 20b or 20c would require greater shear forces than the failure depicted in Figure 20d.

The depth of maximum system reinforcement will not necessarily be the "optimum" embedment depth for the soil-fabric system. Though it is

desirable to place the fabric in a position for maximum strength at minimum deformations, this may not be practicable. Sufficient cover material must be placed to provide for adequate fabric anchorage and protection from fabric damage which might occur by aggregate actions, such as abrasion and puncture. The true optimum depth for fabric placement then, will be at the minimum depth possible with the provisions that:

1. This depth is not less than the depth of maximum system reinforcement,

2. Adequate fabric anchorage is provided for, and

3. Sufficient cover material exists for fabric protection.

It has been theorized above, that the increase in the initial deformation modulus of the soil-fabric system, over that for the no-fabric system, is the result of "interference with the shear failure pattern." An explanation for the remaining portion of the curves shown in Figures 11 through 18 must also be given.

The "flat" portion of the curve, occurring between the initial and second modulus, is representative of a general shear failure of the system. The second modulus, depending upon fabric location, may be caused by one of several phenomena.

As shear failure occurs above the fabric, the soil is in a state of plastic deformation, but as the shear surface approaches the fabric, the soil is forced back into a state of elastic deformation. A new shear path must be assumed once the soil returns to a state of elastic deformation, and the second modulus may be representative of this phenomenon. Also, the soil-fabric system may undergo several of these transformations before developing a load sufficient to induce shear failure below the fabric.

Shear failure below the fabric layer will be accompanied by the development of membrane-type support. Once this occurs, a "final" deformation modulus will occur and control the system deformations. If the fabric is stressed to failure, all reinforcing effects will be eliminated and the soil-fabric system will behave as a "no-fabric" system.

The number of deformation moduli which may occur in a soil-fabric system will vary with site conditions. Other than "site-specific" conditions, controlling factors will include fabric embedment depth and size of loaded area. The only effect which fabric will have on the system, is with respect to the "final" deformation modulus. High fabric tensile moduli and high ultimate fabric strengths will distribute higher loads over a much larger area than will "weak" fabrics, and result in higher ultimate bearing capacities. In most cases however, all fabrics placed at the "optimum" embedment depth will provide essentially the same reinforcement for normal design loads.

CHAPTER V

CONCLUSIONS AND RECOMMENDATIONS

Conclusions

Literature Survey

As a result of the literature review, numerous points were noted and are stated below:

1. Prior to this research all reinforcing effects have been credited to the reinforcing mechanisms of lateral restraint and membrane-type action.

2. Little or no reinforcing effects have been noted from the majority of tests and case studies on soil-fabric systems until excessive deformations have occurred.

3. Most reinforcing effects of fabric have been measured as consequential effects from fabric being placed as a separation medium.

From the above points it may be concluded then that there exists a need for further testing of fabric in the reinforcing mode as opposed to separation mode. The identification of a mechanism by which substantial reinforcement may be achieved with minimal deflections will be of great importance to civil engineering construction technology and to the basic understanding of the behavior of fabrics.

Preliminary Fabric Testing

Most important points of interest noted from results of tension testing, creep testing, and direct shear testing have been noted in previous reports. The majority of the research project and thus results and discussions, dealt with load bearing tests. Several important points noted from preliminary testing should, however, be restated:

1. Direct shear testing results indicated the need for realistic normal loading to be used during direct shear testing, when ϕ_{SF} is an important design parameter.

2. Creep testing results indicated that no estimates of fabric creep tendencies can be assumed, based upon manufacturing process or fabric chemical composition.

Load Bearing Tests

Interpretation of the results of load bearing tests resulted in many important observations with regard to fabric reinforcement mechanisms and fabric behaviors. These conclusions are listed below, not necessarily in order of importance:

1. Fabric placed in a reinforcement mode shows definite improvement over reinforcement effects noted for fabric when placed at depths more representative of those found when fabric is placed in the separation mode.

2. Results vary with fabric embedment depth.

3. An embedment depth exists which will provide minimum deformation with maximum reinforcement; this depth is termed: "depth of maximum system reinforcement."

4. The mechanism responsible for this behavior has been identified

as one different from previously defined mechanisms and is termed "interference with shear failure surface patterns."

5. The behavior of the soil-fabric system with the fabric placed in the reinforcement mode is one in which there is an initial deformation modulus greater than that for the no-fabric system, followed by a slight shear failure for the material above the fabric, and then a second deformation modulus which may be attributed to additional elastic deformation of the soil.

6. The depth of embedment for maximum system reinforcement is independent of whether the strength gain desired is contained in the bounds of the first or a subsequent modulus.

7. The optimum fabric embedment depth for utilizing this reinforcing mechanism in road, airport runway, or other foundation construction, is the minimum depth which can be achieved providing:

   a. A depth not less than the depth of maximum system reinforcement,
   b. Adequate anchorage, and
   c. Sufficient cover material for fabric protection.

From the above conclusions it is obvious that the net results of this research is identification of a reinforcing mechanism not previously identified but one that is of primary importance for the use of fabric as reinforcement.

Recommendations for Further Research

Limiting factors of this testing procedure are as follows:

1. Fabric prestressing was limited in this study.
2. Only one soil in one condition was used.

3. Only four fabrics were used in the test procedure.

4. Only two sizes of loading plates were used.

5. The loading apparatus as designed was not capable of applying loads at the very small increments needed to better delineate the transition period from the initial modulus to second modulus (if important).

6. No cyclic loading was performed.

Considering the above shortcomings of the testing program it is recommended that the testing apparatus be fine-tuned so that it will be functionable for the application of small load increments. Additionally, tests should be performed on a wide range of soil conditions and fabrics. The effects of cyclic loading should be evaluated so that future recommendations on the selection of fabrics may be made with regard to these items. Pretensioning should be performed over a wide range for various fabrics so that the effects of prestressing or lateral restraint may be observed.

BIBLIOGRAPHY

1. Holtz, Robert B., "Reinforced Earthworks Mechanics." Final Technical Report, National Science Foundation Grant No. ENG 74-17810, School of Civil Engineering, Prudue University, West Lafayette, Indiana, August, 1978.

2. Jessberger, H. L., "Load-Bearing Behavior of a Gravel Subbase-Non-Woven Fabric-Soft Subgrade System." Proceedings, International Conference on the Use of Fabrics in Geotechniques, Paris, Vol. I, April, 1977, pp. 9-13.

3. Giroud, Jean-Pierre and Laure Noiray, "Design of Geotextile-Reinforced, Unpaved Roads." Preprint of Proceedings, Specialty Session on Geotextiles, American Society of Civil Engineers National Meeting, Portland, Oregon, April, 1980.

4. Fowler, J., T. A. Haliburton, and J. P. Langan, "Analysis of Fabric-Reinforced Embankment Test Section at Pinto Pass, Mobile, Alabama." Technical Report, Dredging Operations Technical Support Project, Enviornmental Laboratory, U. S. Army Engineer Waterways Experiment Station, Vicksburg, Mississippi, January, 1980.

5. Sorlie, A., "The Effect of Fabrics on Pavement Strength-Plate Bearing Tests in the Laboratory." Proceedings, International Conference on the Use of Fabrics in Geotechniques, Vol. I, Paris, 1977, pp. 15-18.

6. Kinney, T. C. and E. J. Barenberg, "Mechanisms by Which Fabric Stabilizes Aggregate Layers on Soft Subgrades." Miscellaneous Paper, Geotechnical Laboratory, U. S. Army Engineer Waterways Experiment Station, Vicksburg, Mississippi, February, 1978.

7. Bender, David A. and Ernest J. Barenberg, "Design and Behavior of Soil-Fabric-Aggregate Systems." Preprint of Paper Presented at 57th Annual Meeting of Transportation Research Board, Washington, D. C., January, 1978.

8. Haliburton, T. A., C. C. Anglin, and Jack D. Lawmaster, "Selections of Geotechnical Fabrics for Embankment Reinforcement." School of Civil Engineering, Oklahoma State University, Stillwater, Oklahoma, May, 1978.

9. Haliburton, T. A., C. C. Anglin, and Jack D. Lawmaster, "Testing of Geotechnical Fabrics for Use as Reinforcement." Geotechnical Testing Journal, American Society for Testing Materials, Philadelphia, Vol. I, No. 4, December, 1978, pp. 203-212.

APPENDIX A

PHOTOGRAPHS AND STRESS-STRAIN DATA FOR FABRIC TENSION TESTS

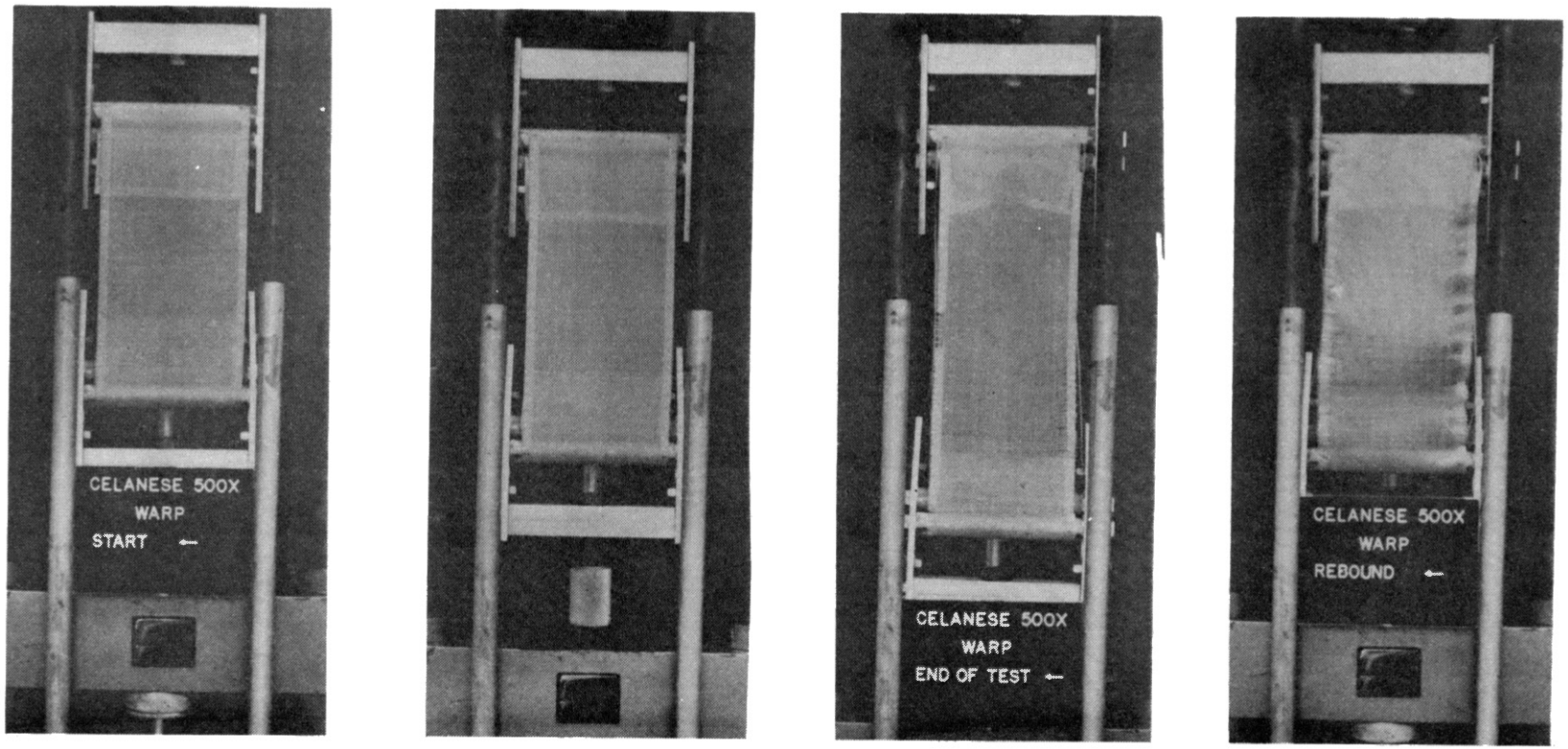

Figure 22. Photographs of Celanese 500X-Warp Direction in Tension Testing at (Left to Right) Start, 10 Percent Strain, Failure, and After "Elastic" Rebound

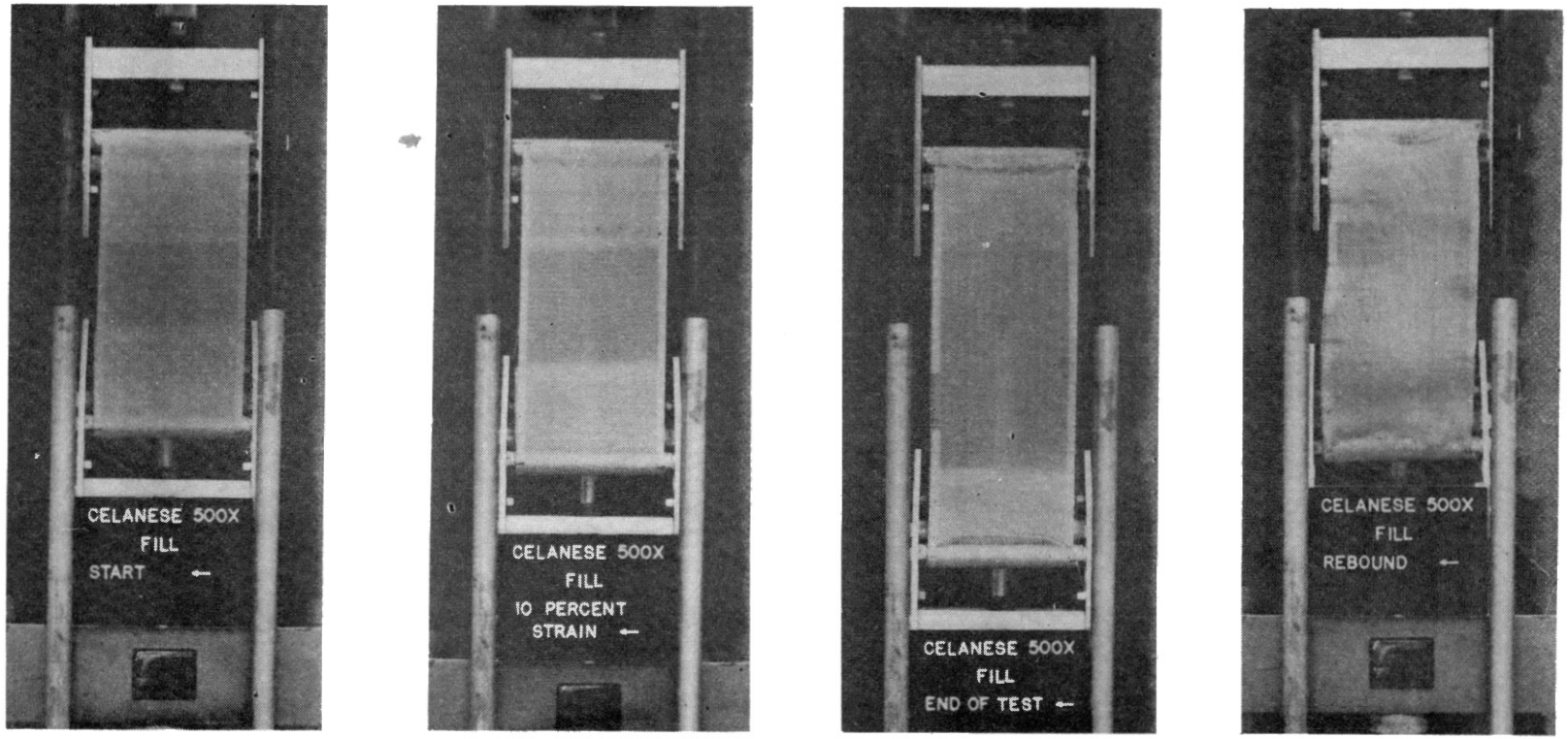

Figure 23. Photographs of Celanese 500X-Fill Direction in Tension Testing at (Left to Right) Start, 10 Percent Strain, Failure, and After "Elastic" Rebound

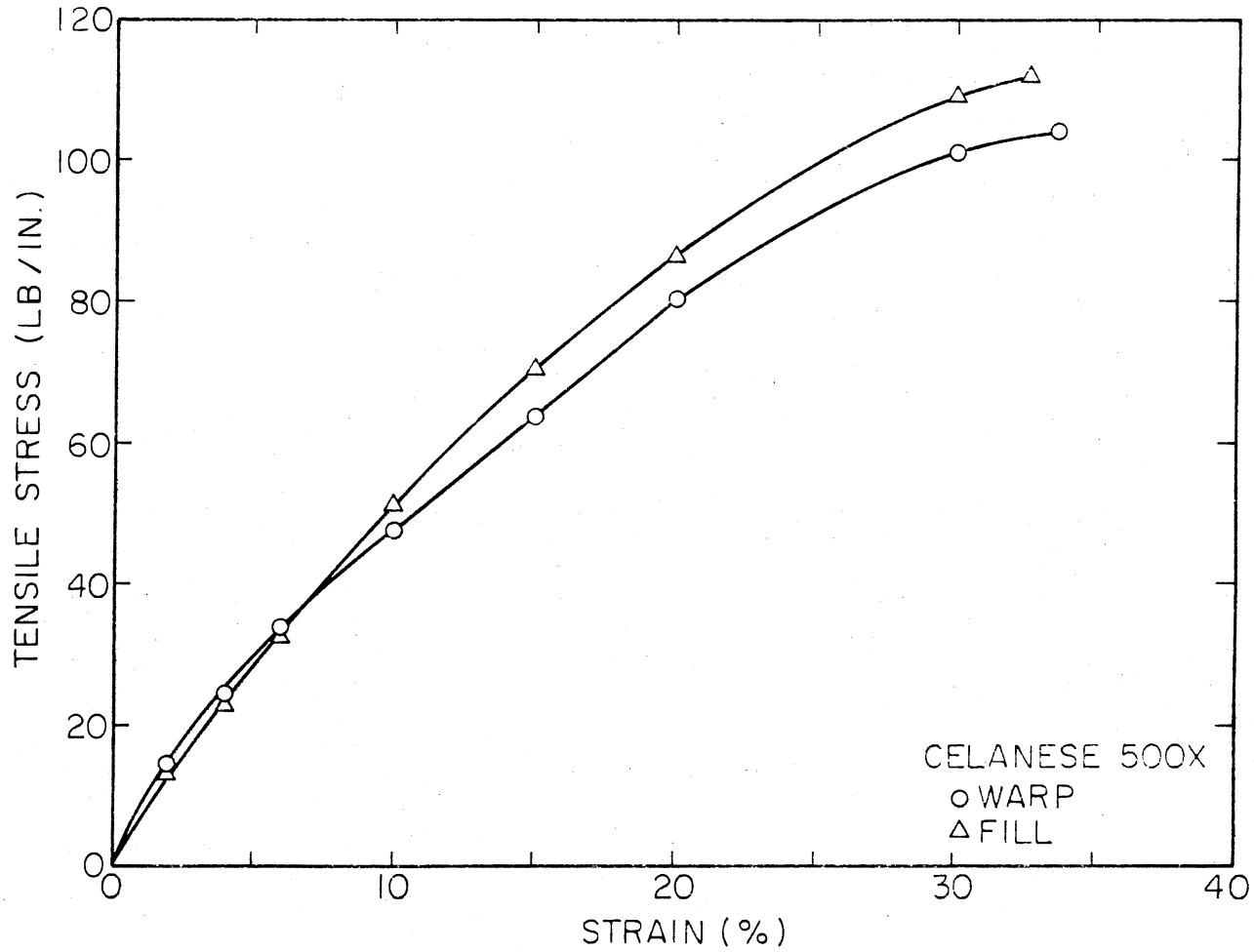

Figure 24. Stress-Strain Data for Celanese 500X in Uniaxial Testing

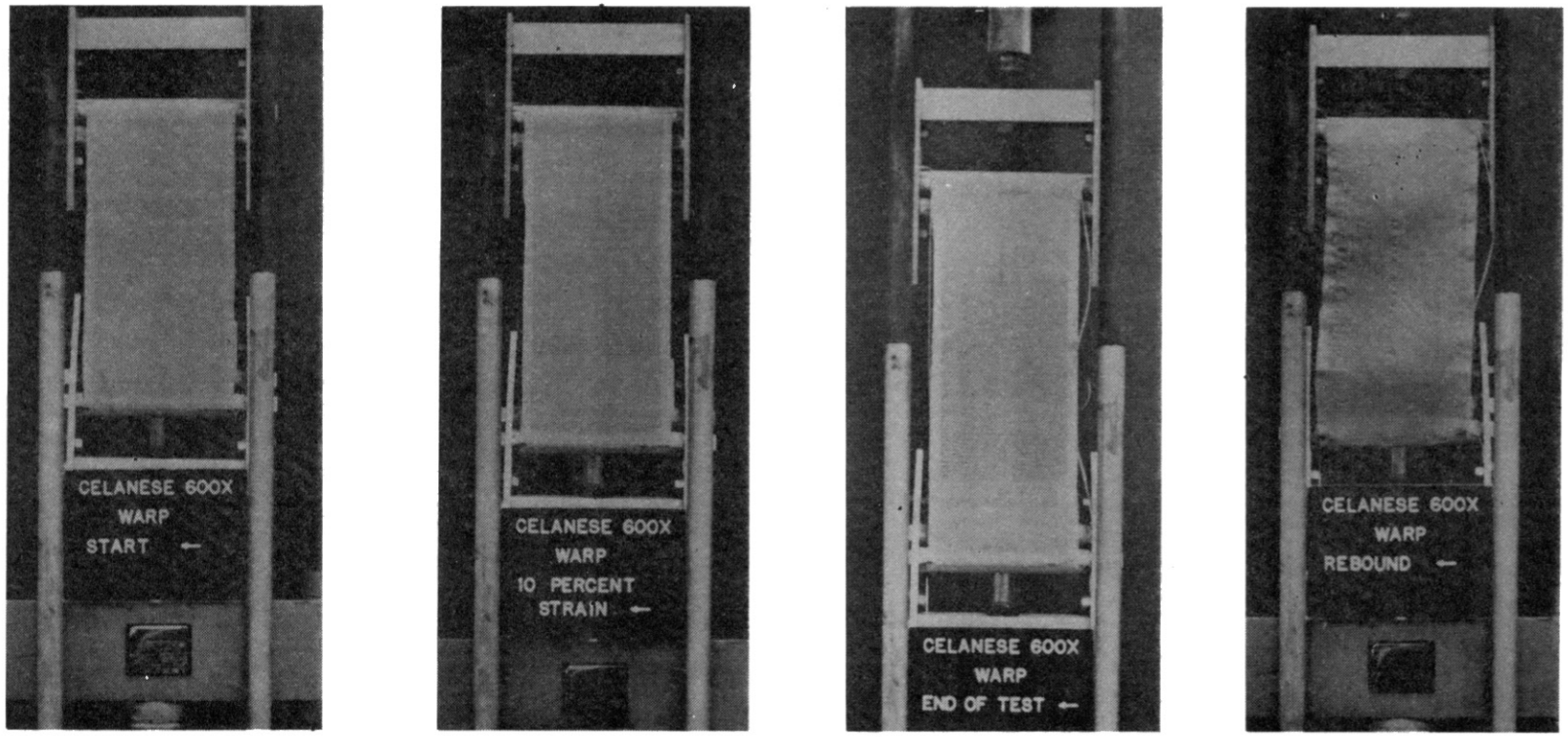

Figure 25. Photographs of Celanese 600X-Warp Direction in Tension Testing at (Left to Right) Start, 10 Percent Strain, Failure, and After "Elastic" Rebound

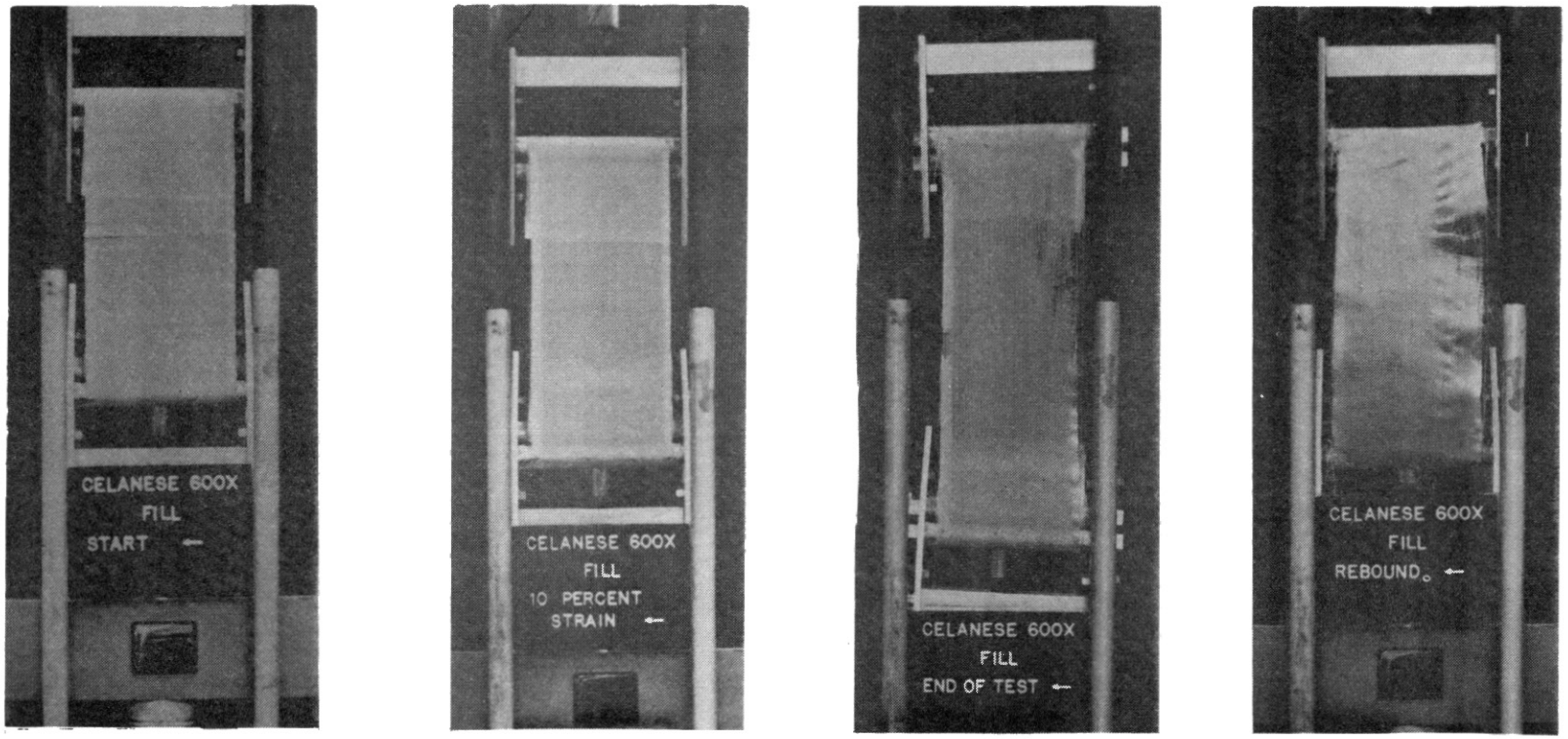

Figure 26. Photographs of Celanese 600X-Fill Direction in Tension Testing at (Left to Right) Start, 10 Percent Strain, Failure, and After "Elastic" Rebound

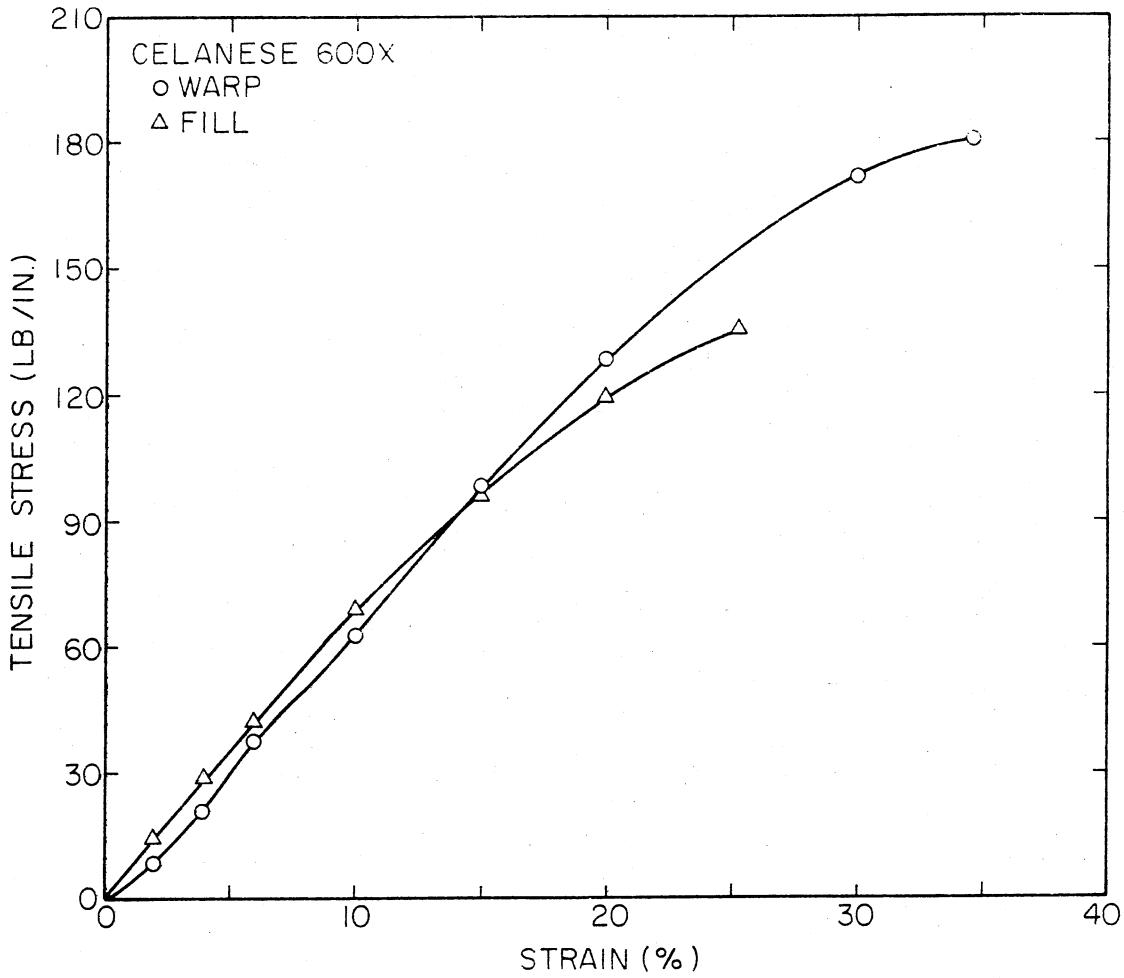

Figure 27. Stress-Strain Data for Celanese 600X in Uniaxial Testing

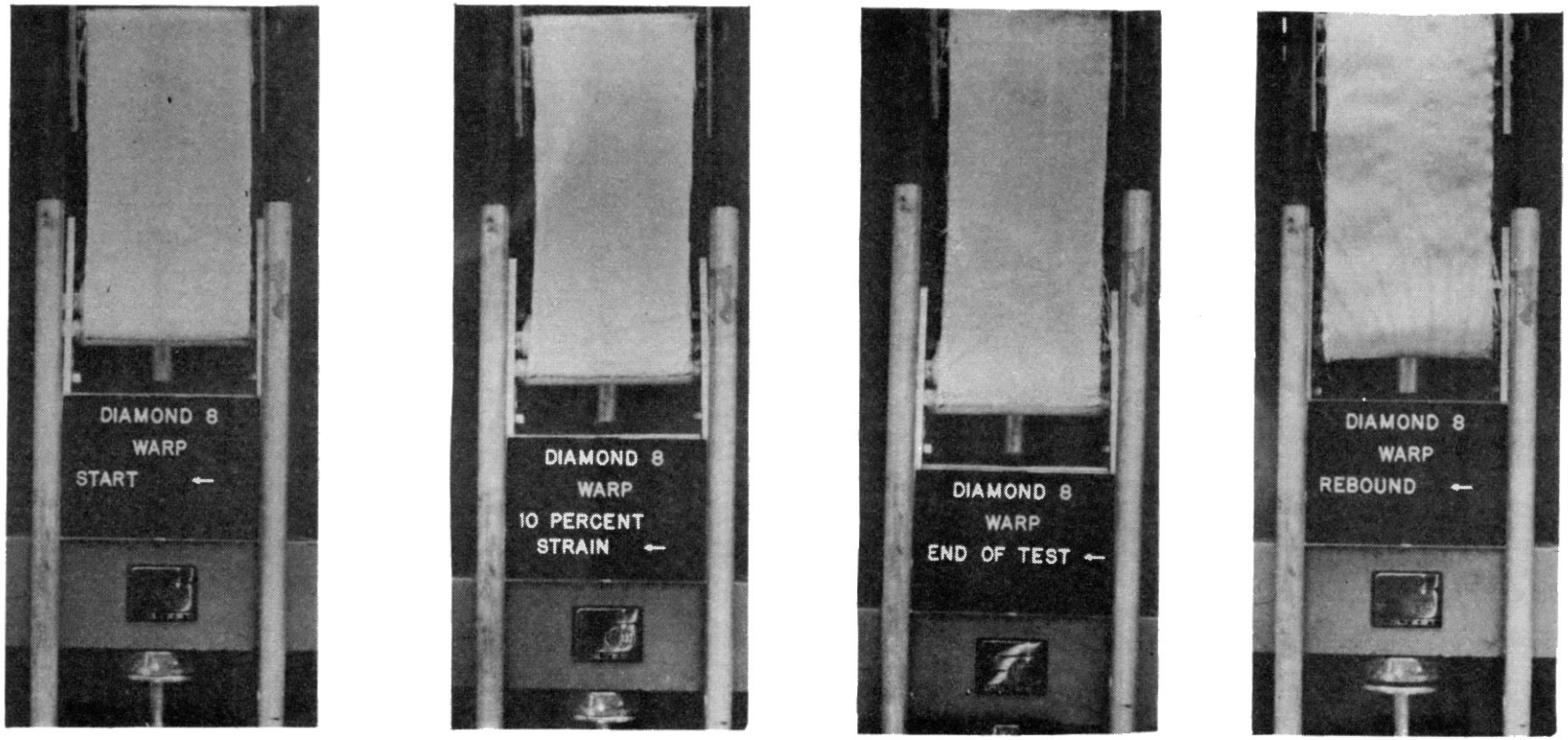

Figure 28. Photographs of Diamond 8-Warp Direction in Tension Testing at (Left to Right) Start, 10 Percent Strain, Failure, and After "Elastic" Rebound

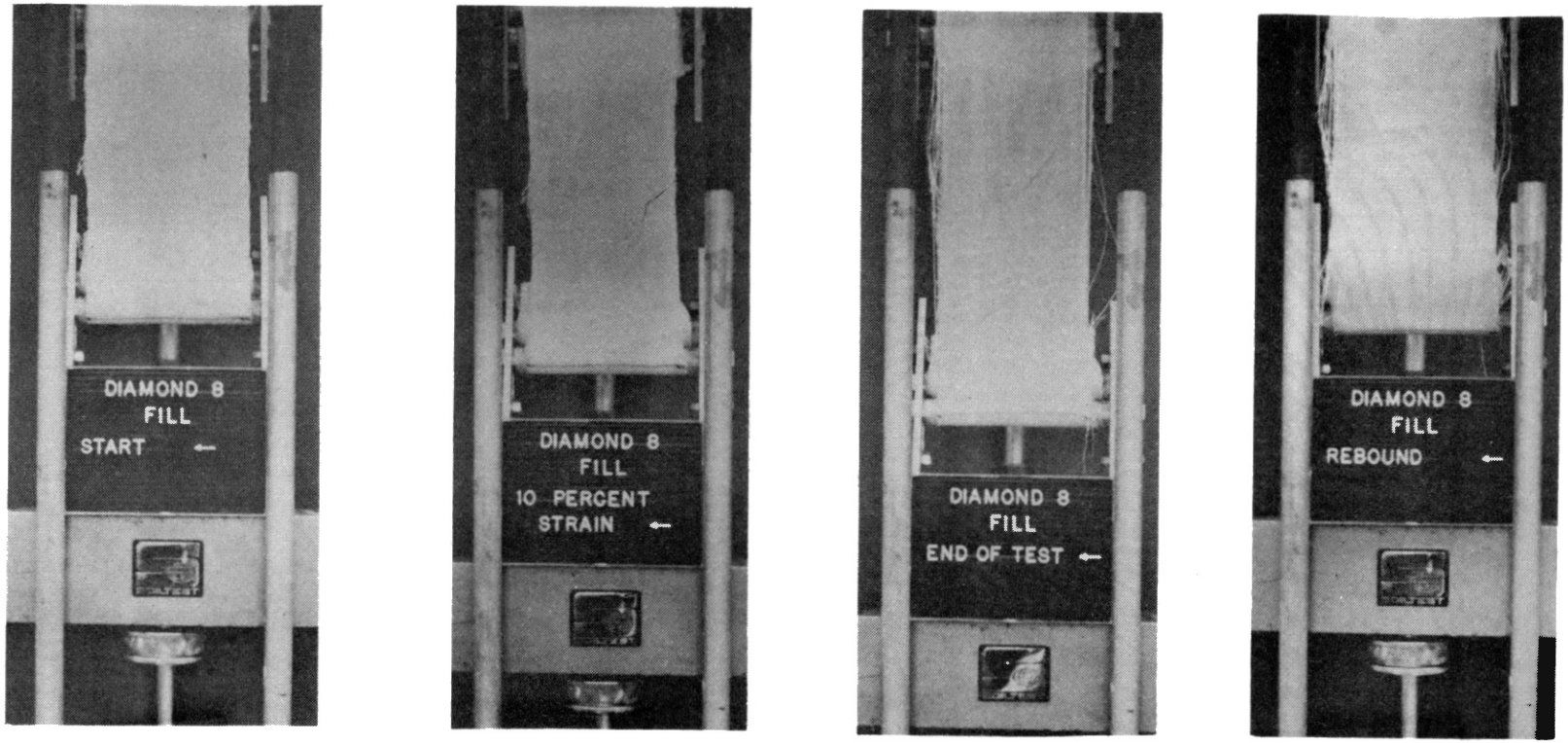

Figure 29. Photographs of Diamond 8-Fill Direction in Tension Testing at (Left to Right) Start, 10 Percent Strain, Failure, and After "Elastic" Rebound

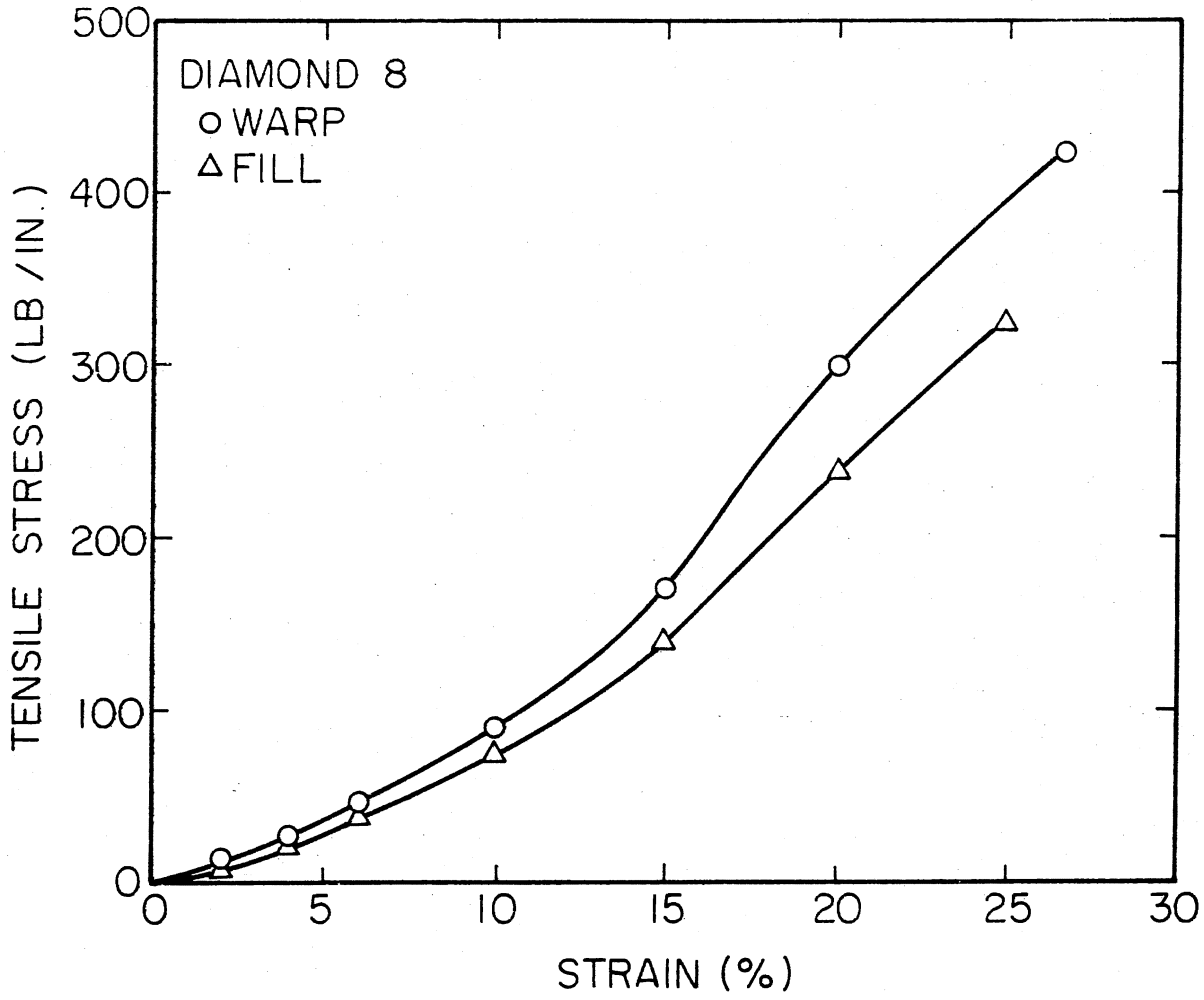

Figure 30. Stress-Strain Data for Diamond 8 in Uniaxial Testing

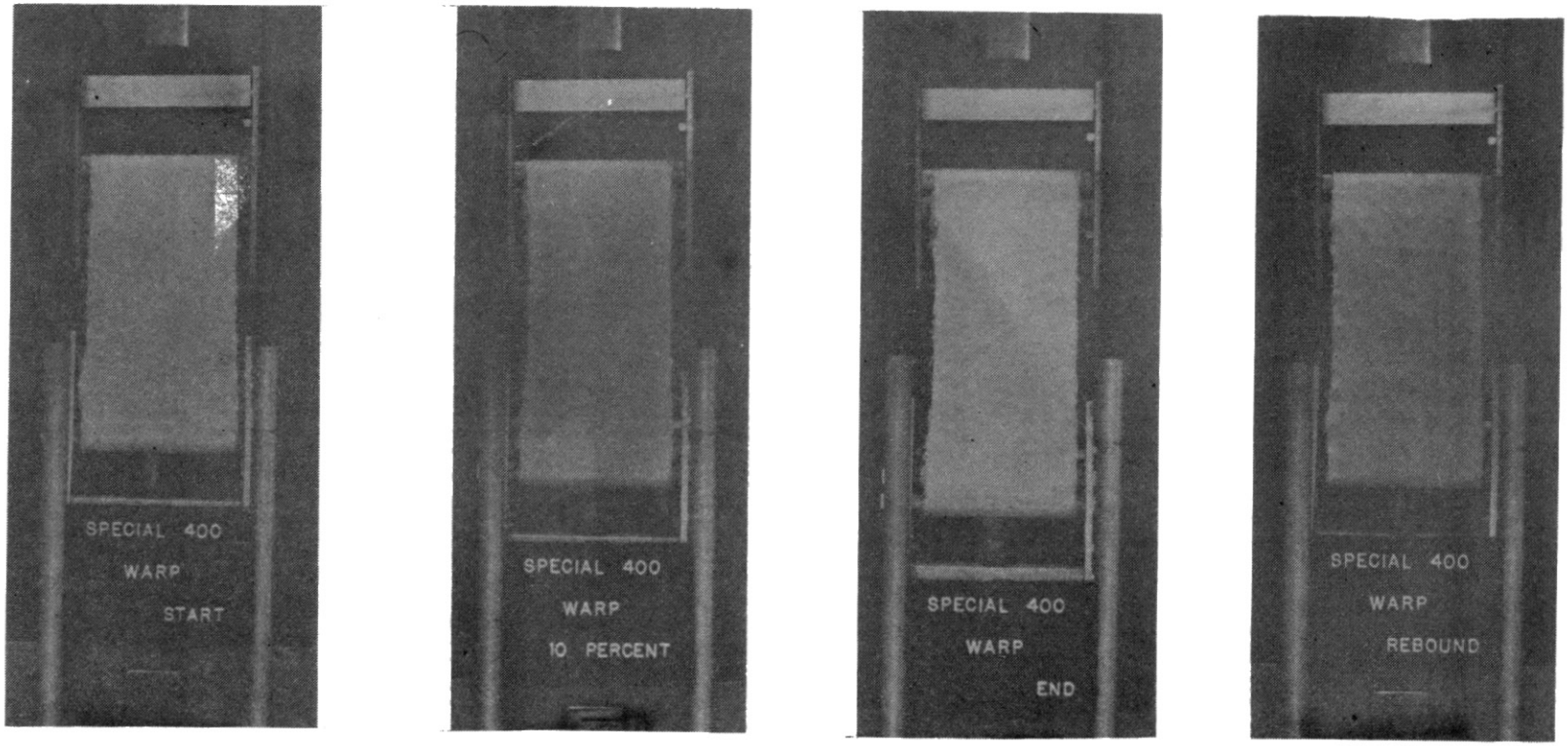

Figure 31. Photographs of Special 400-Warp Direction in Tension Testing at (Left to Right) Start, 10 Percent Strain, Failure, and After "Elastic" Rebound

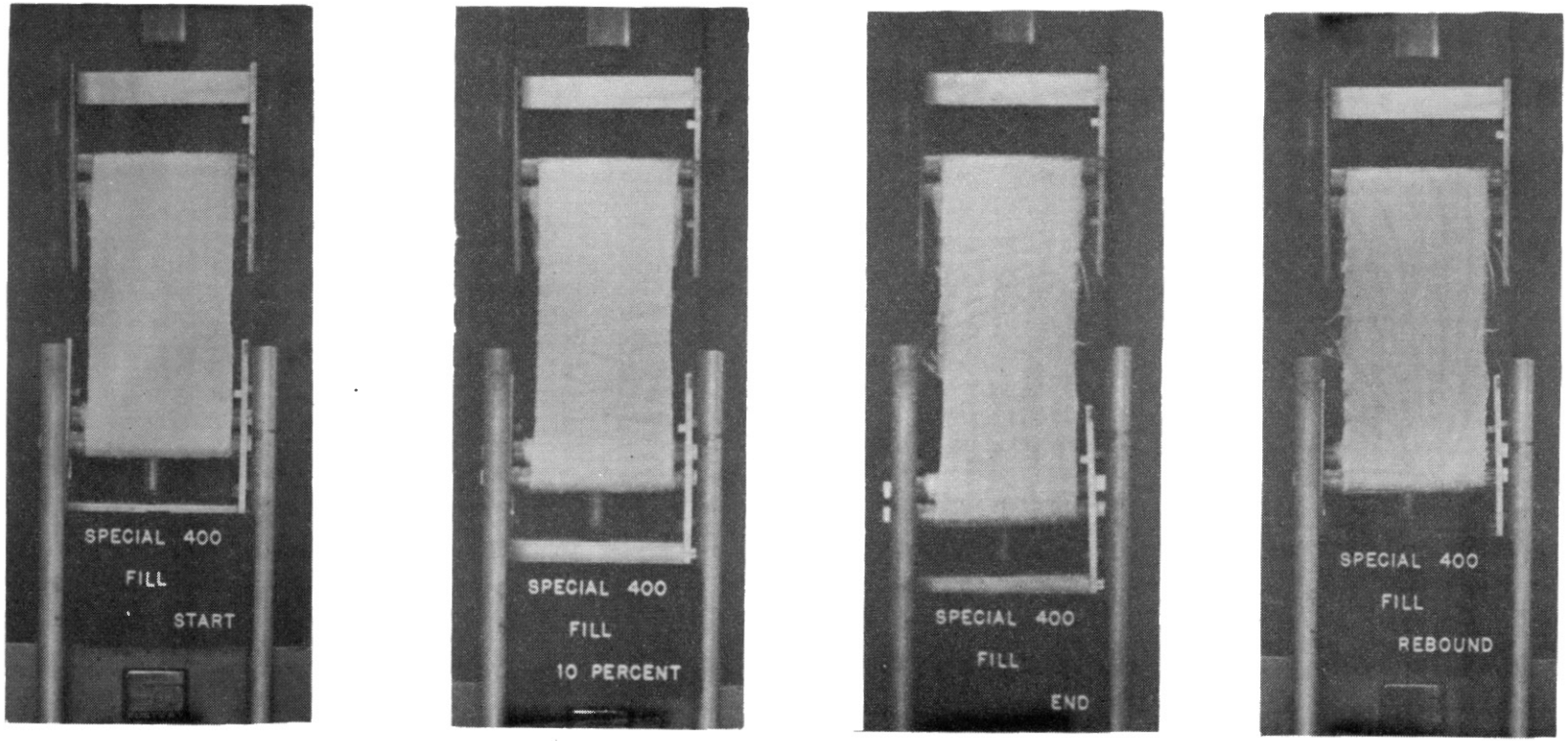

Figure 32. Photographs of Special 400-Fill Direction in Tension Testing at (Left to Right) Start, 10 Percent Strain, Failure, and After "Elastic" Rebound

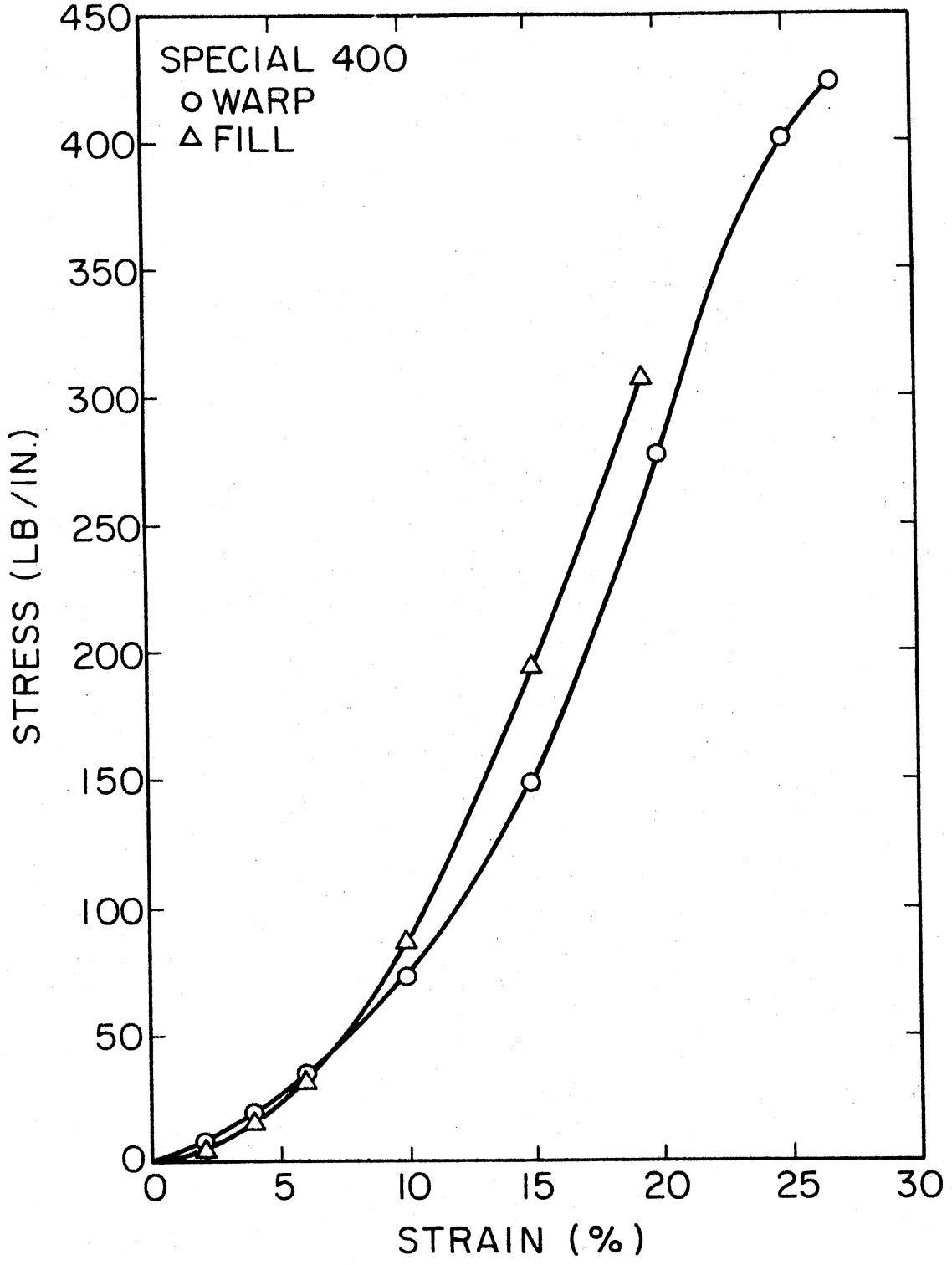

Figure 33. Stress-Strain Data for Special 400 in Uniaxial Testing

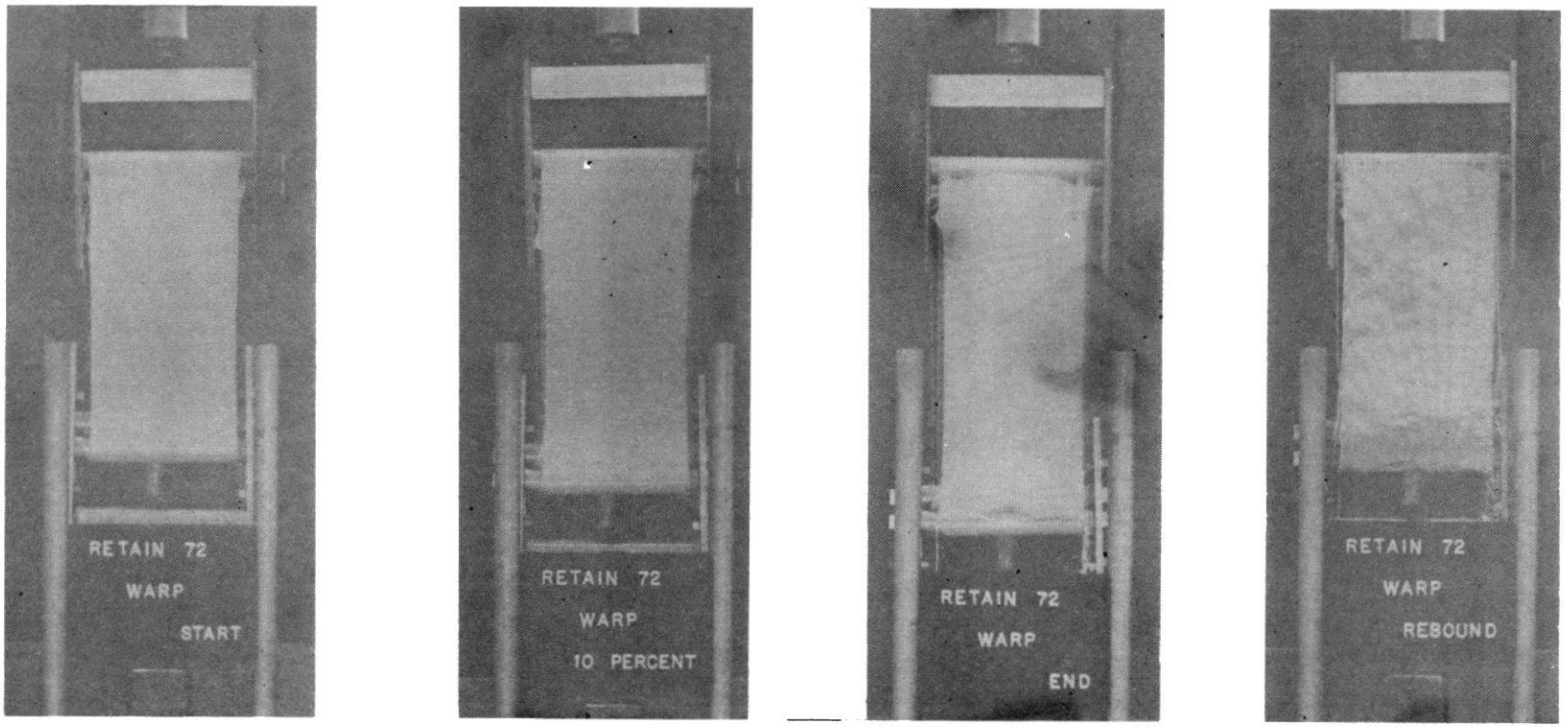

Figure 34. Photographs of Retain 72-Warp Direction in Tension Testing at (Left to Right) Start, 10 Percent Strain, Failure, and After "Elastic" Rebound

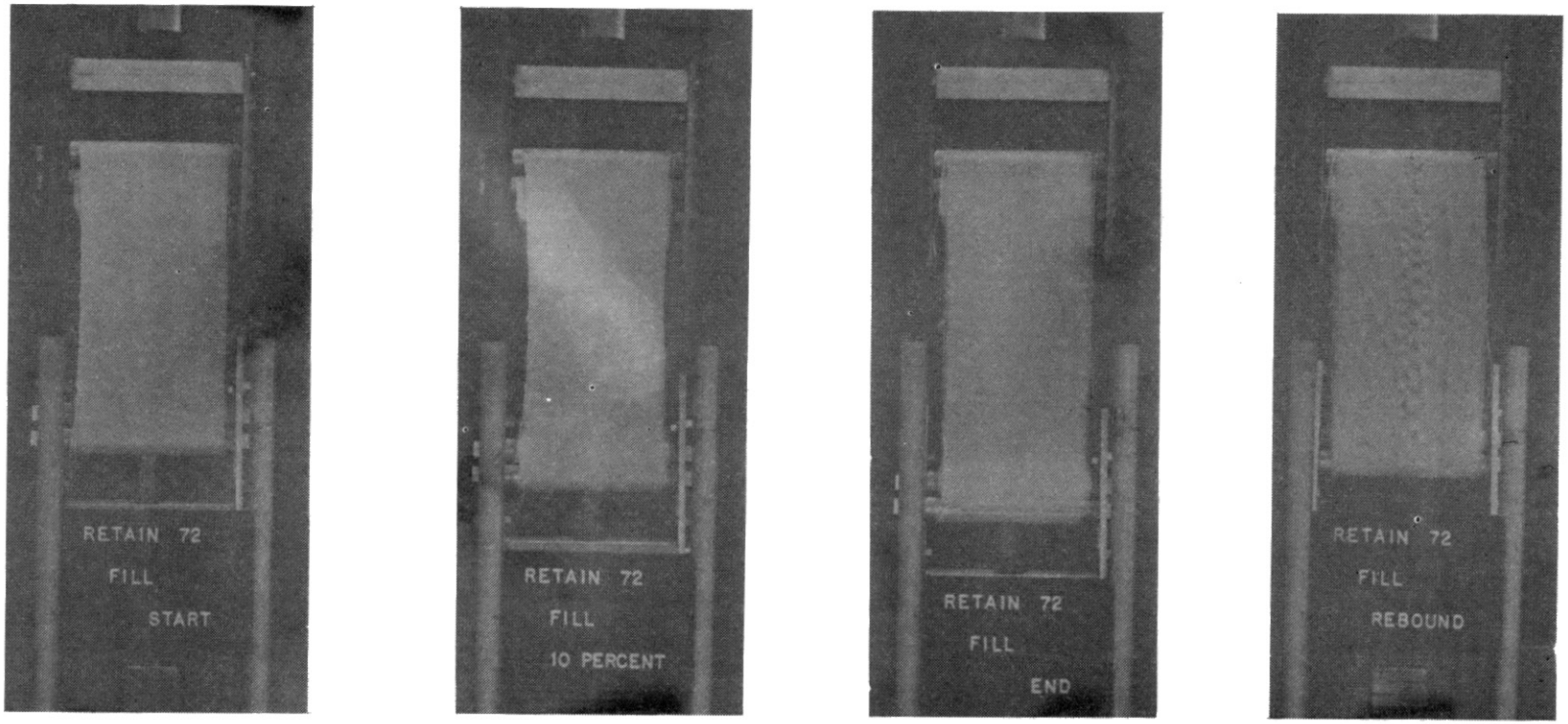

Figure 35. Photographs of Retain 72-Fill Direction in Tension Testing at (Left to Right) Start, 10 Percent Strain, Failure, and After "Elastic" Rebound

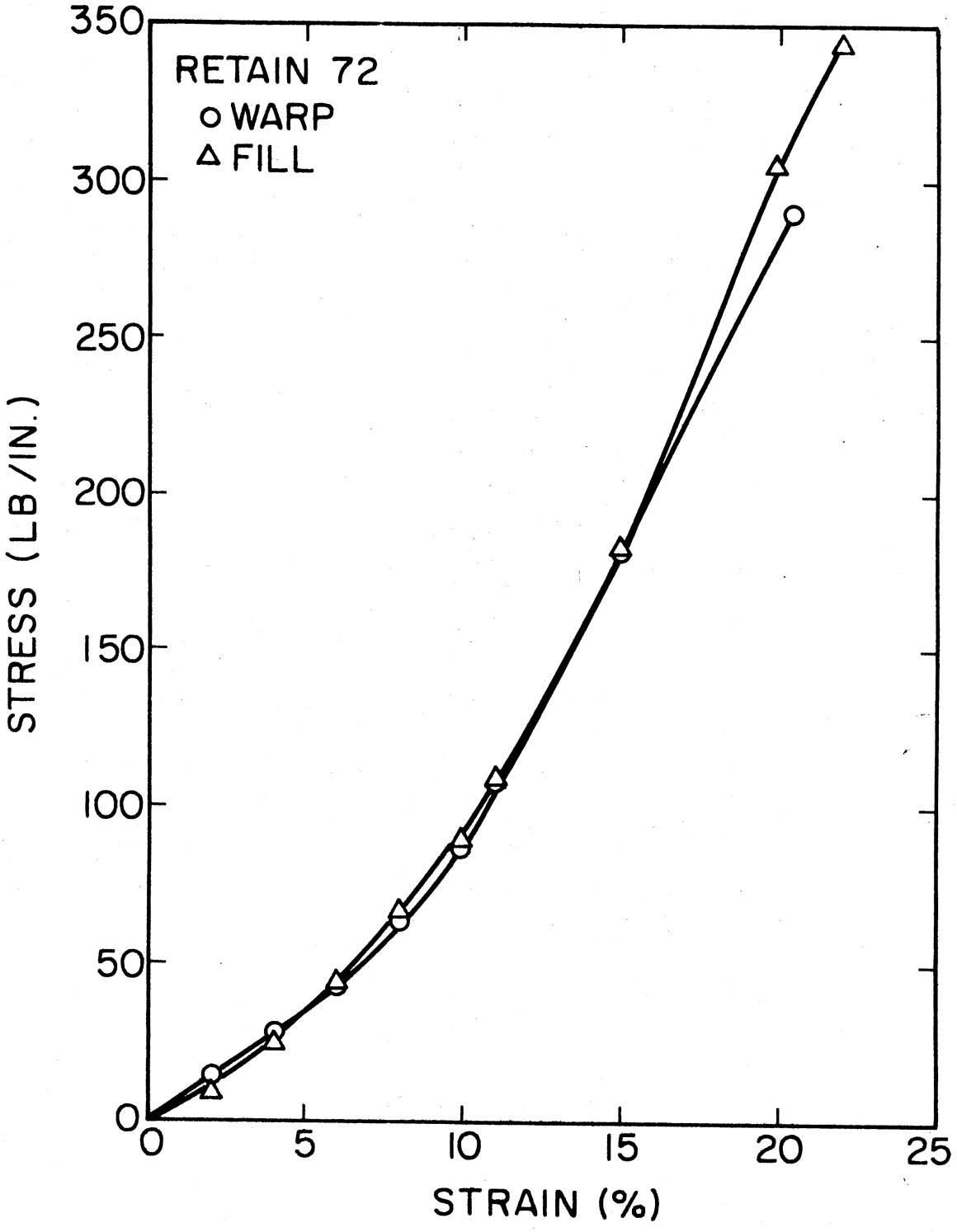

Figure 36. Stress-Strain Data for Retain 72 in Uniaxial Testing

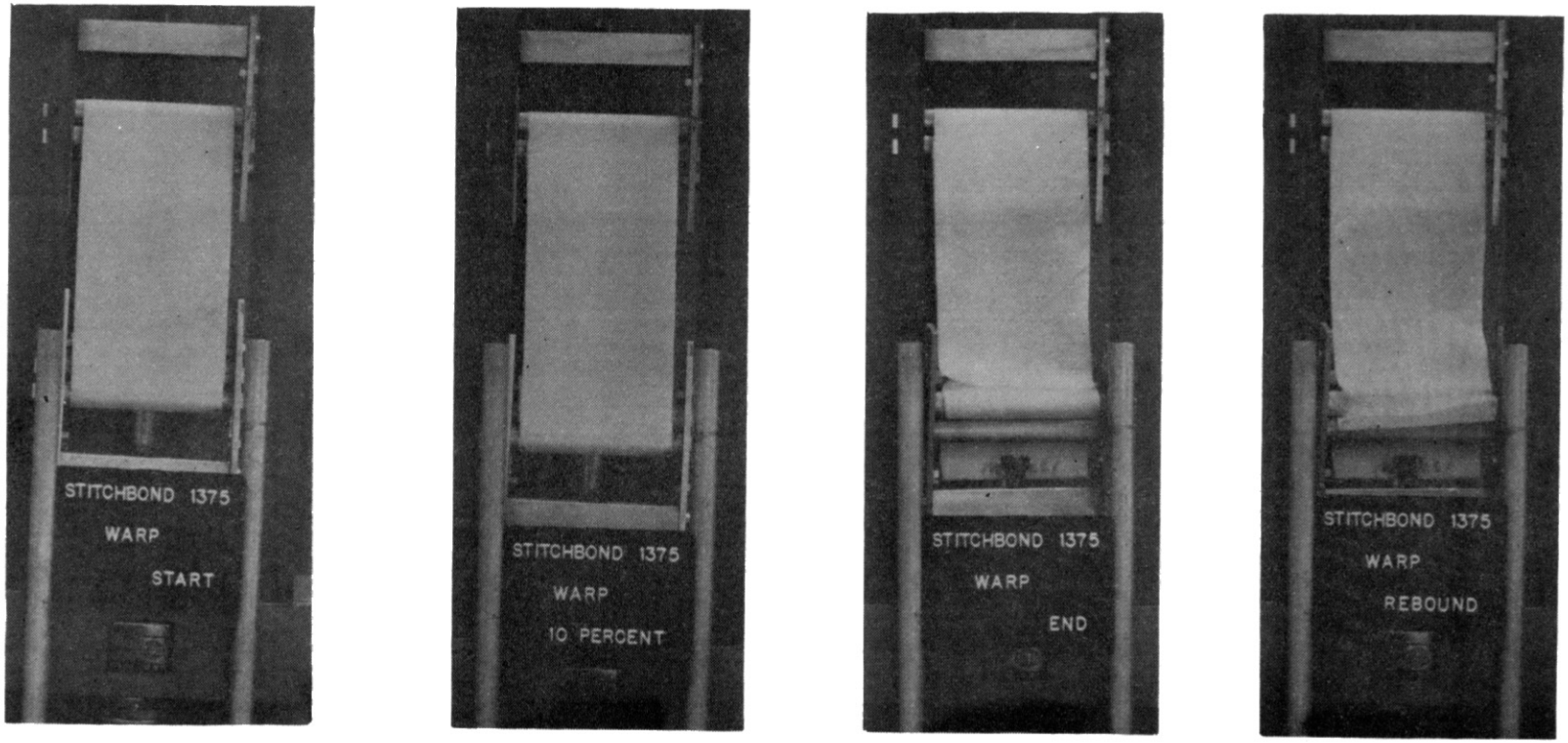

Figure 37. Photographs of Stitchbond 1375-Warp Direction in Tension Testing at (Left to Right) Start, 10 Percent Strain, Failure, and After "Elastic" Rebound

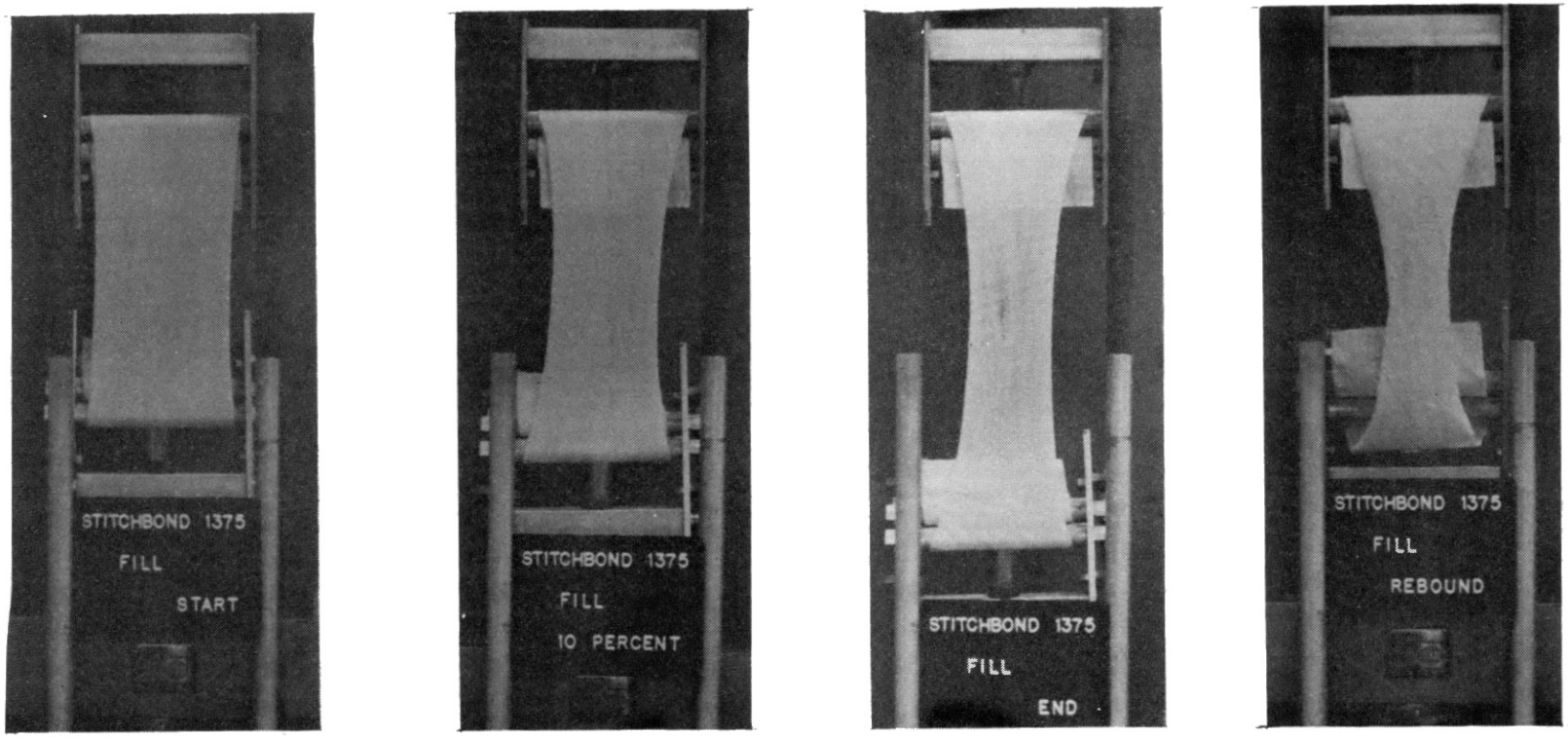

Figure 38. Photographs of Stitchbond 1375-Fill Direction in Tension Testing at (Left to Right) Start, 10 Percent Strain, Failure, and After "Elastic" Rebound

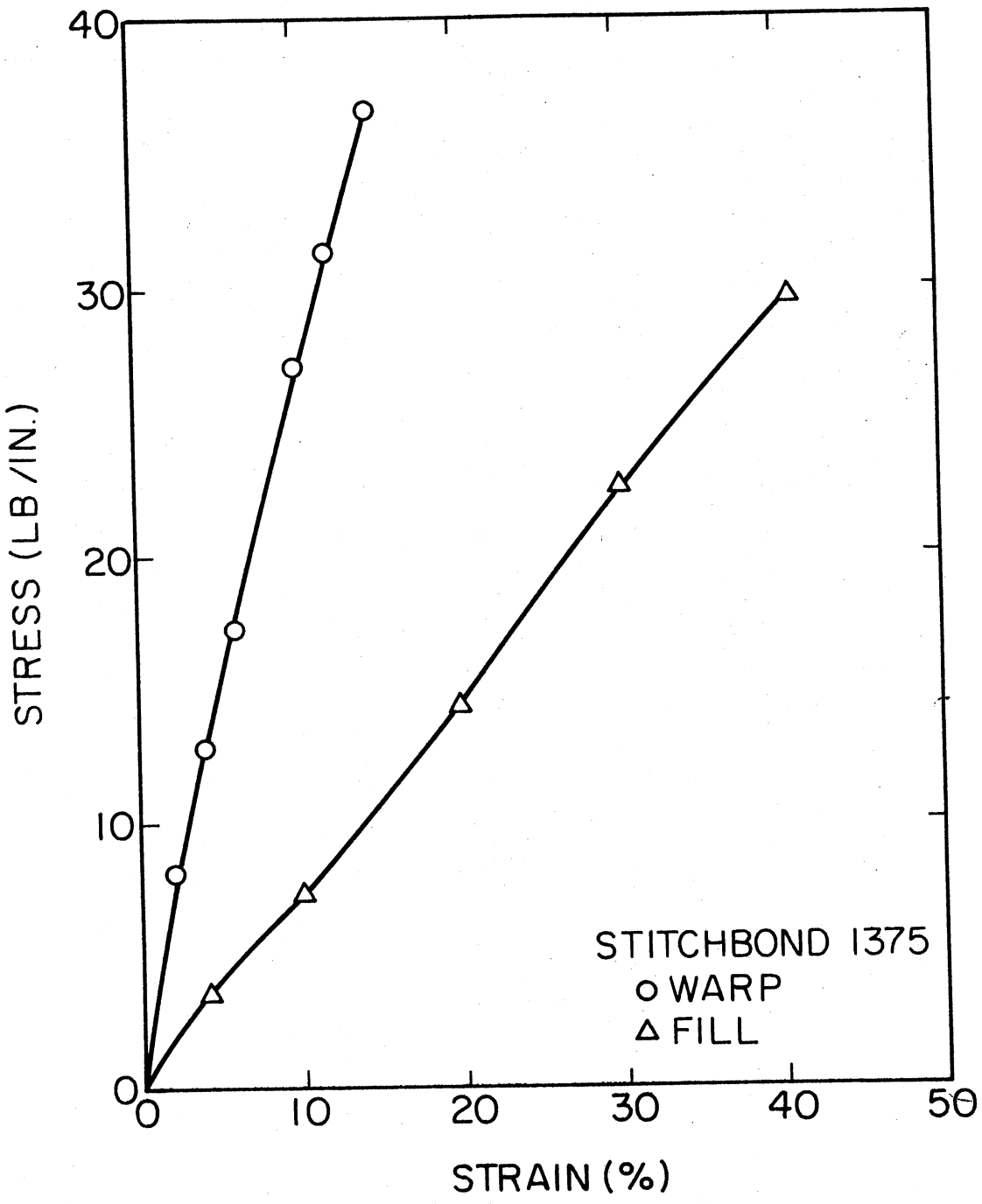

Figure 39. Stress-Strain Data for Stitchbond 1375 in Uniaxial Testing

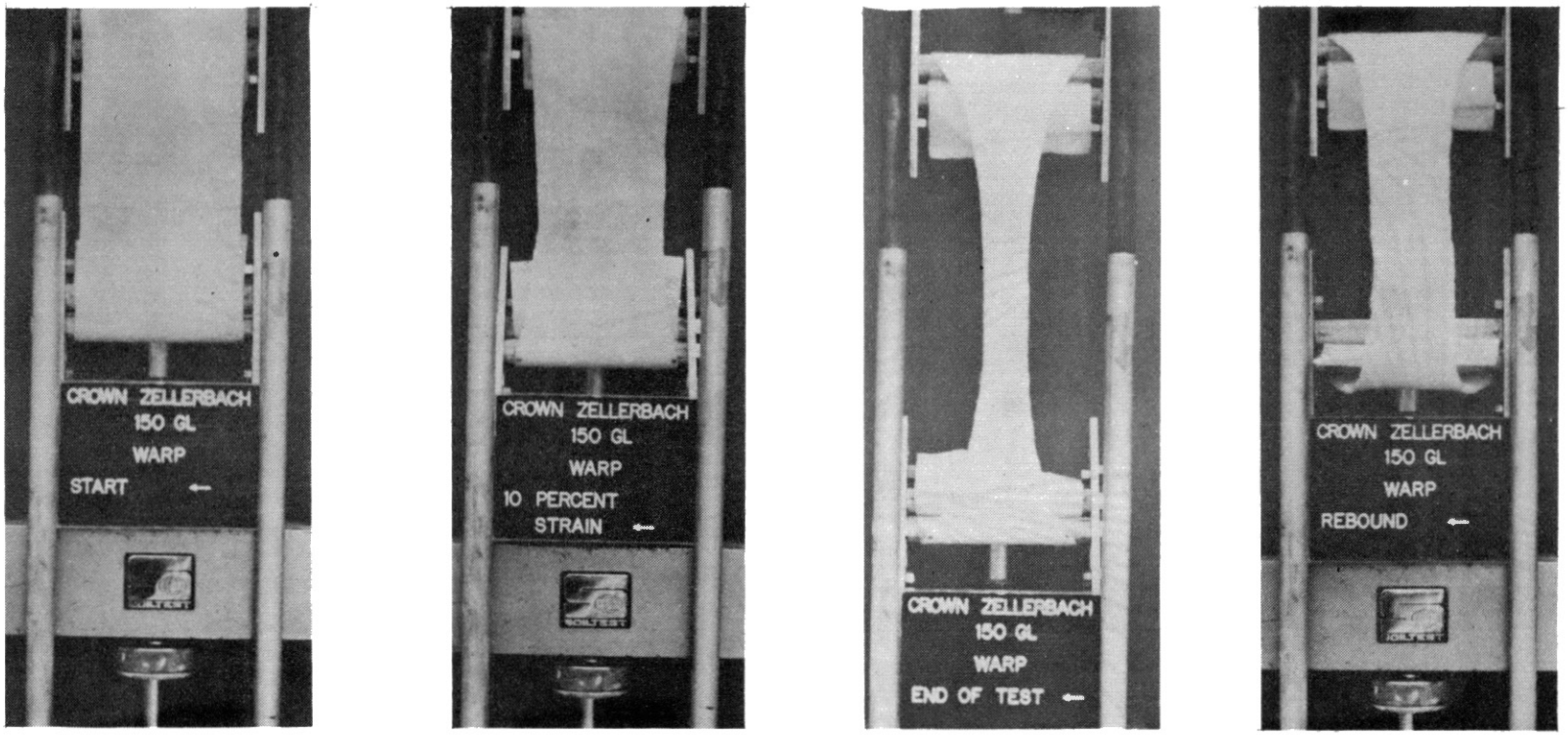

Figure 40. Photographs of Fibretex 150-Warp Direction in Tension Testing at (Left to Right) Start, 10 Percent Strain, Failure, and After "Elastic" Rebound

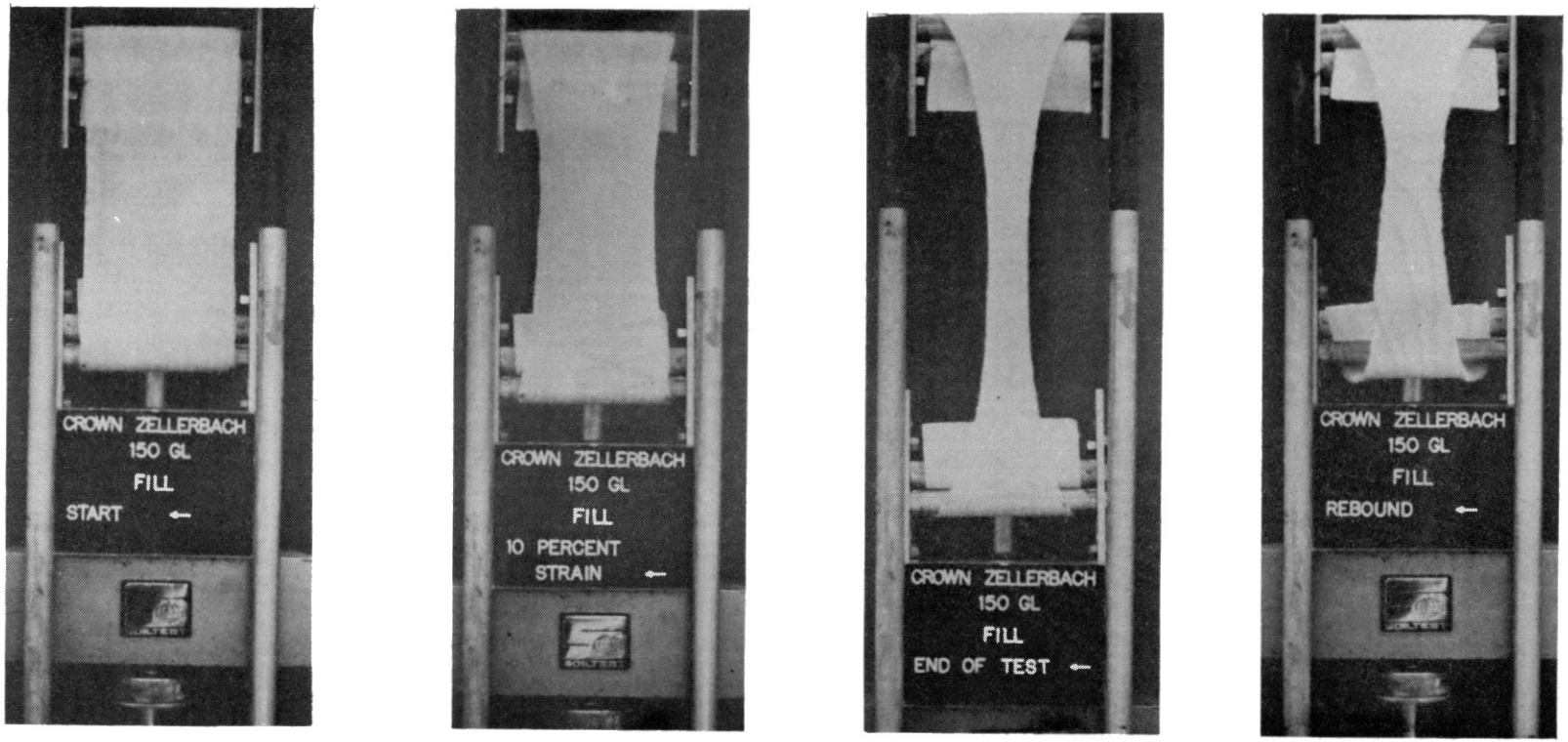

Figure 41. Photographs of Fibretex 150-Fill Direction in Tension Testing at (Left to Right) Start, 10 Percent Strain, Failure, and After "Elastic" Rebound

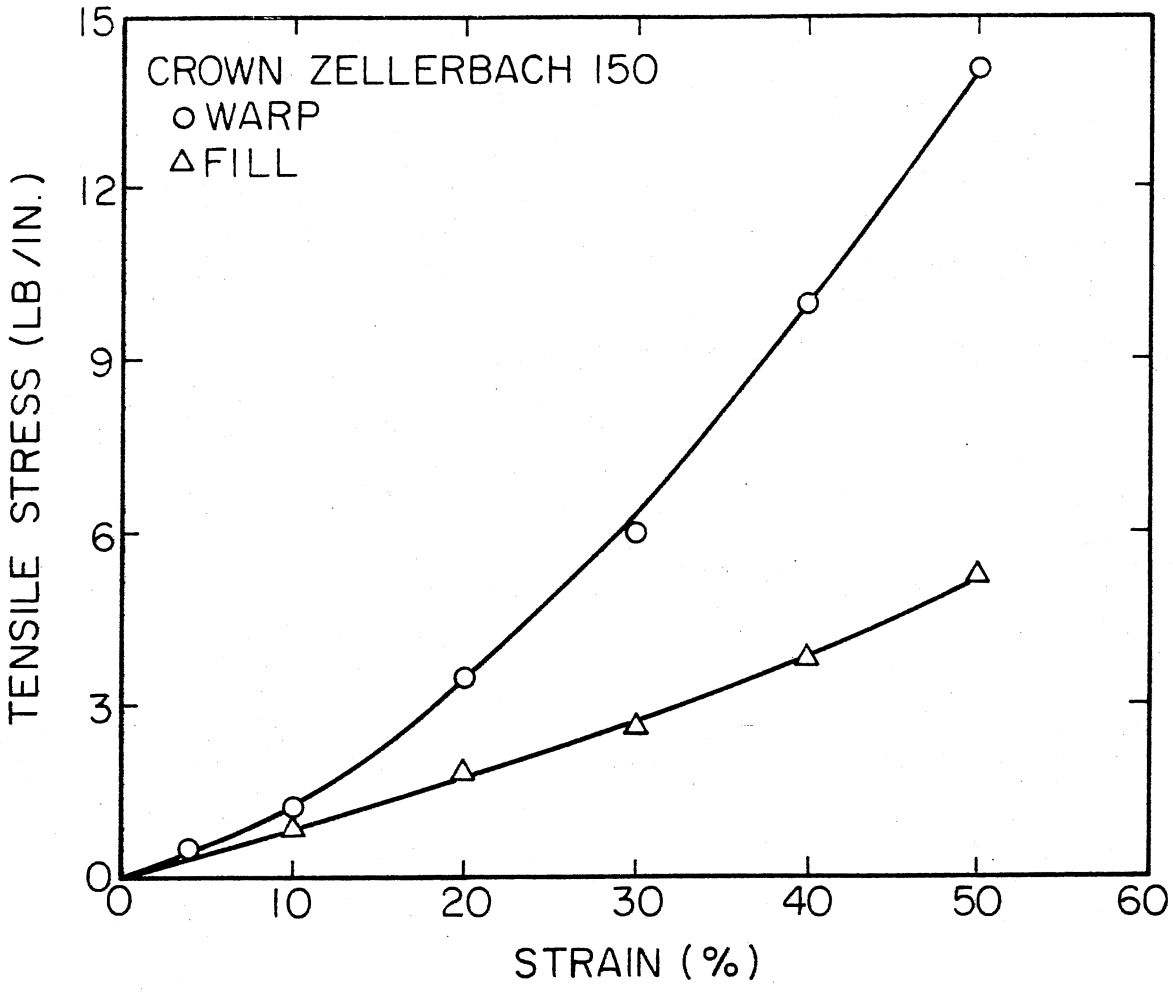

Figure 42. Stress-Strain Data for Fibretex 150 in Uniaxial Testing

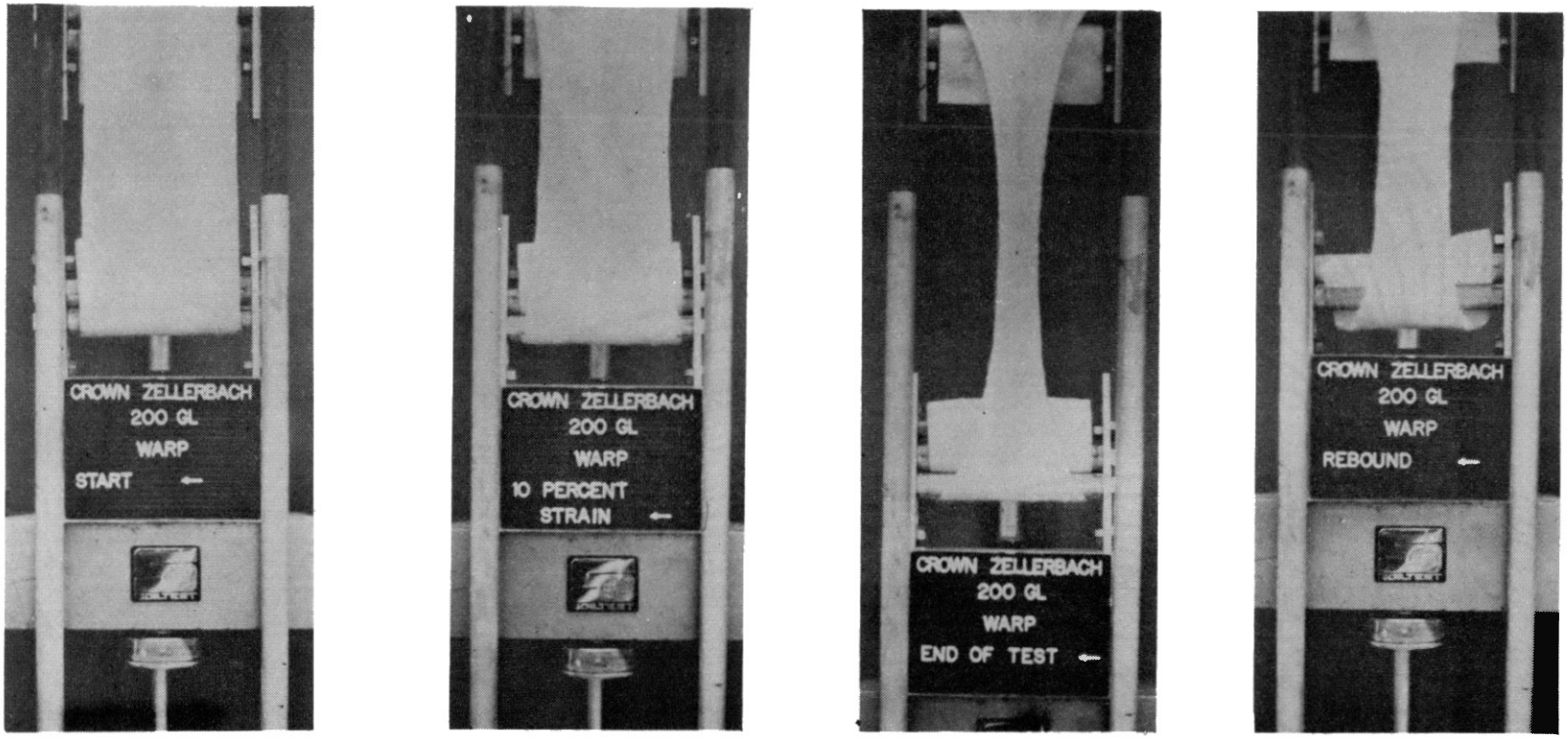

Figure 43. Photographs of Fibretex 200-Warp Direction in Tension Testing at (Left to Right) Start, 10 Percent Strain, Failure, and After "Elastic" Rebound

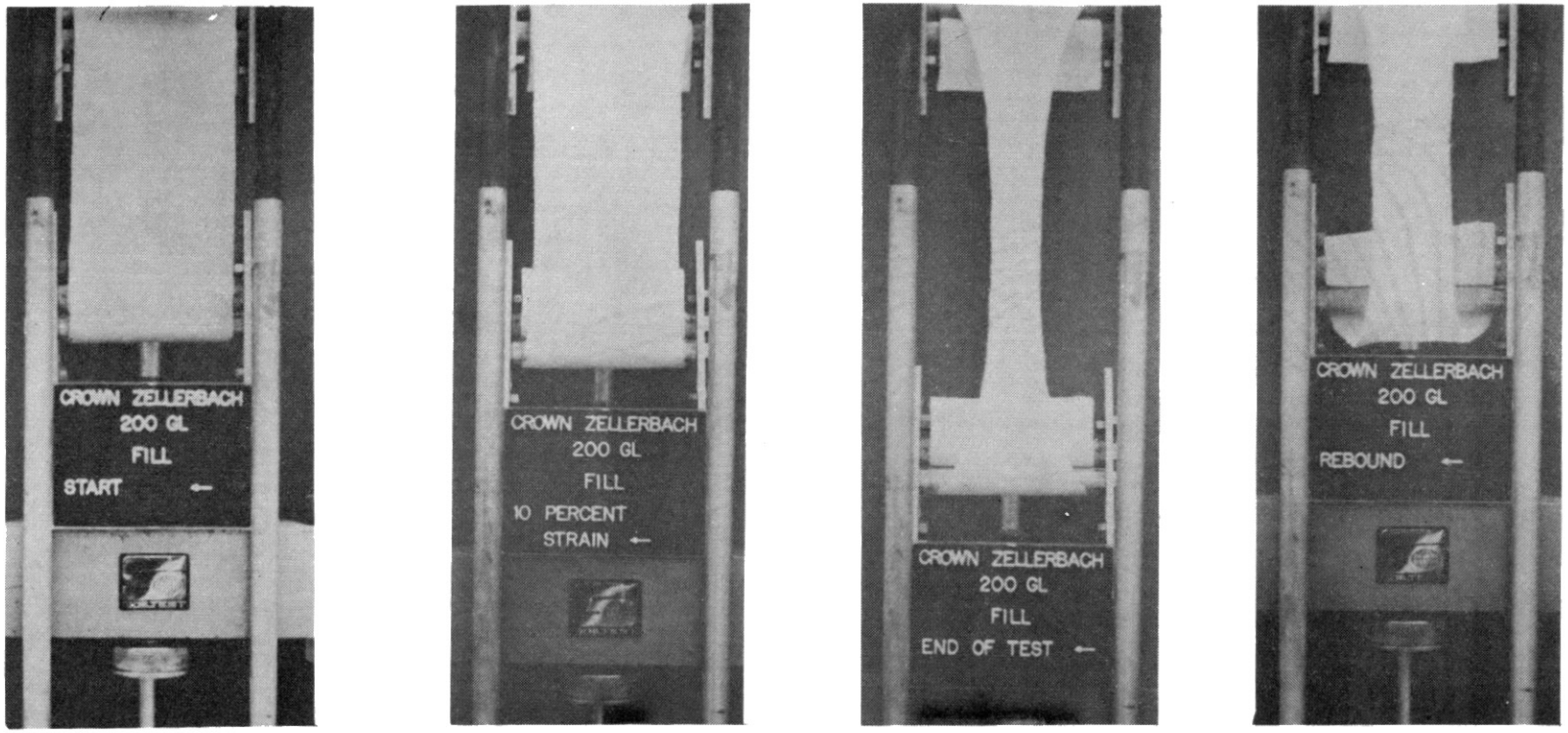

Figure 44. Photographs of Fibretex 200-Fill Direction in Tension Testing at (Left to Right) Start, 10 Percent Strain, Failure, and After "Elastic" Rebound

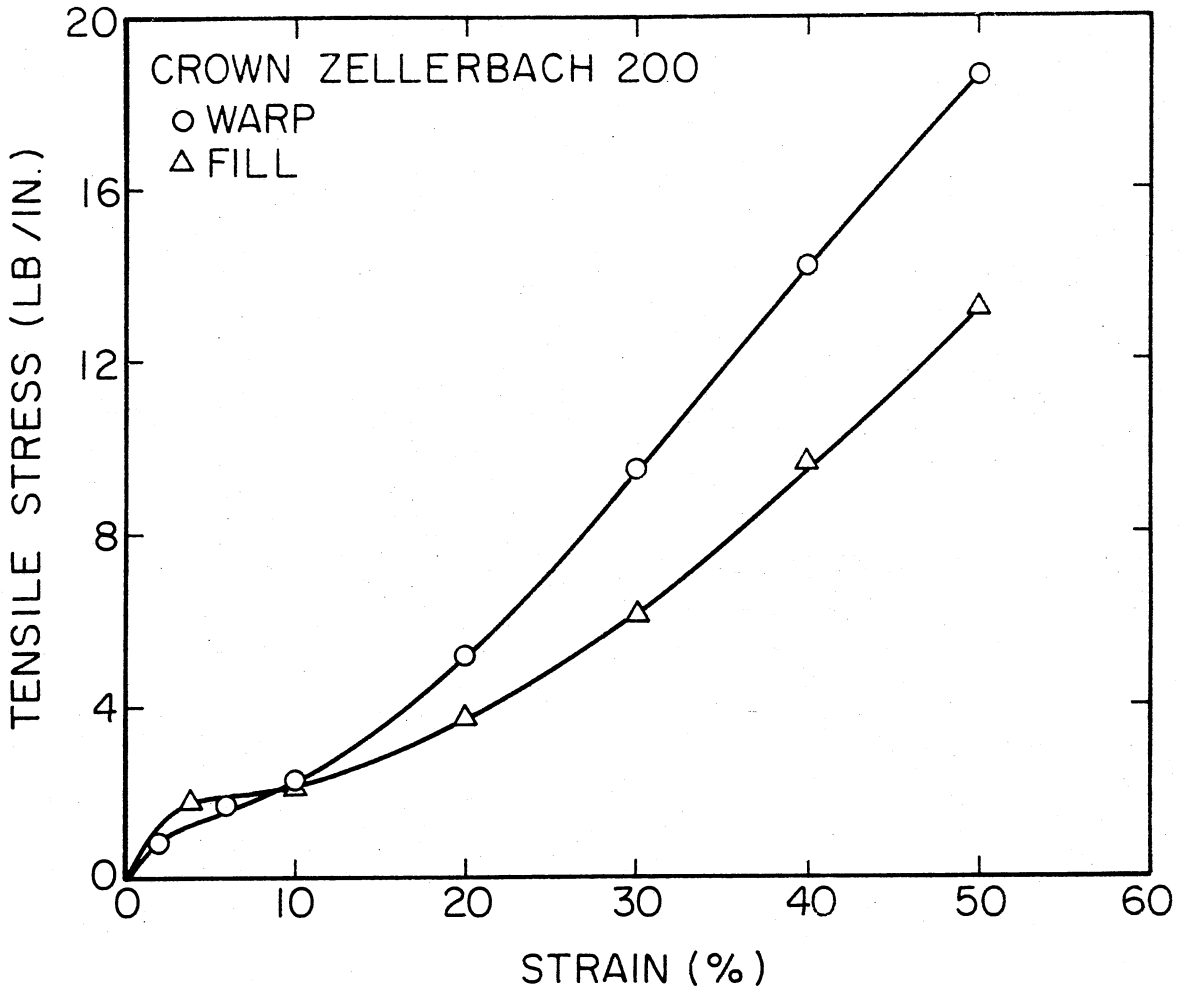

Figure 45. Stress-Strain Data for Fibretex 200 in Uniaxial Testing

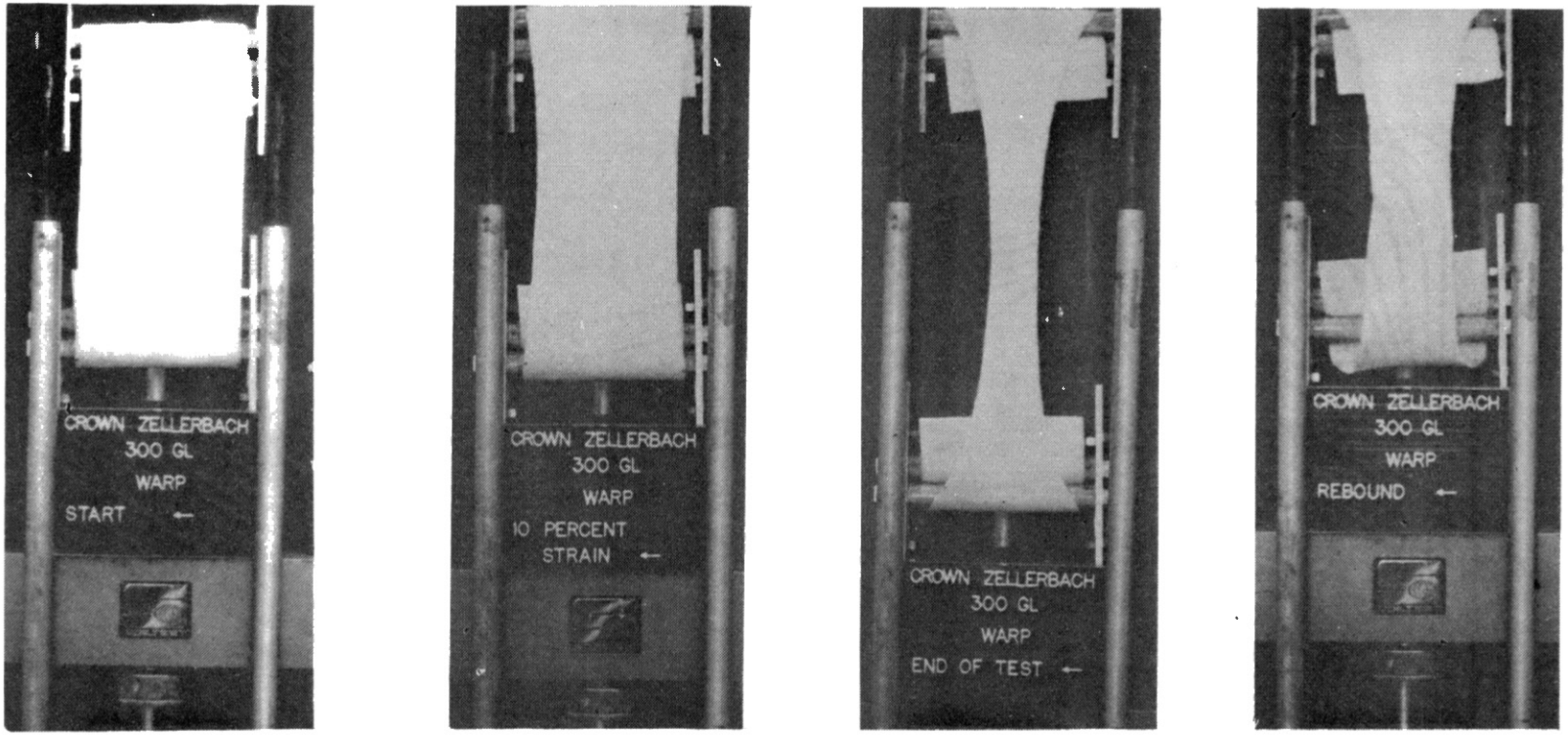

Figure 46. Photograph of Fibretex 300-Warp Direction in Tension Testing at (Left to Right) Start, 10 Percent Strain, Failure, and After "Elastic" Rebound

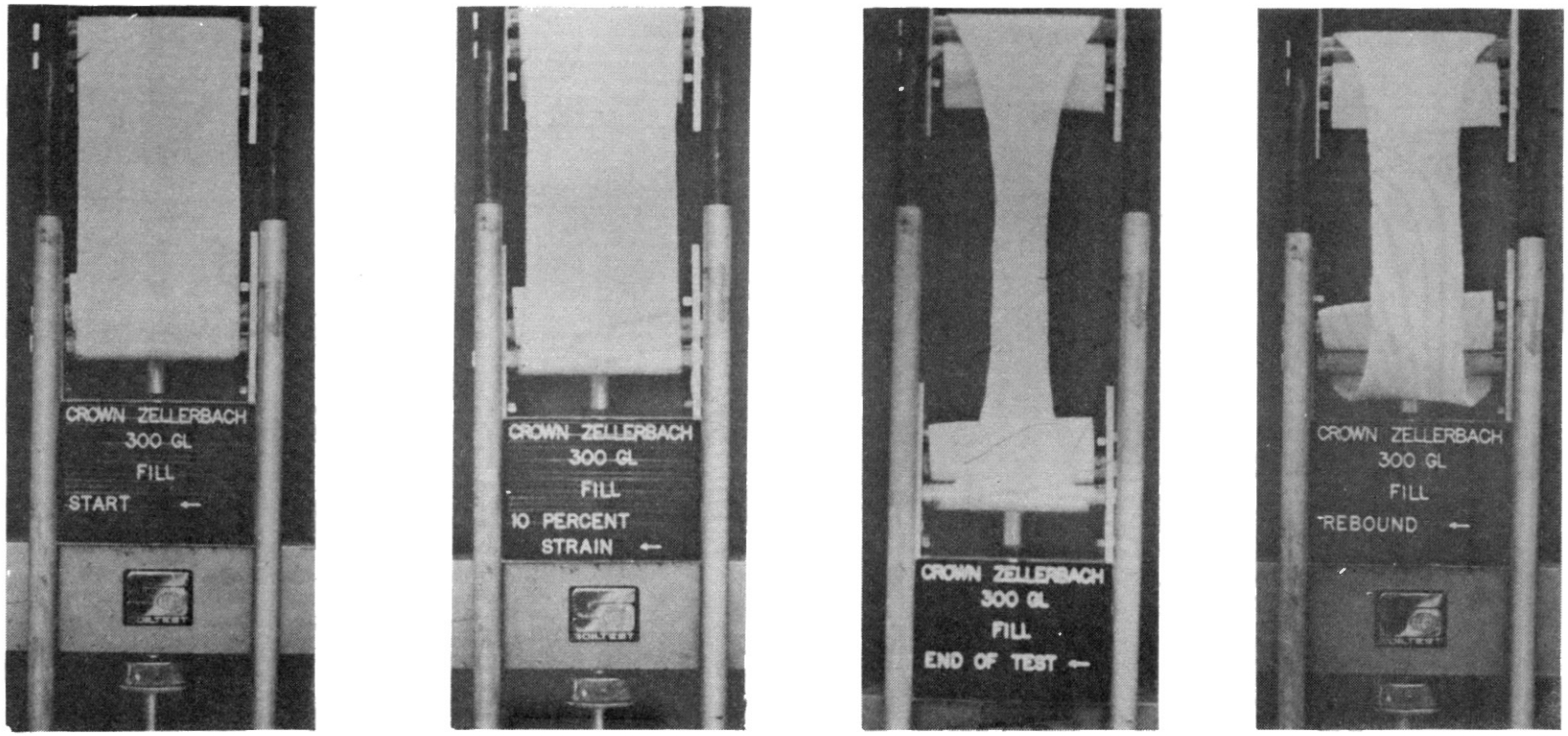

Figure 47. Photographs of Fibretex 300-Fill Direction in Tension Testing at (Left to Right) Start, 10 Percent Strain, Failure, and After "Elastic" Rebound

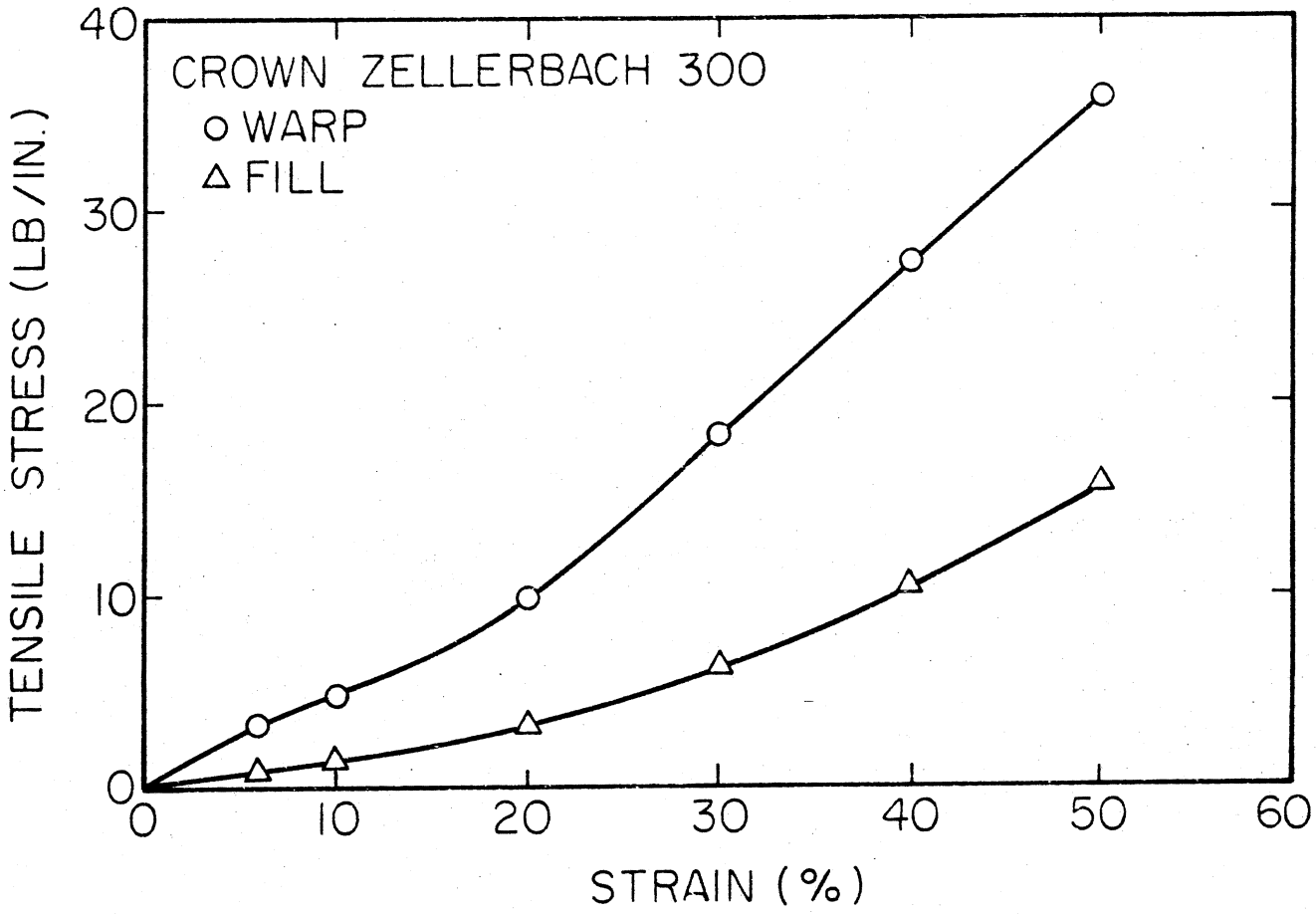

Figure 48. Stress-Strain Data for Fibretex 300 in Uniaxial Testing

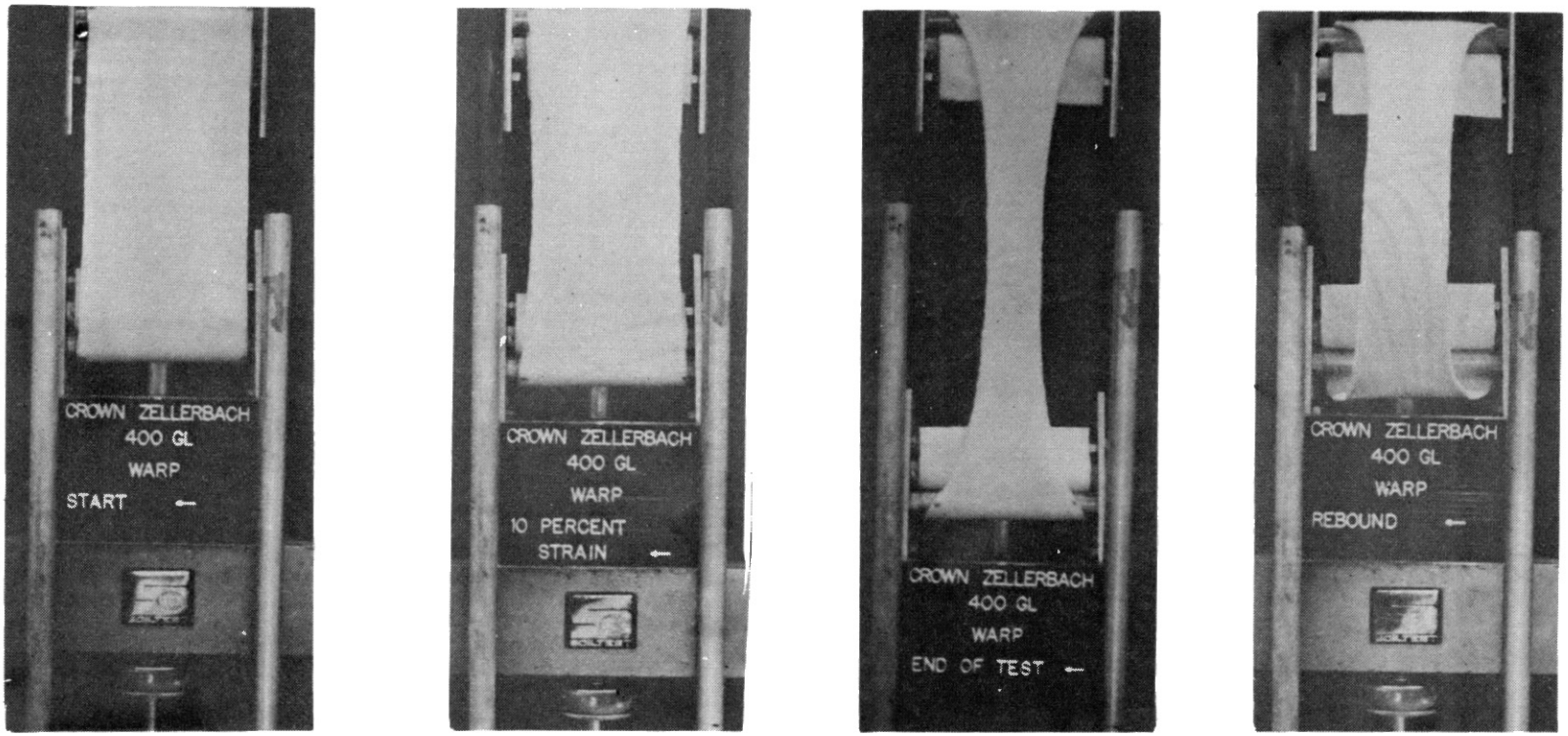

Figure 49. Photographs of Fibretex 400-Warp Direction in Tension Testing at (Left to Right) Start, 10 Percent Strain, Failure, and After "Elastic" Rebound

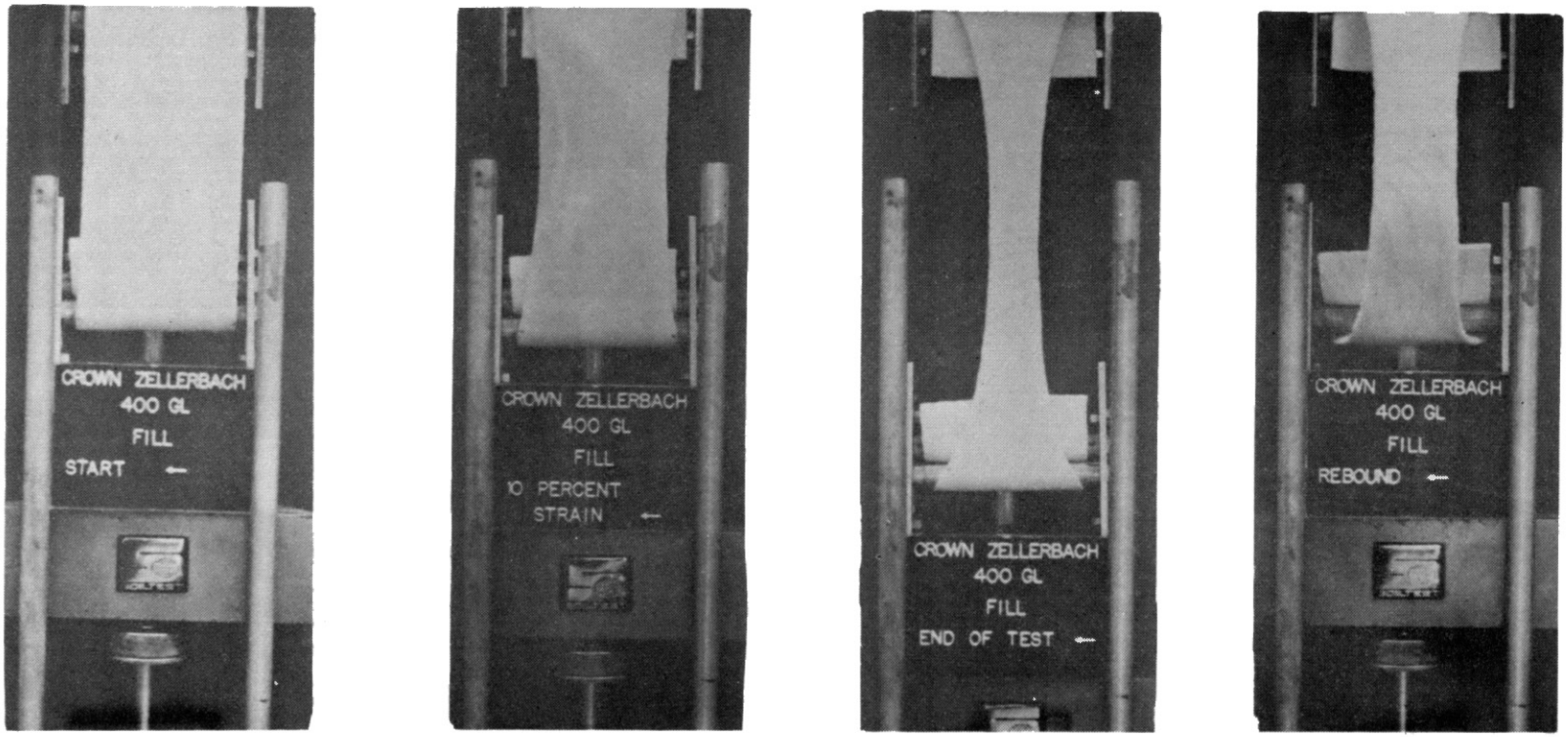

Figure 50. Photographs of Fibretex 400-Fill Direction in Tension Testing at (Left to Right) Start, 10 Percent Strain, Failure, and After "Elastic" Rebound

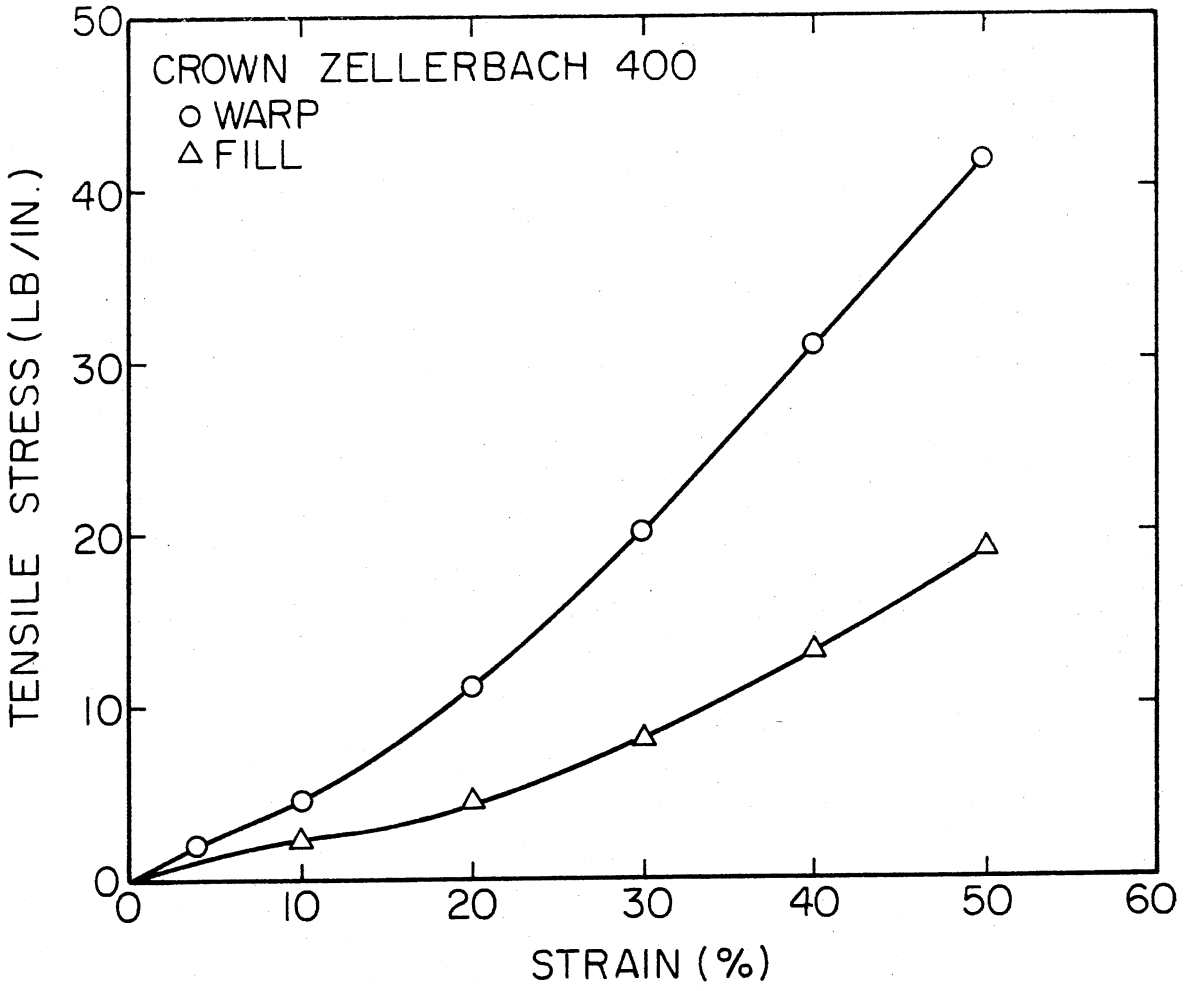

Figure 51. Stress-Strain Data for Fibretex 400 in Uniaxial Testing

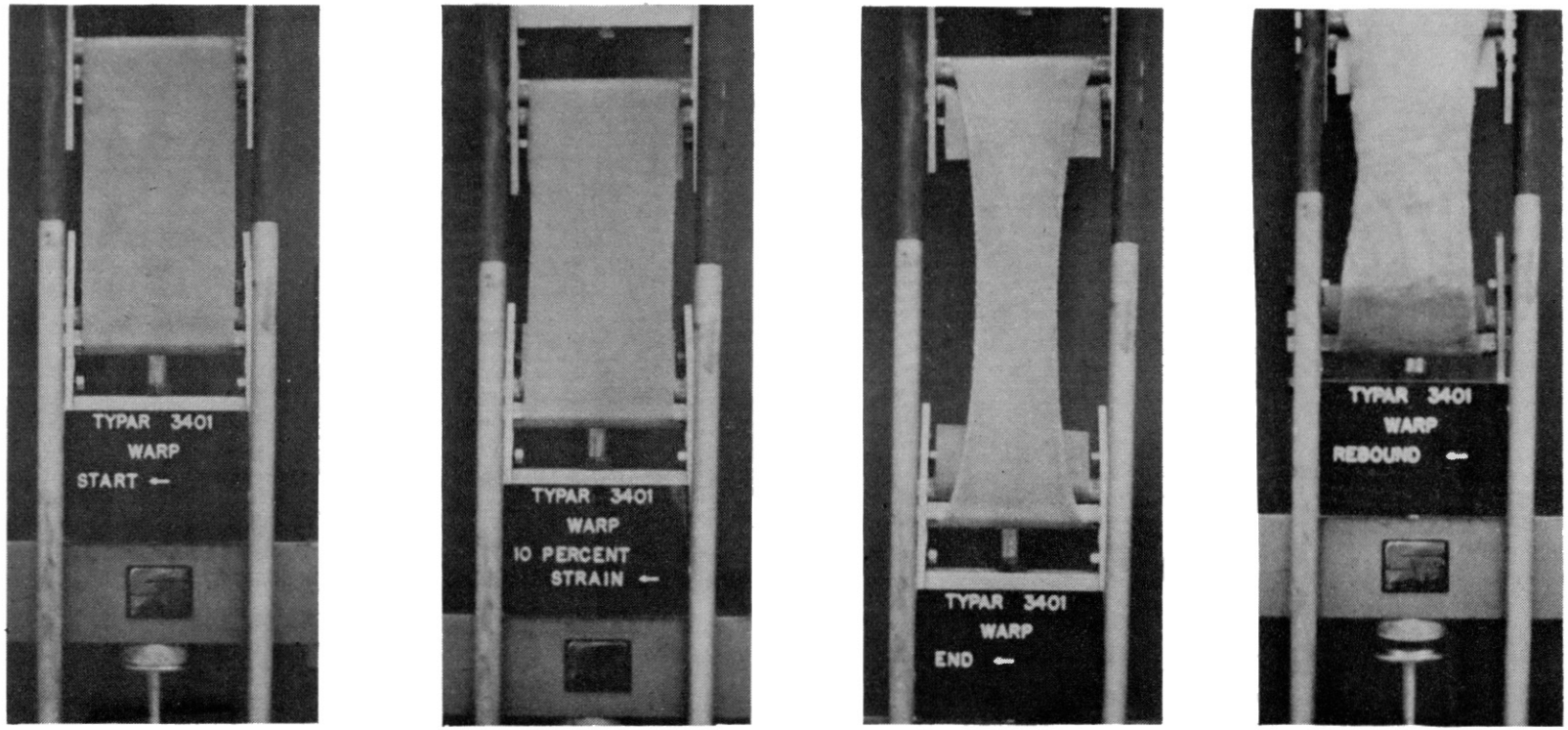

Figure 52. Photographs of Typar 3401-Warp Direction in Tension Testing at (Left to Right) Start, 10 Percent Strain, Failure, and After "Elastic" Rebound

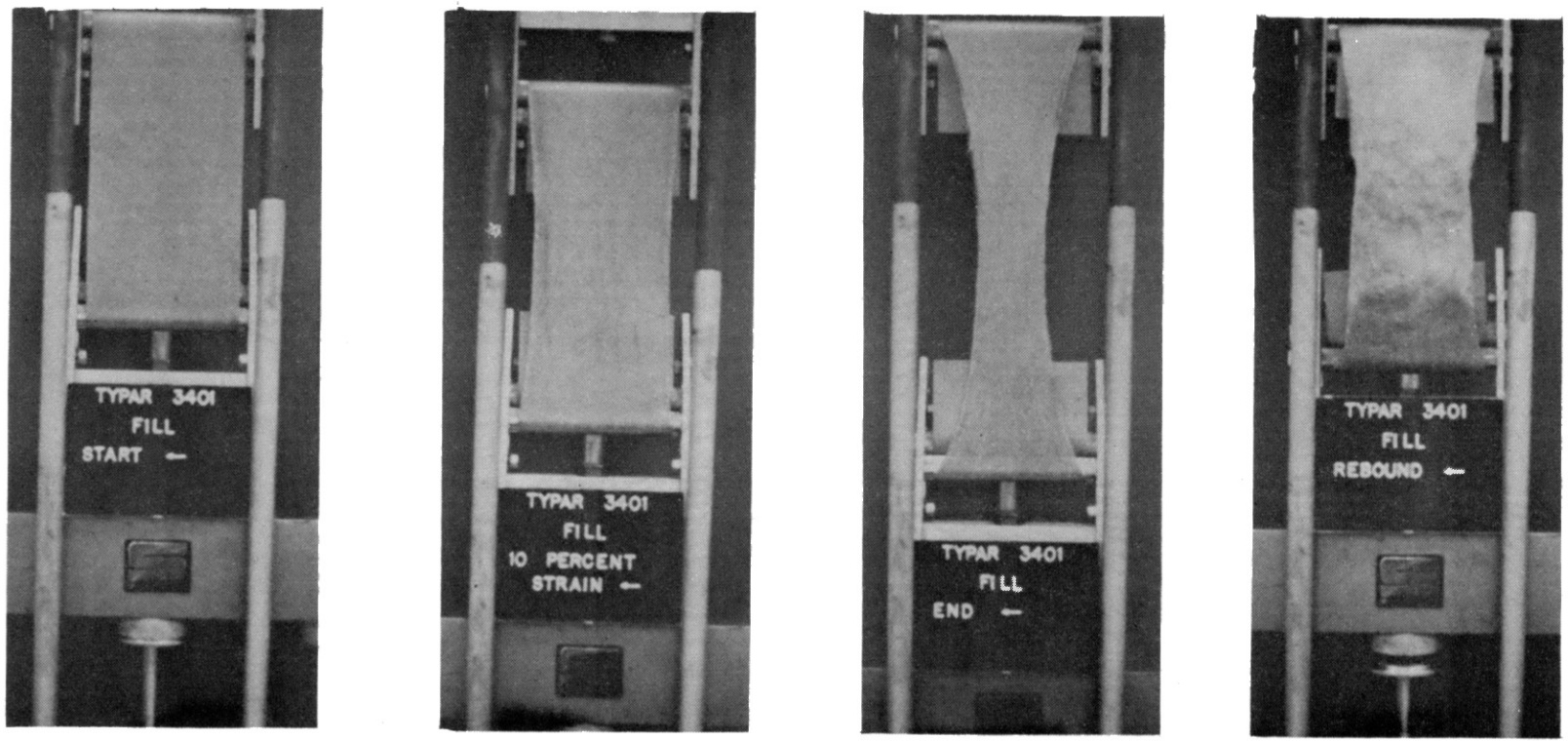

Figure 53. Photographs of Typar 3401-Fill Direction in Tension Testing at (Left to Right) Start, 10 Percent Strain, Failure, and After "Elastic" Rebound

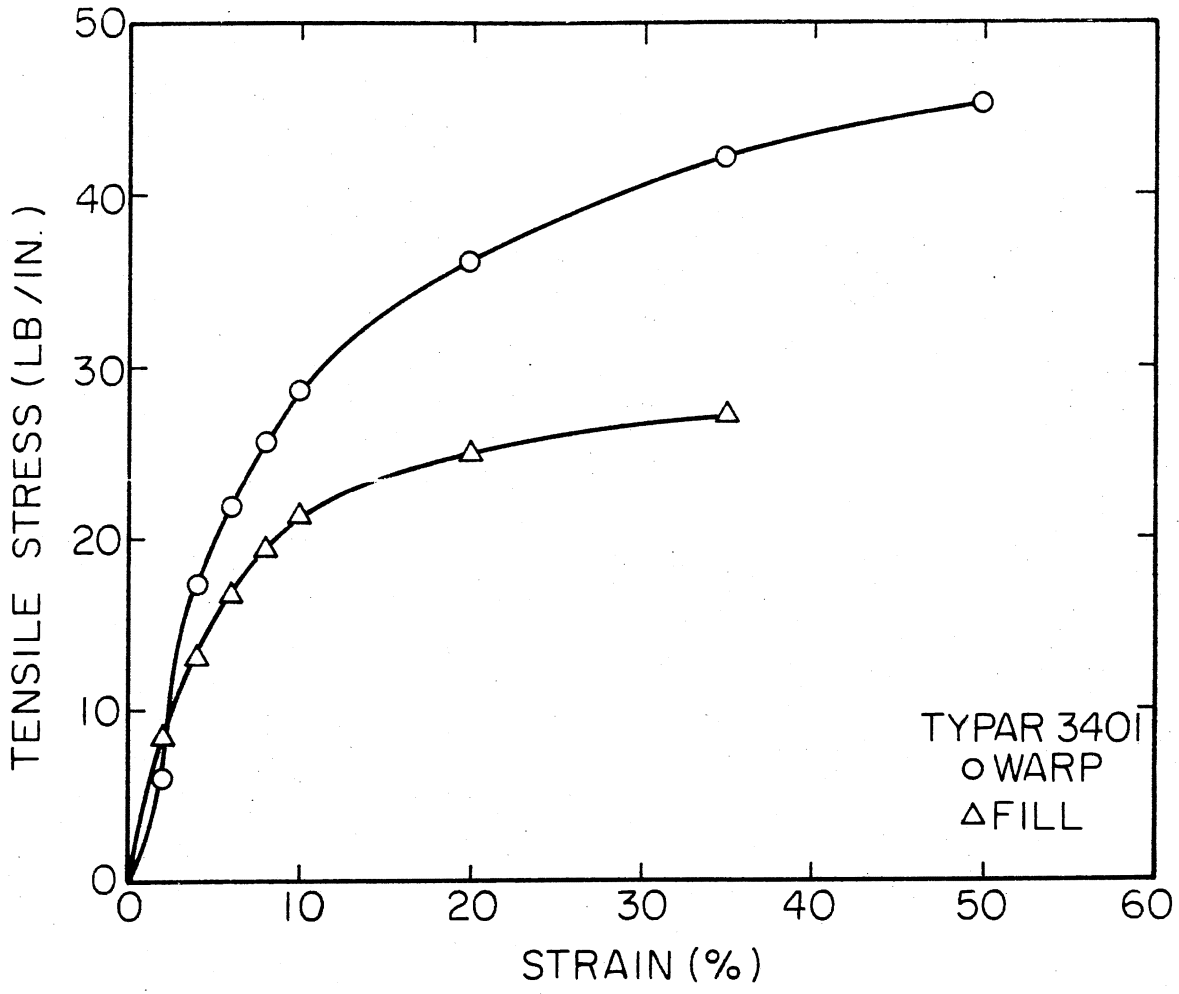

Figure 54. Stress-Strain Data for Typar 3401 in Uniaxial Testing

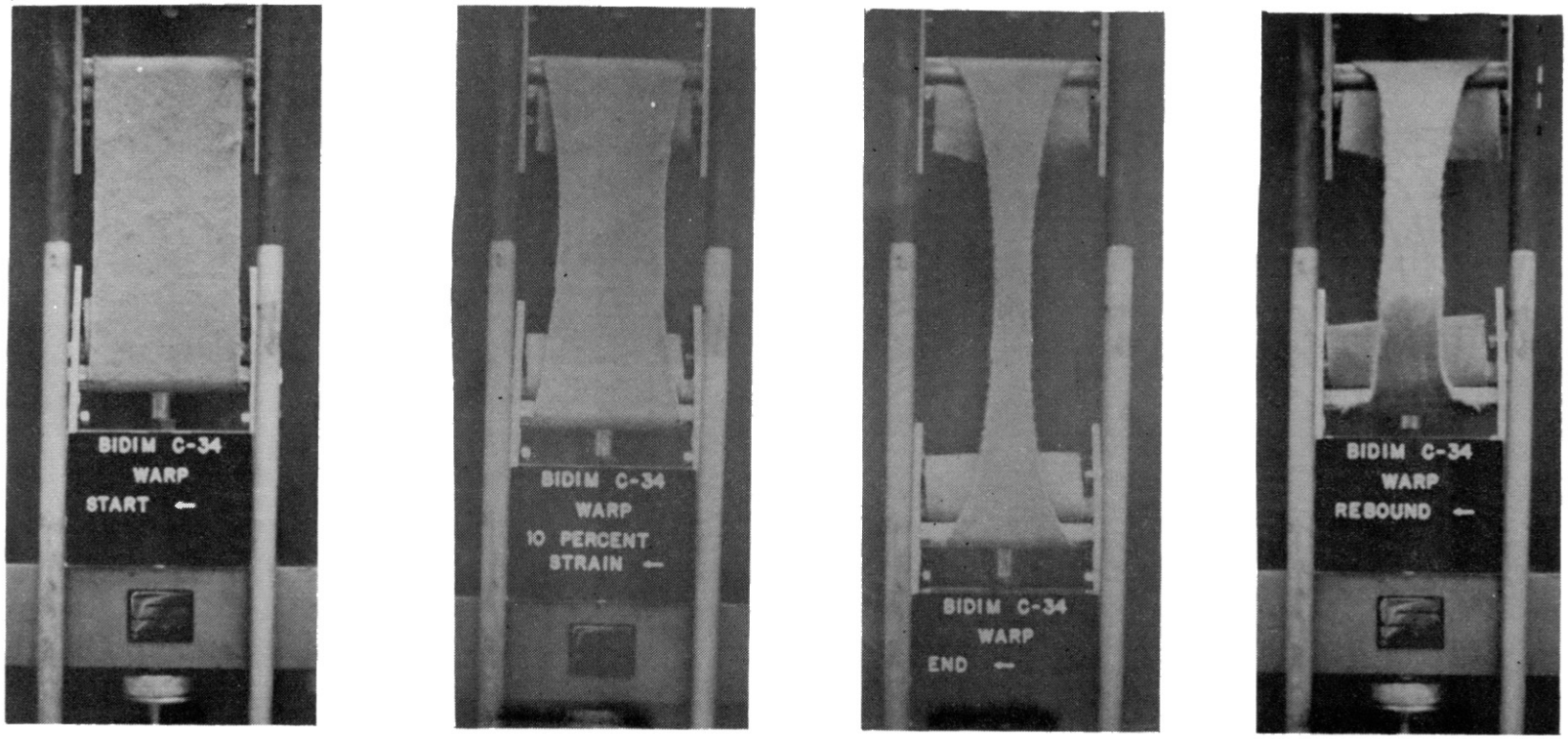

Figure 55. Photographs of Bidim C-34-Warp Direction in Tension Testing at (Left to Right) Start, 10 Percent Strain, Failure, and After "Elastic" Rebound

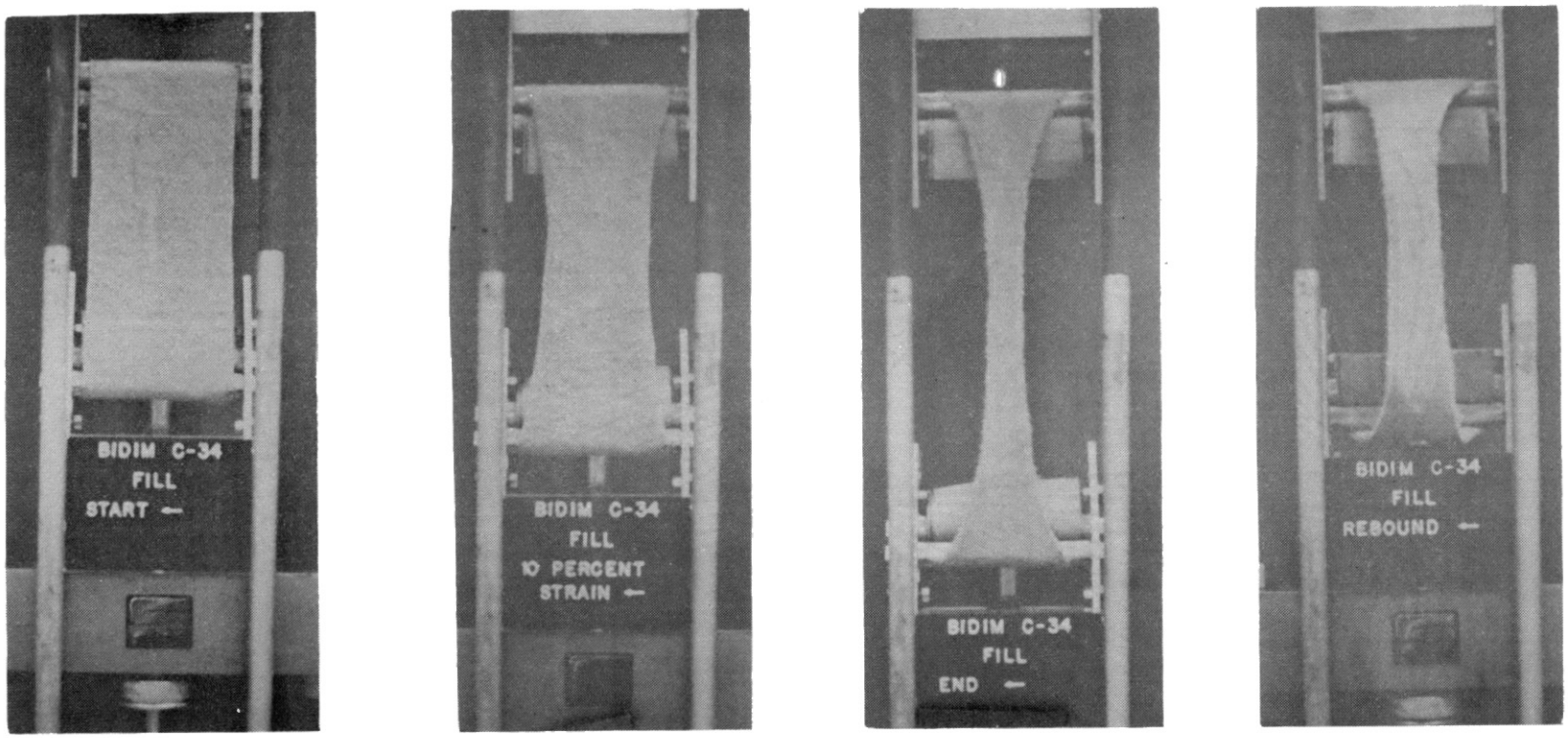

Figure 56. Photographs of Bidim C-34-Fill Direction in Tension Testing at (Left to Right) Start, 10 Percent Strain, Failure, and After "Elastic" Rebound

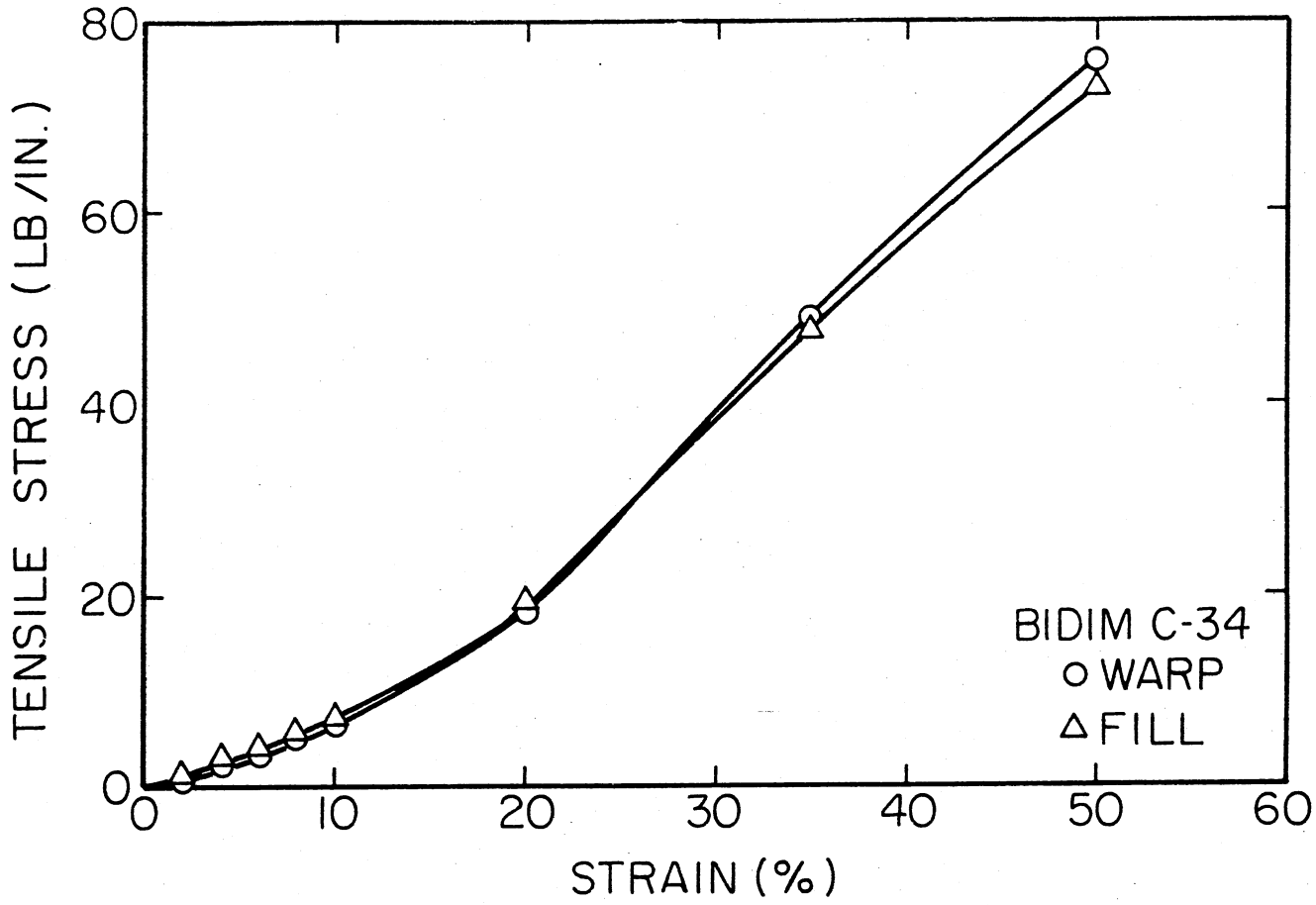

Figure 57. Stress-Strain Data for Bidim C-34 in Uniaxial Testing

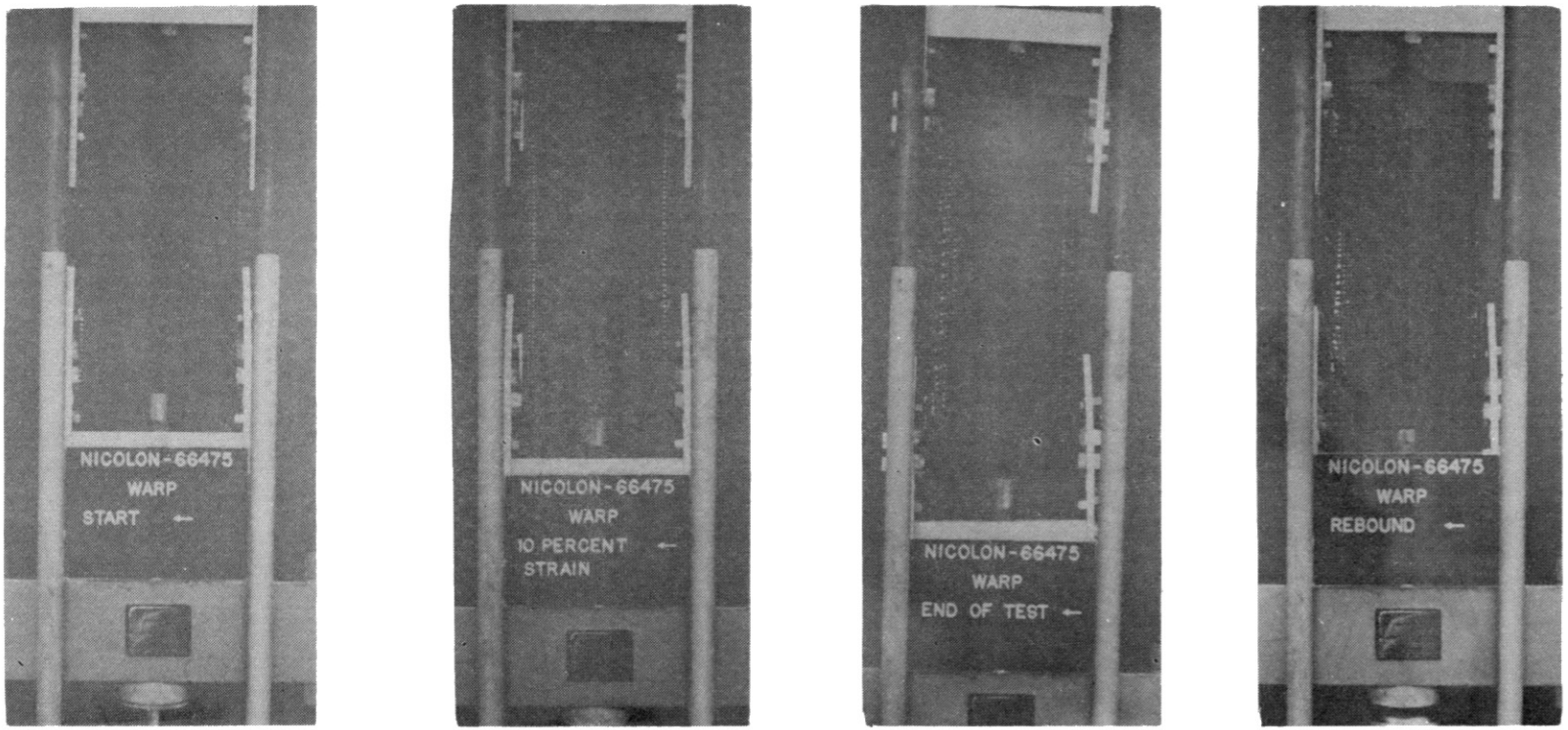

Figure 58. Photographs of Nicolon 66475-Warp Direction in Tension Testing at (Left to Right) Start, 10 Percent Strain, Failure, and After "Elastic" Rebound

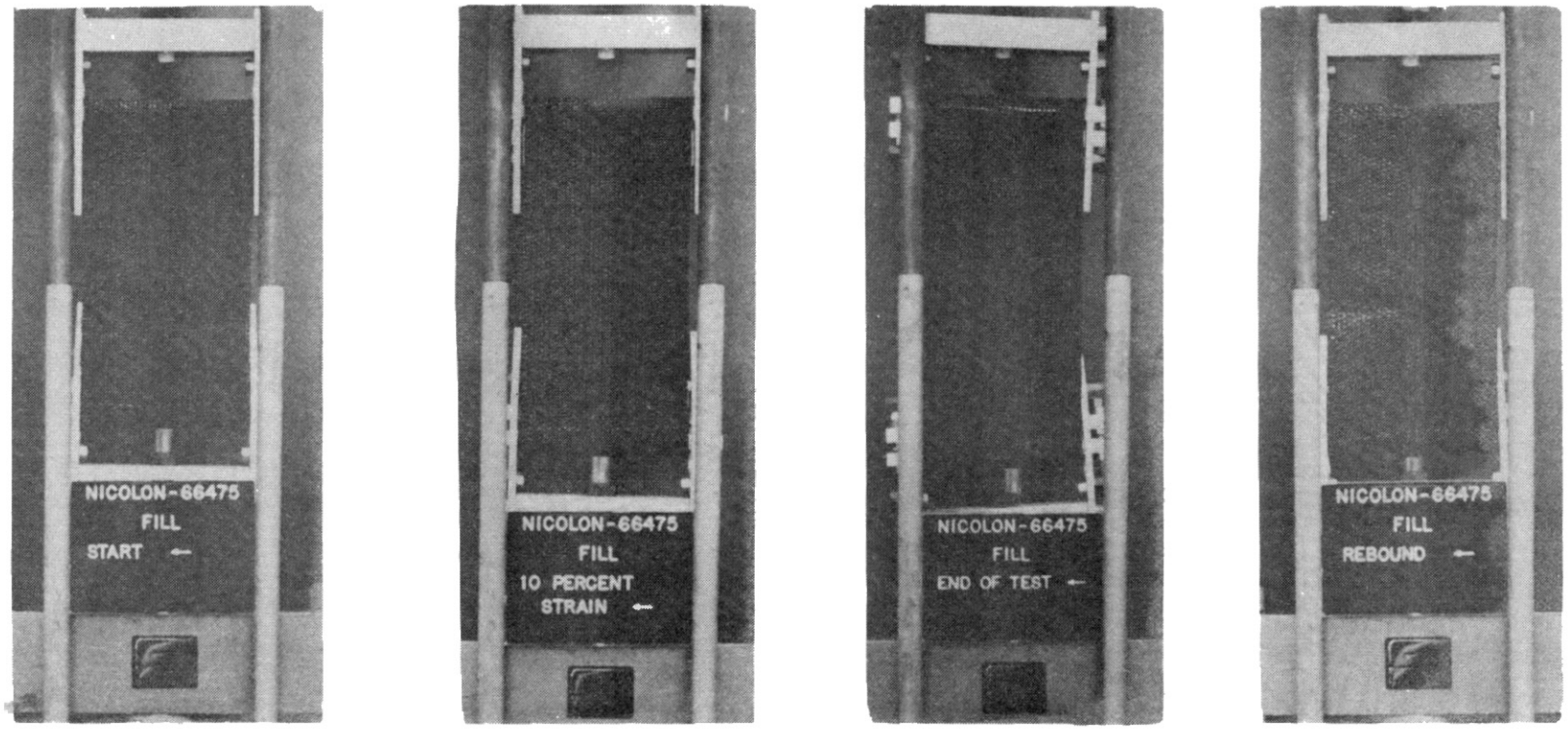

Figure 59. Photographs of Nicolon 66475-Fill Direction in Tension Testing at (Left to Right) Start, 10 Percent Strain, Failure, and After "Elastic" Rebound

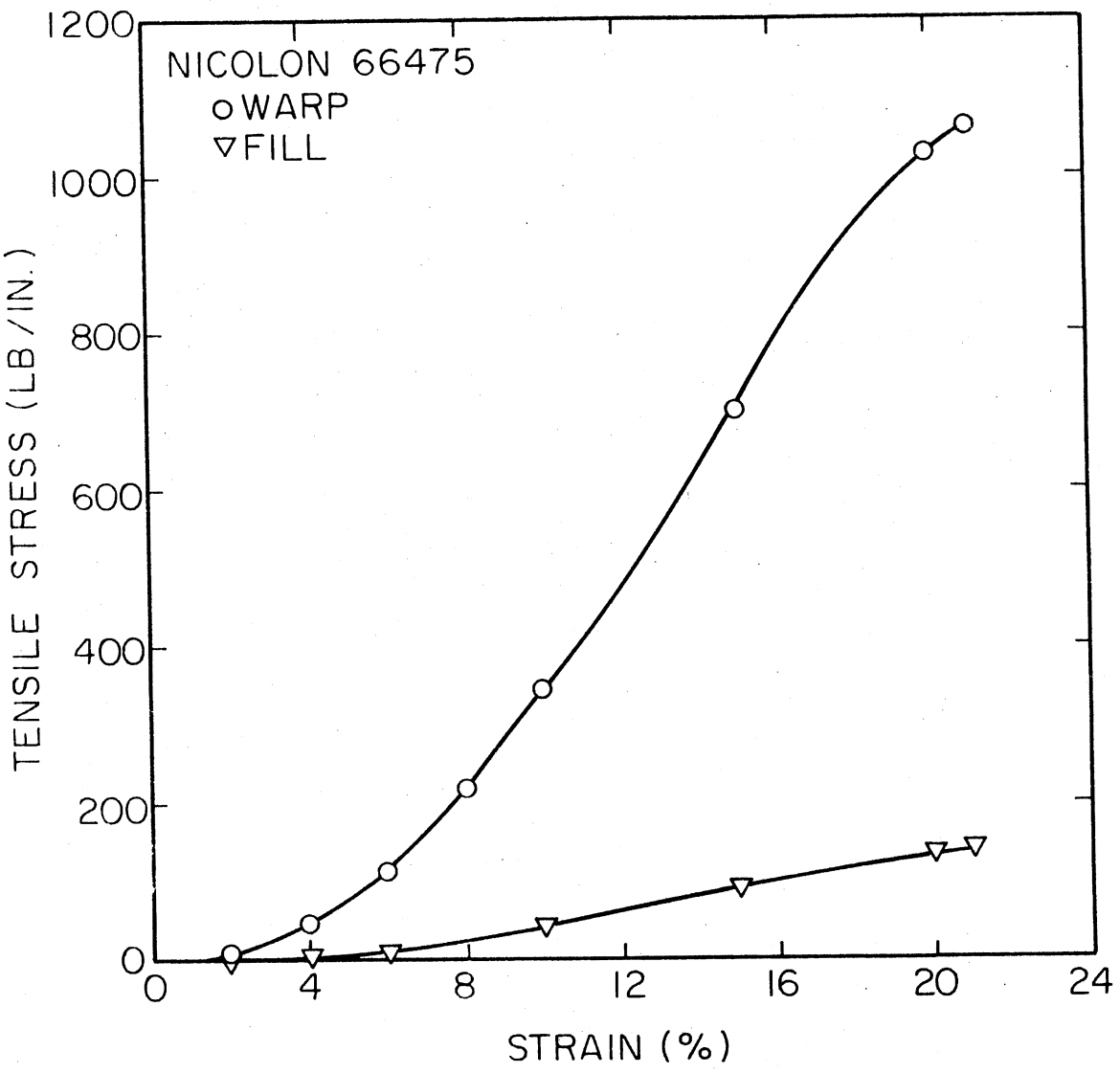

Figure 60. Stress-Strain Data for Nicolon 66475 in Uniaxial Testing

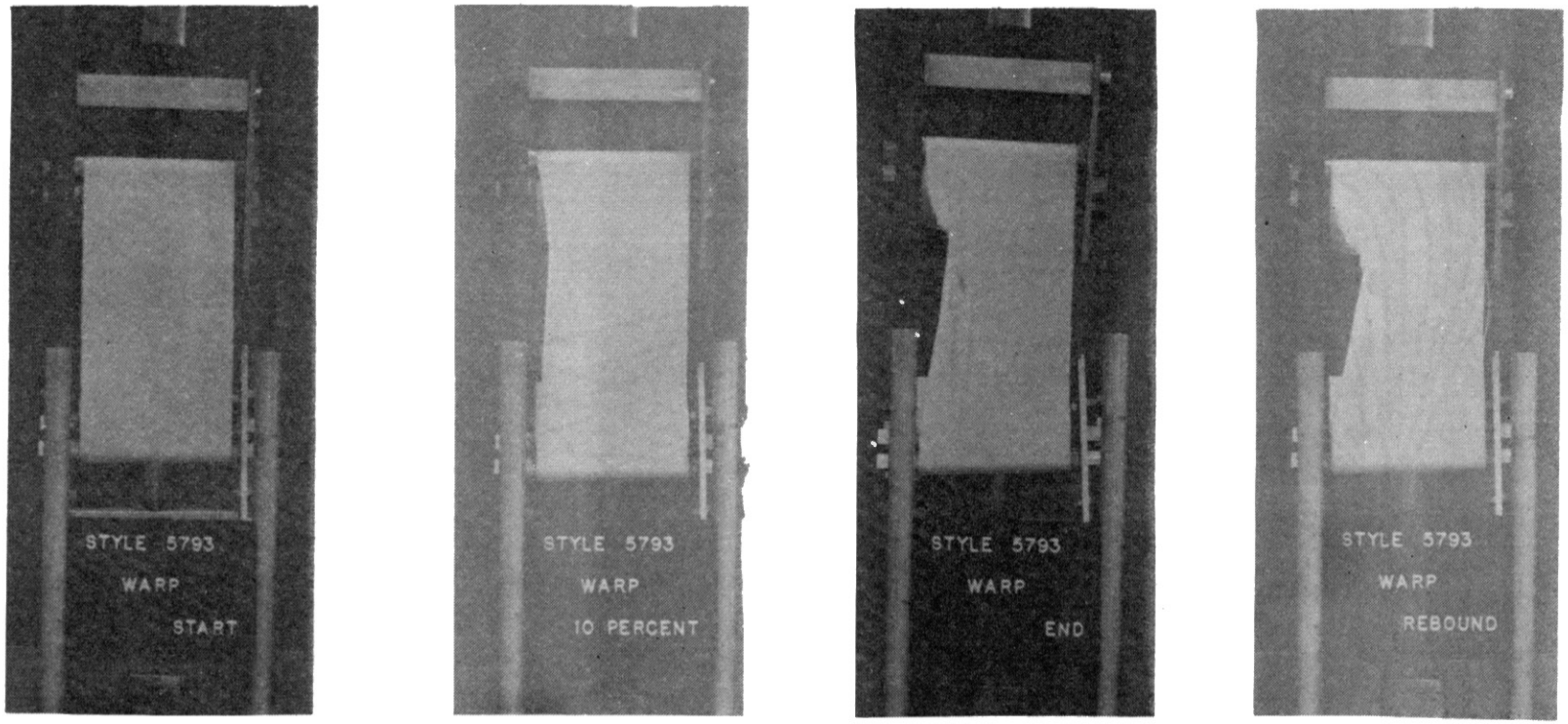

Figure 61. Photographs of Style 5793-Warp Direction in Tension Testing at (Left to Right) Start, 10 Percent Strain, Failure, and After "Elastic" Rebound

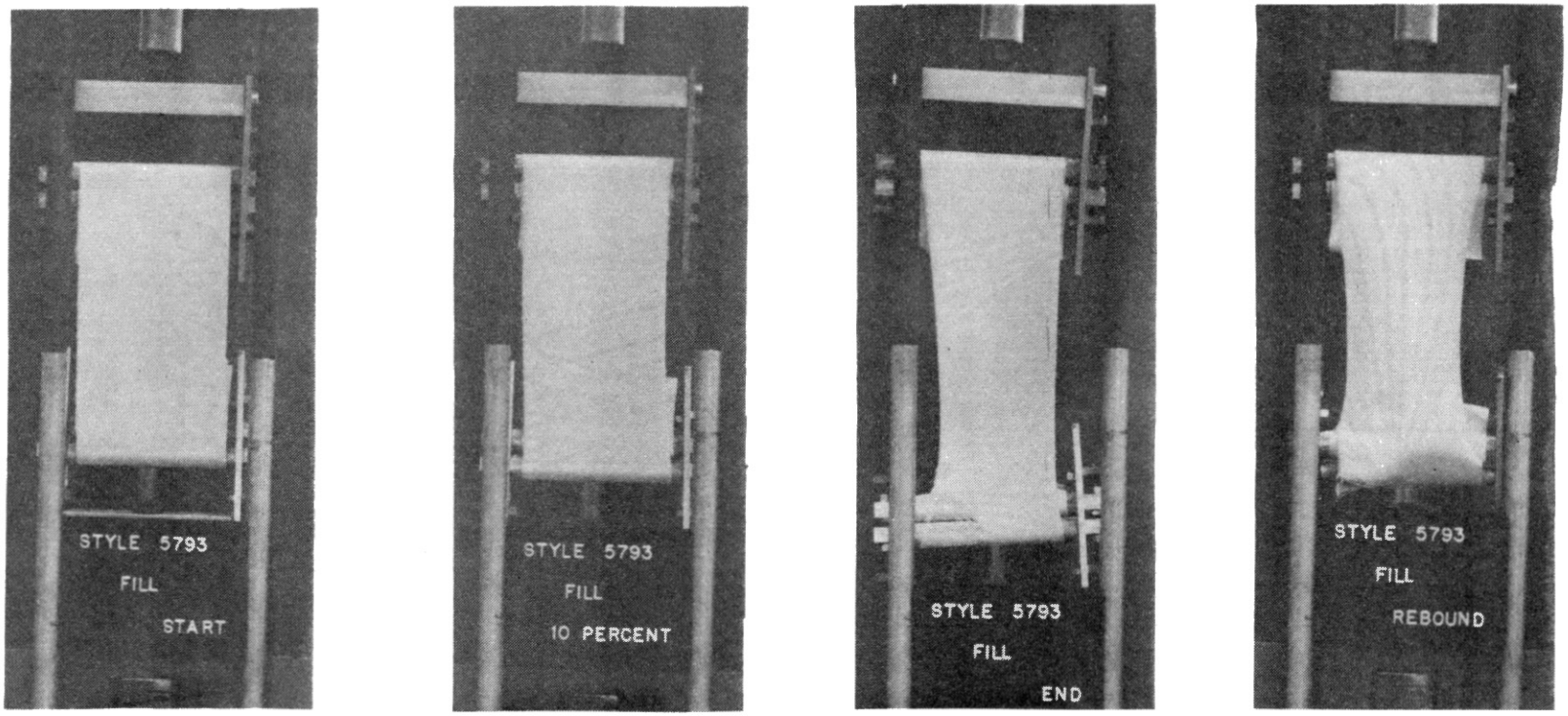

Figure 62. Photographs of Style 5793-Fill Direction in Tension Testing at (Left to Right) Start, 10 Percent Strain, Failure, and After "Elastic" Rebound

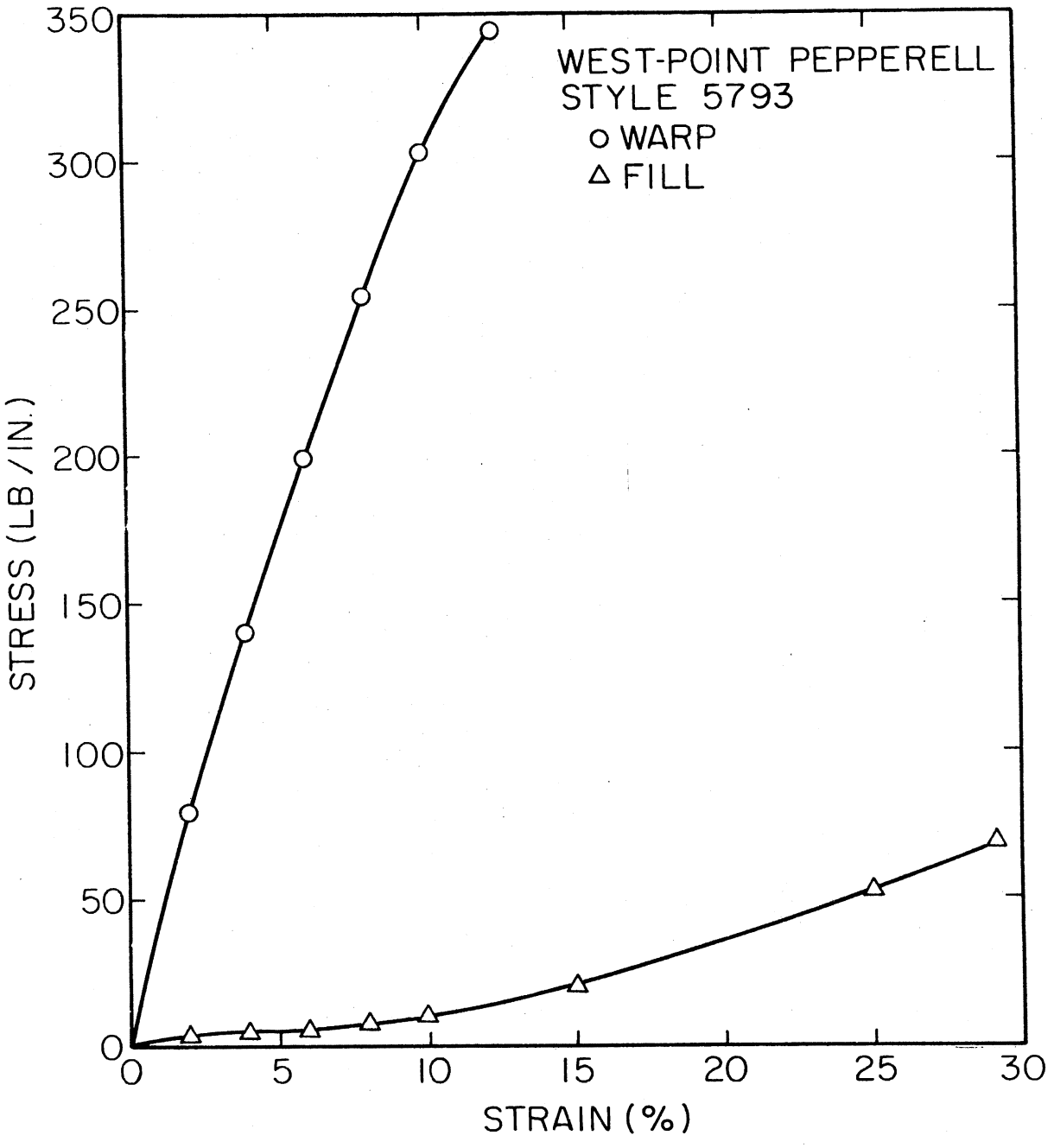

Figure 63. Stress-Strain Data for Style 5793 in Uniaxial Testing

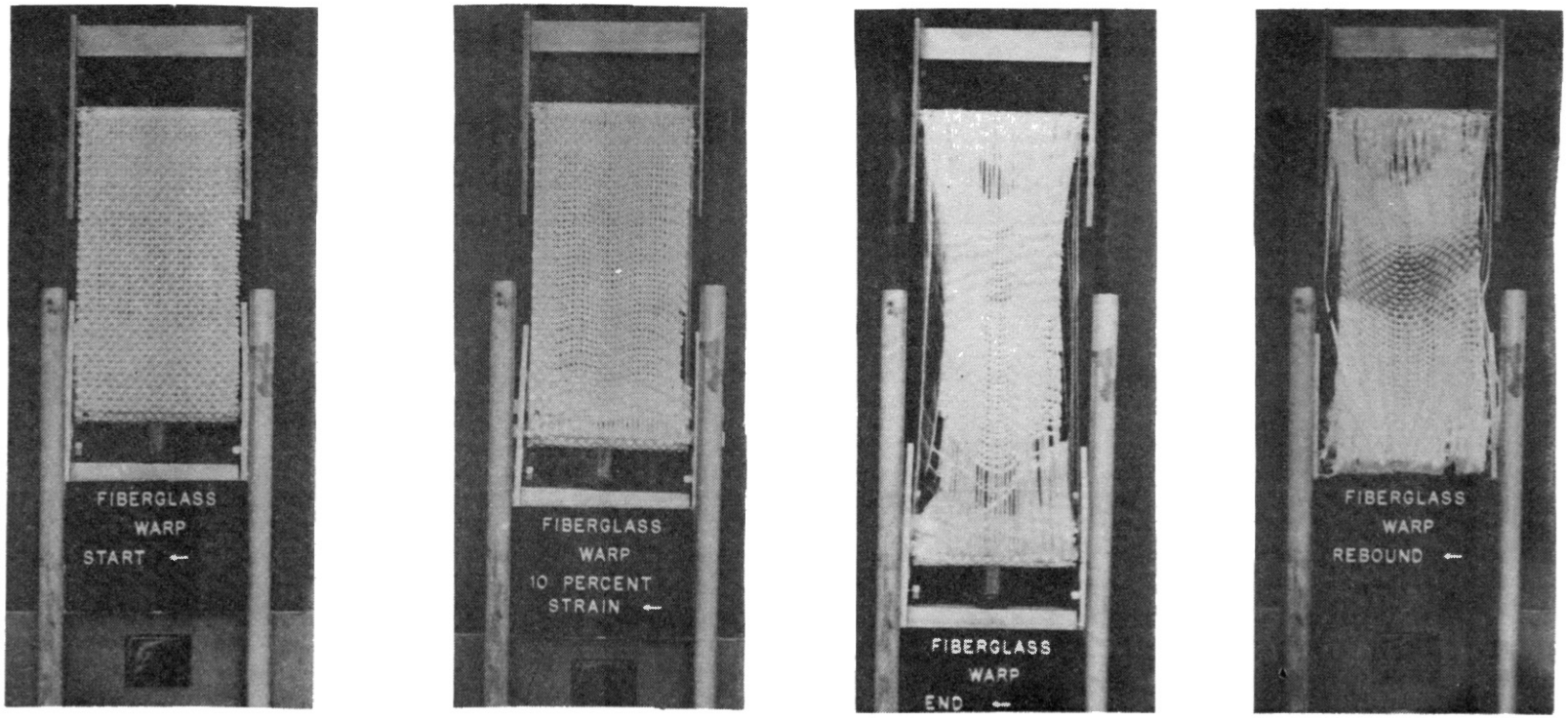

Figure 64. Photographs of Corning Fiberglass Fabric-Warp Direction in Tension Testing at (Left to Right) Start, 10 Percent Strain, Failure, and After "Elastic" Rebound

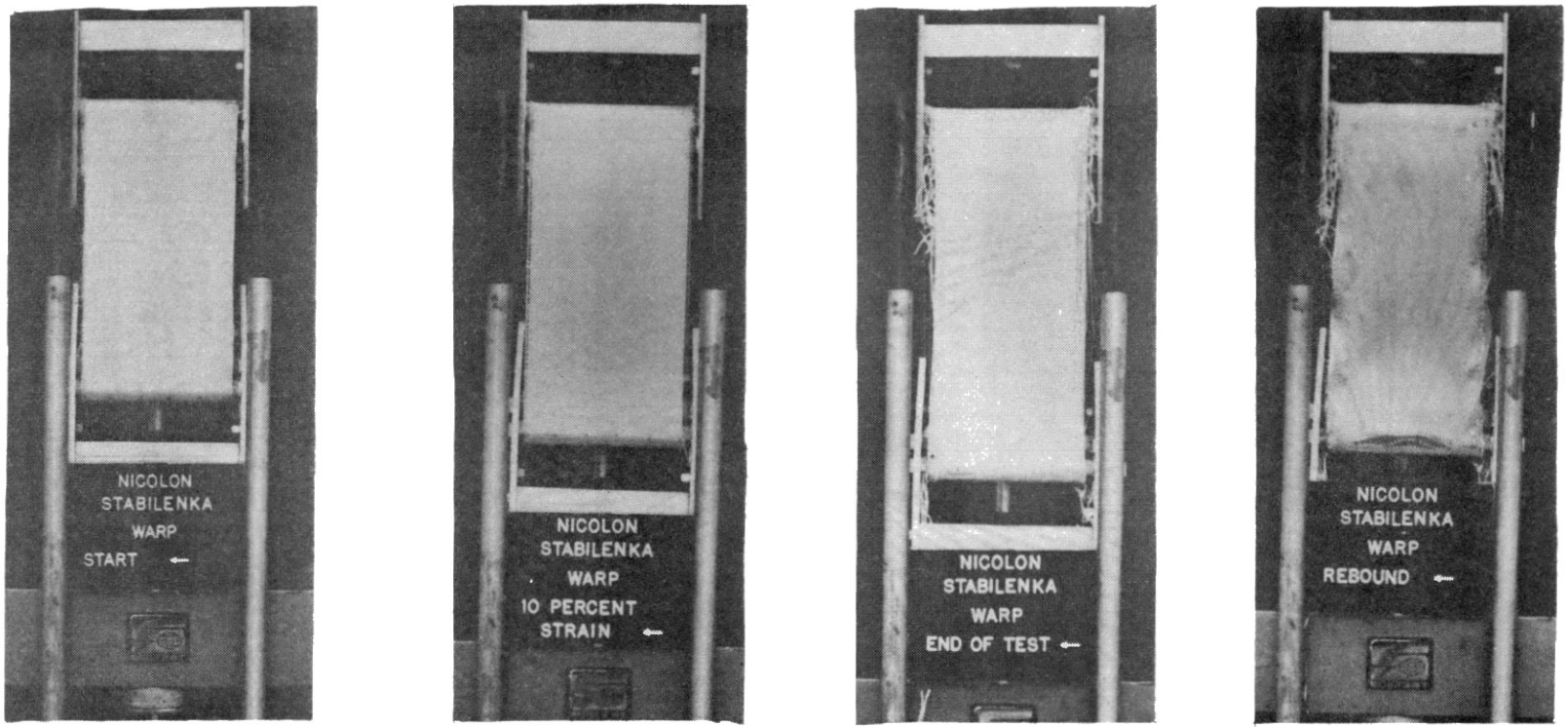

Figure 65. Photographs of Stabilenka 200-Warp Direction in Tension Testing at (Left to Right) Start, 10 Percent Strain, Failure, and After "Elastic" Rebound

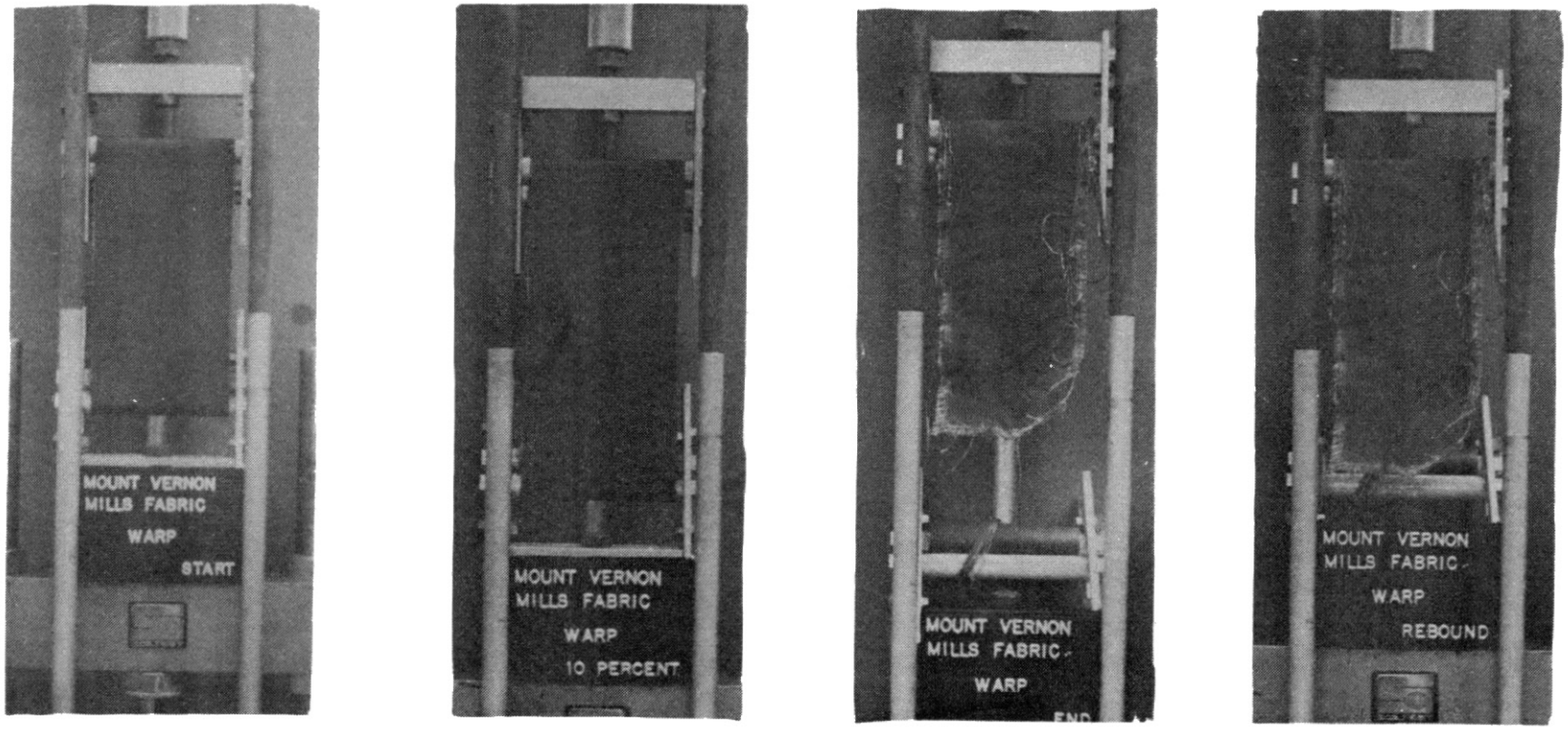

Figure 66. Photographs of Stabilenka 200-Fill Direction in Tension Testing at (Left to Right) Start, 10 Percent Strain, Failure, and After "Elastic" Rebound

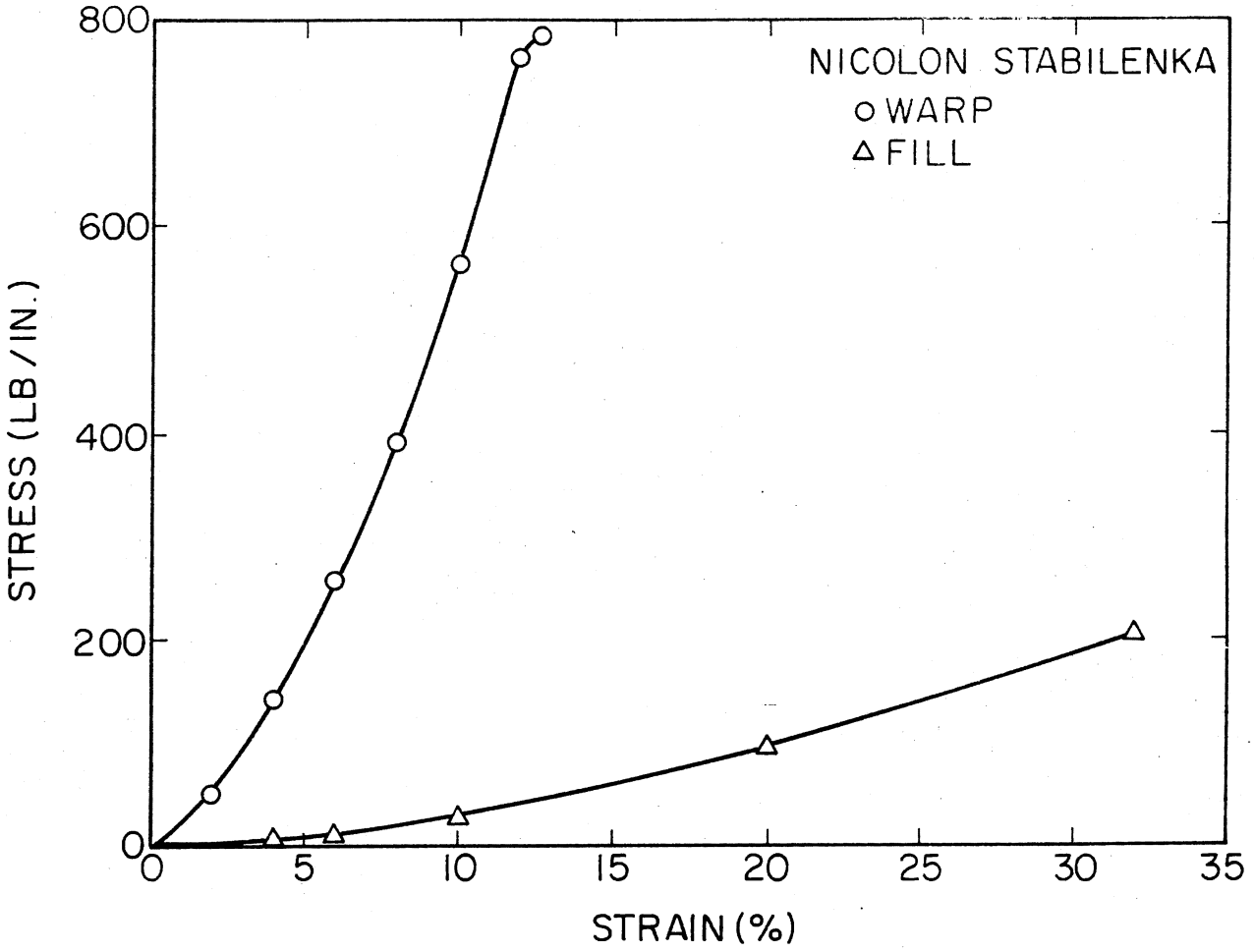

Figure 67. Stress-Strain Data for Stabilenka 200 in Uniaxial Testing

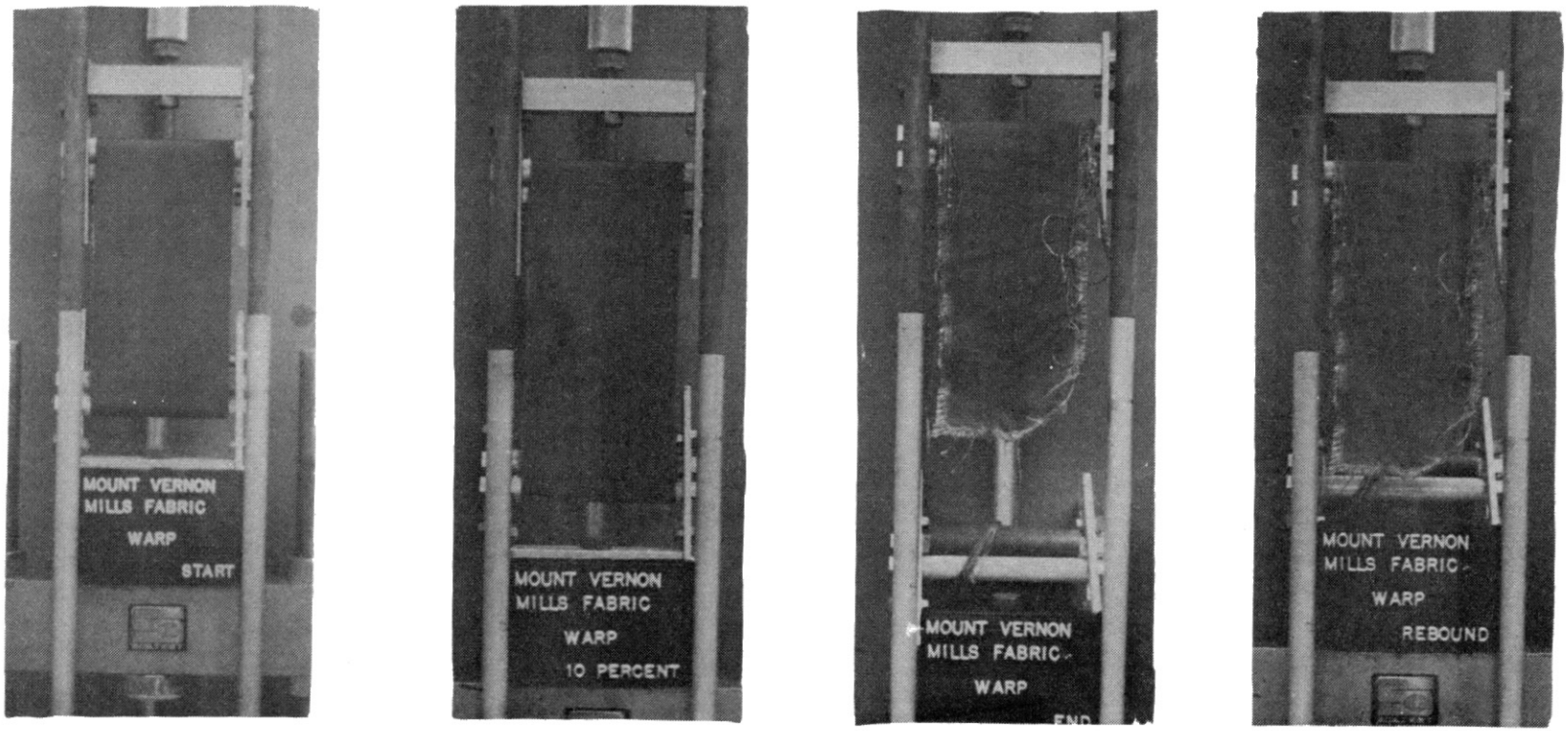

Figure 68. Photographs of Mount Vernon Mills Fabric-Warp Direction in Tension Testing at (Left to Right) Start, 10 Percent Strain, Failure, and After "Elastic" Rebound

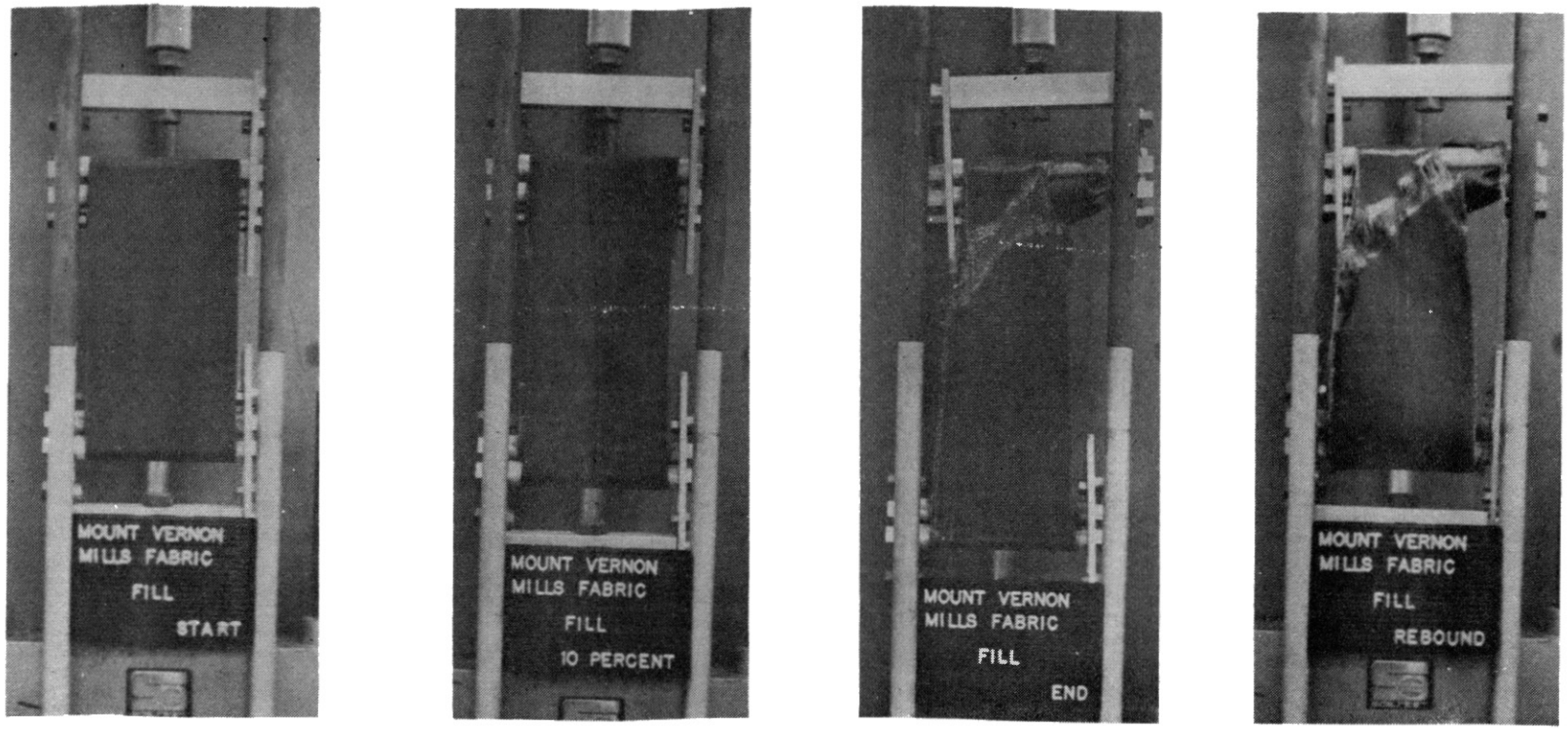

Figure 69. Photographs of Mount Vernon Mills Fabric-Fill Direction in Tension Testing at (Left to Right) Start, 10 Percent Strain, Failure, and After "Elastic" Rebound

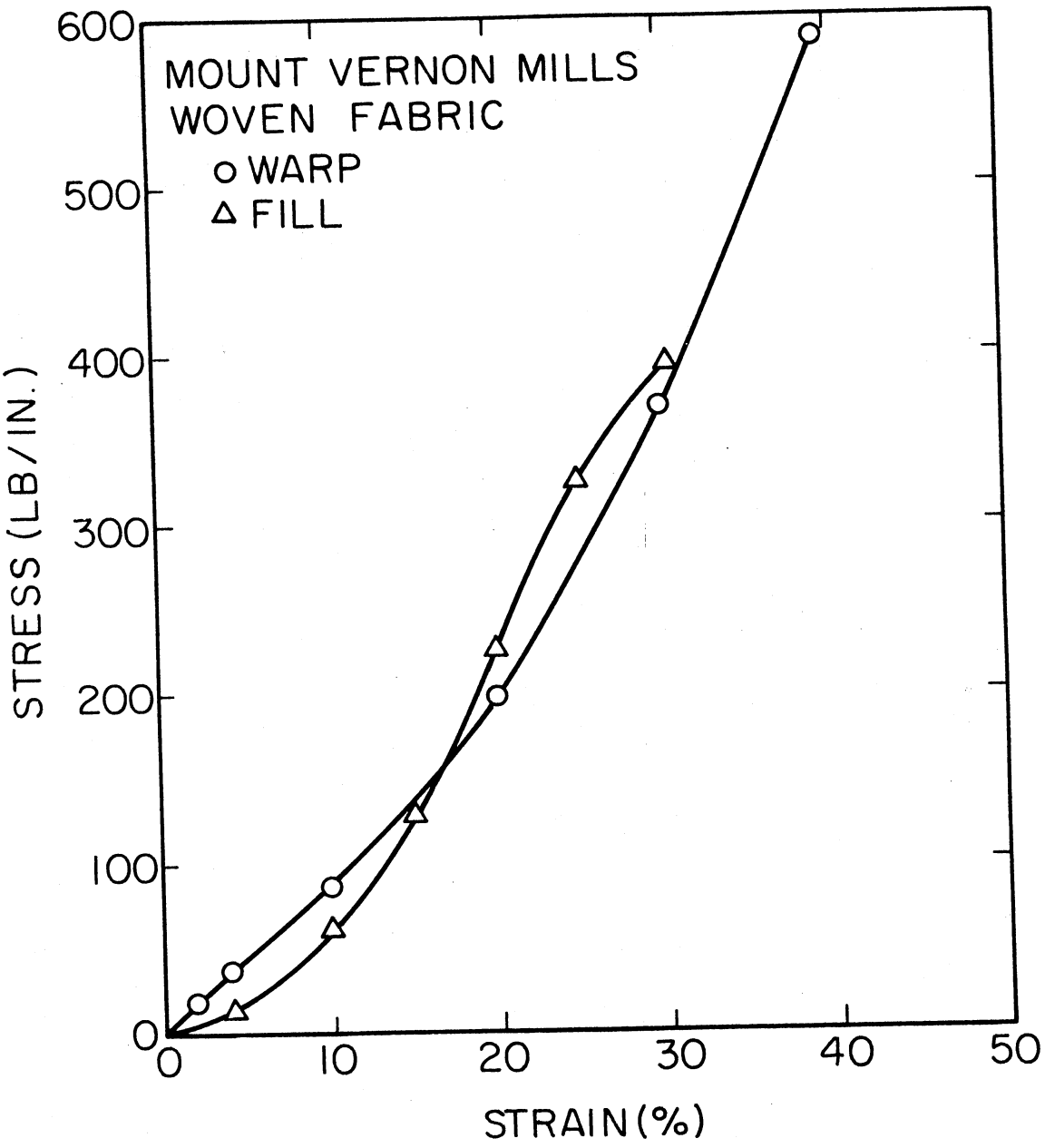

Figure 70. Stress-Strain Data for Mount Vernon Mills Fabric in Uniaxial Testing

APPENDIX B

STRESS-STRAIN DATA FOR LOAD BEARING TESTS

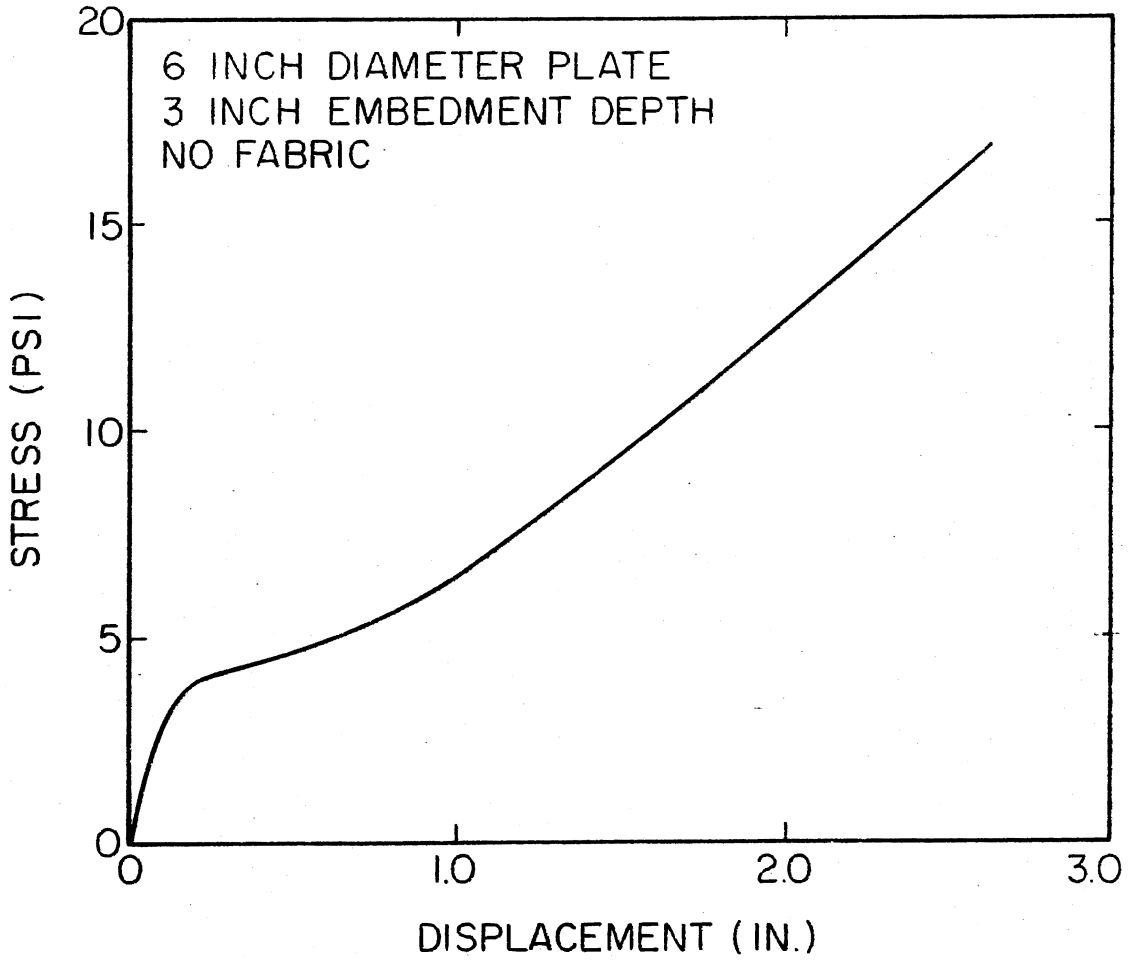

Figure 71. Load Bearing Test Data for a "No-Fabric" System Loaded with a Plate of Diameter B Equal to 6 in., with a 3 in. (0.50B) Thick Top Layer of Sand

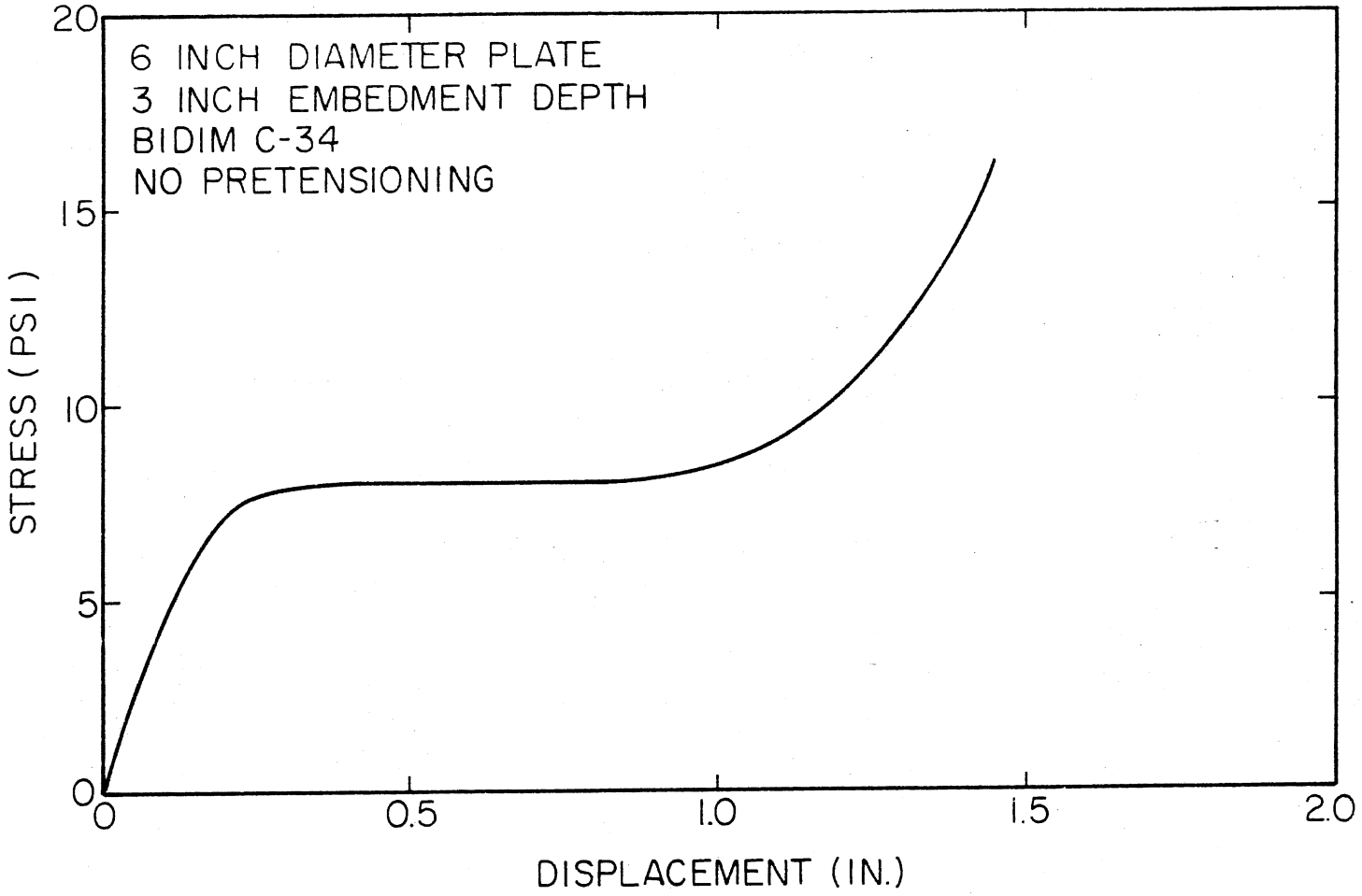

Figure 72. Load Bearing Test Data for Bidim C-34 Loaded with a Plate of Diameter B Equal to 6 in., at an Initial Embedment Depth of 3 in. (0.50B)-No Pretensioning

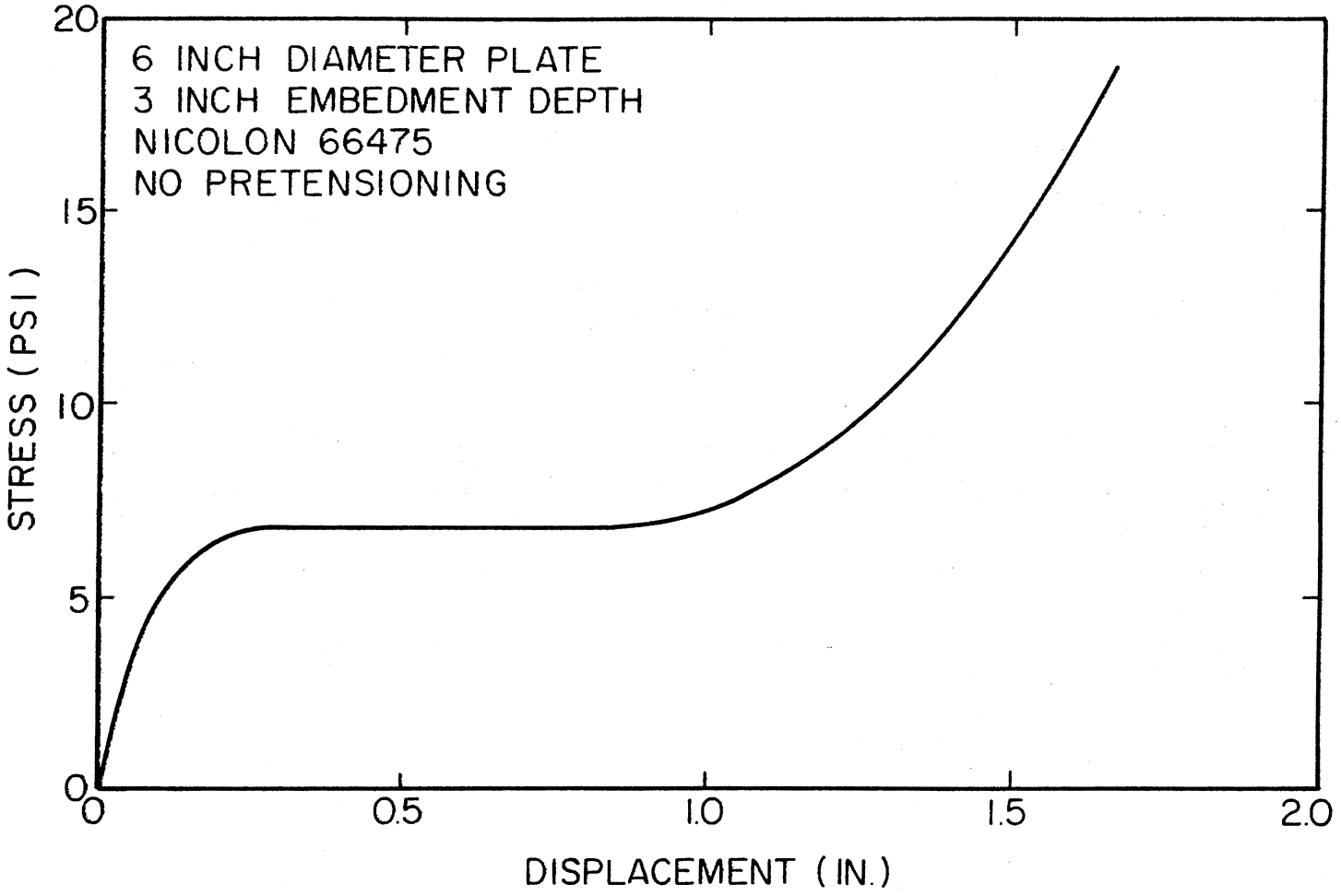

Figure 73. Load Bearing Test Data for Nicolon 66475 Loaded with a Plate of Diameter B Equal to 6 in., at an Initial Embedment Depth of 3 in. (0.50B)-No Pretensioning

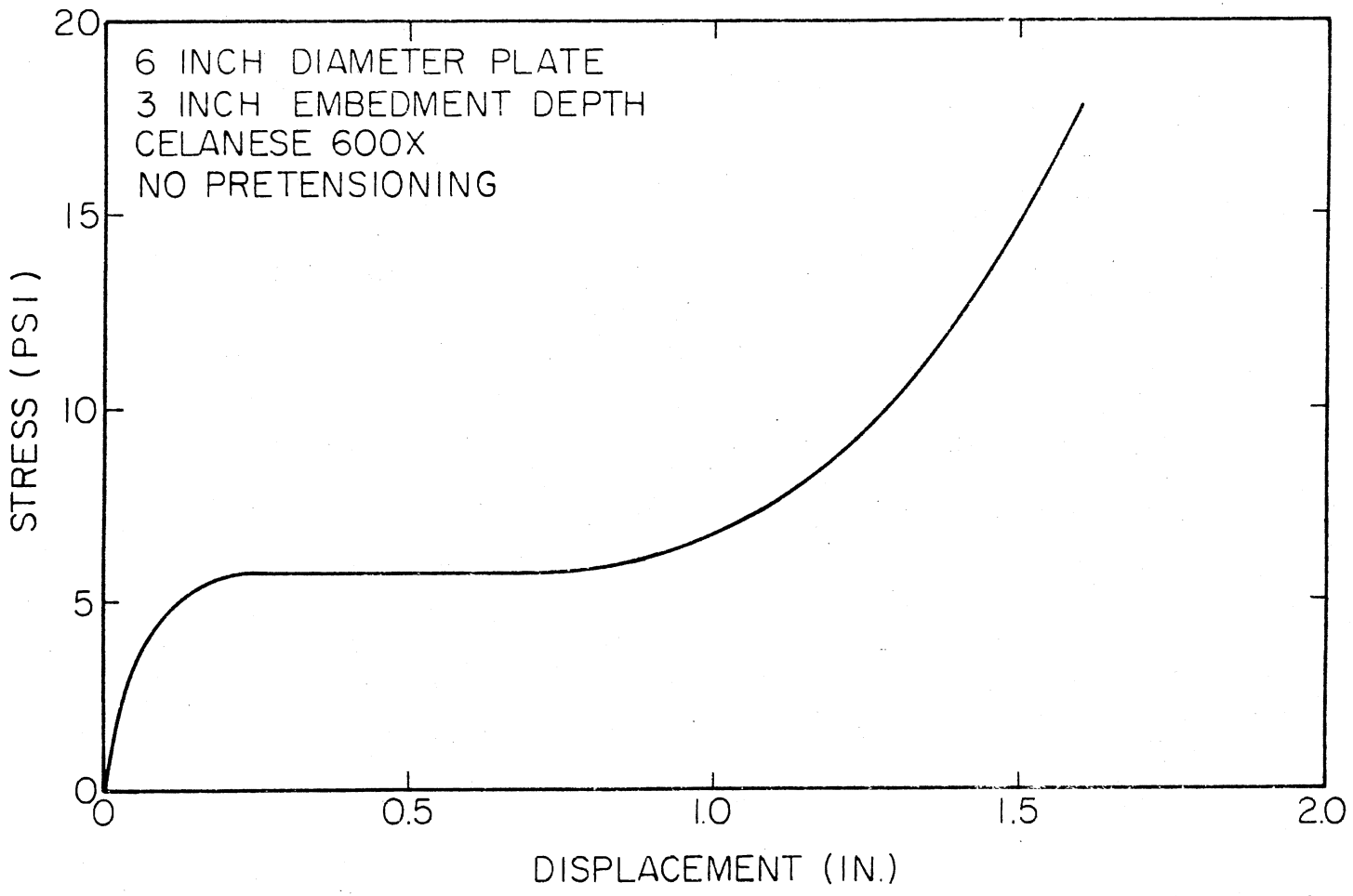

Figure 74. Load Bearing Test Data for Celanese 600X Loaded with a Plate of Diameter B Equal to 6 in., at an Initial Embedment Depth of 3 in. (0.50B)-No Pretensioning

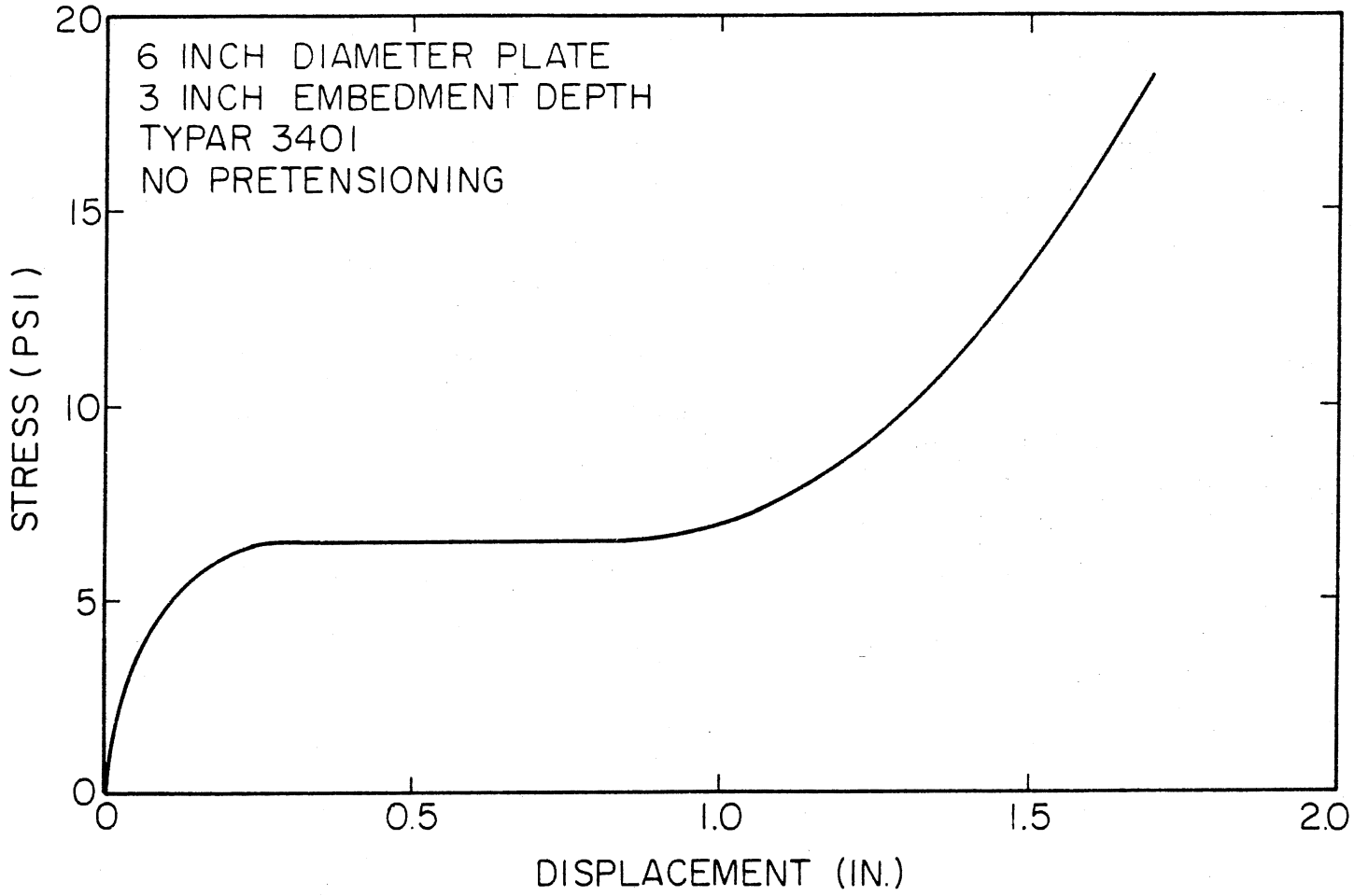

Figure 75. Load Bearing Test Data for Typar 3401 Loaded with a Plate of Diameter B Equal to 6 in., at an Initial Embedment Depth of 3 in. (0.50B)-No Pretensioning

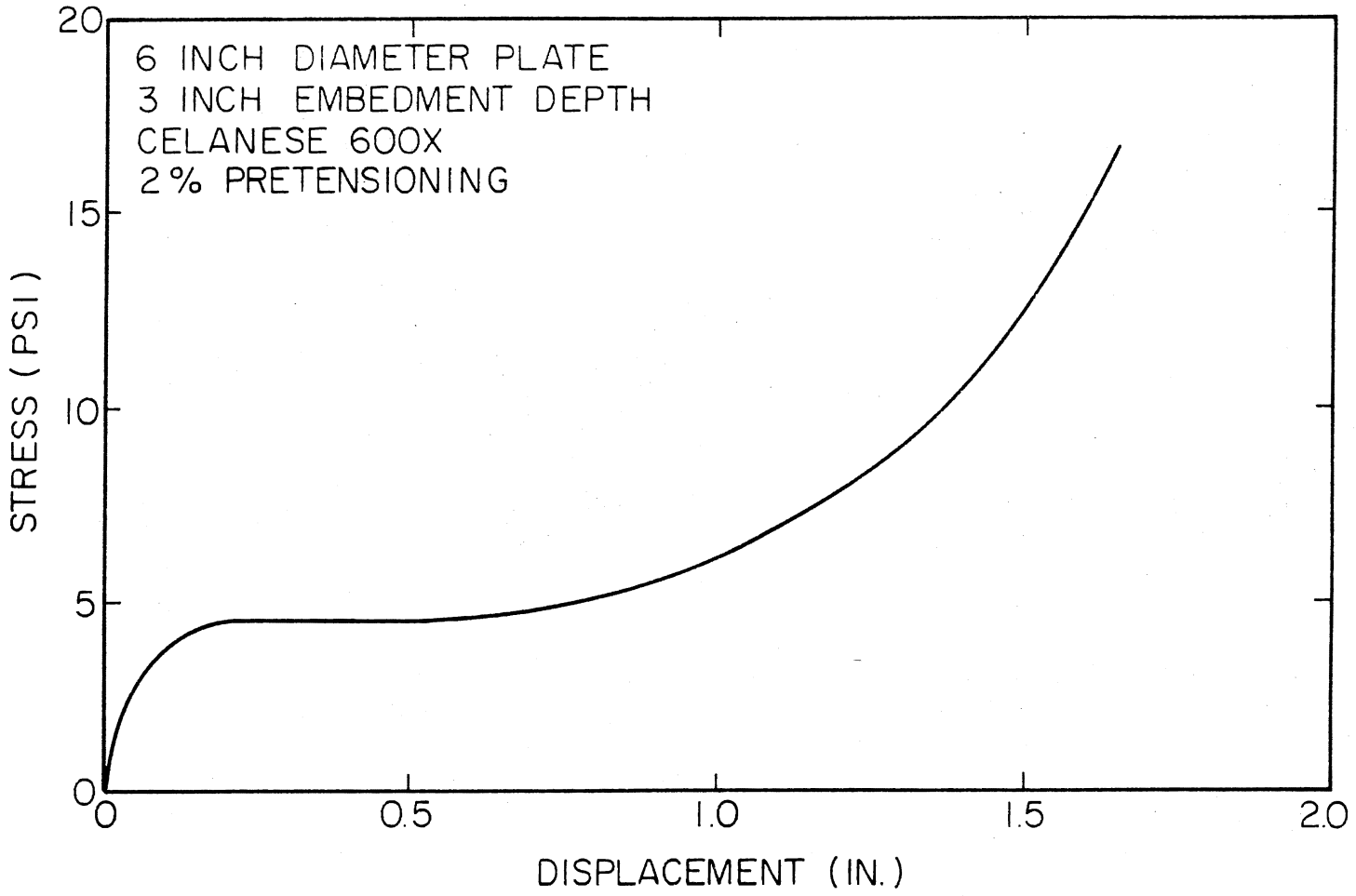

Figure 76. Load Bearing Test Data for Celanese 600X Loaded with a Plate of Diameter B Equal to 6 in., at an Initial Embedment Depth of 3 in. (0.50B)-2 Percent Pretensioning

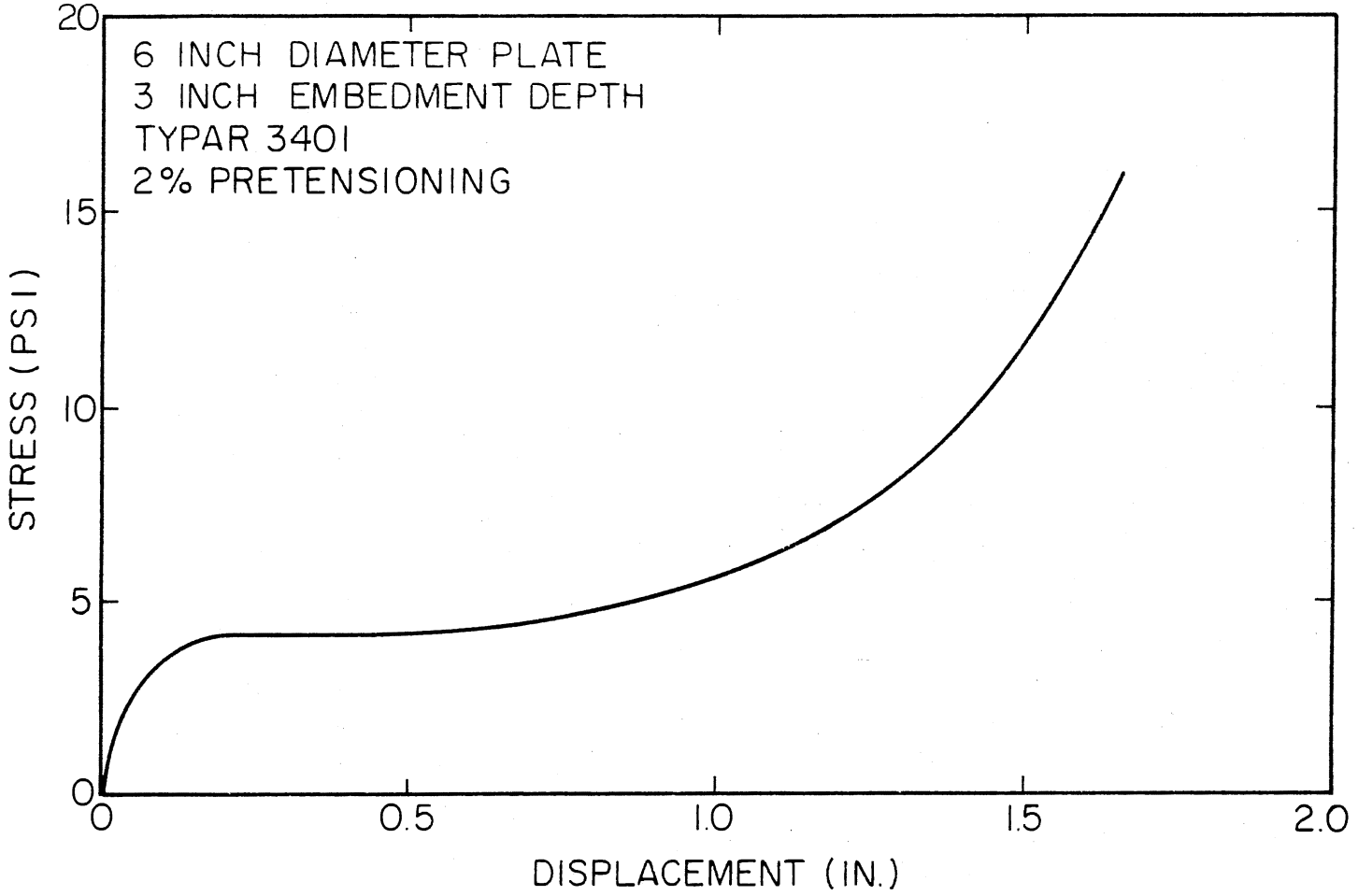

Figure 77. Load Bearing Test Data for Typar 3401 Loaded with a Plate of Diameter B Equal to 6 in., at an Initial Embedment Depth of 3 in. (0.50B)-2 Percent Pretensioning

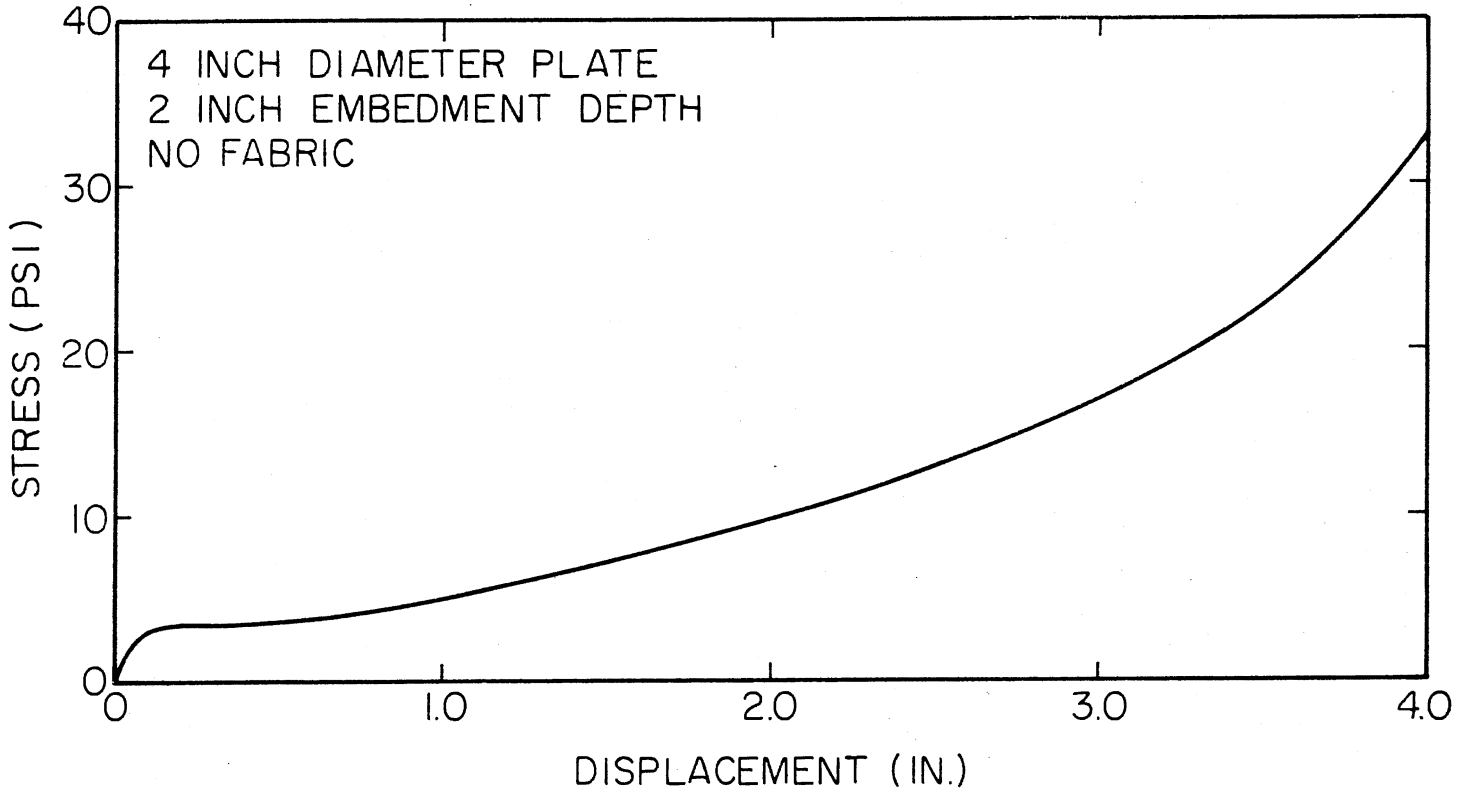

Figure 78. Load Bearing Test Data for a "No-Fabric" System Loaded with a Plate of Diameter B Equal to 4 in., with a 2 in. (0.50B) Thick Top Layer of Sand

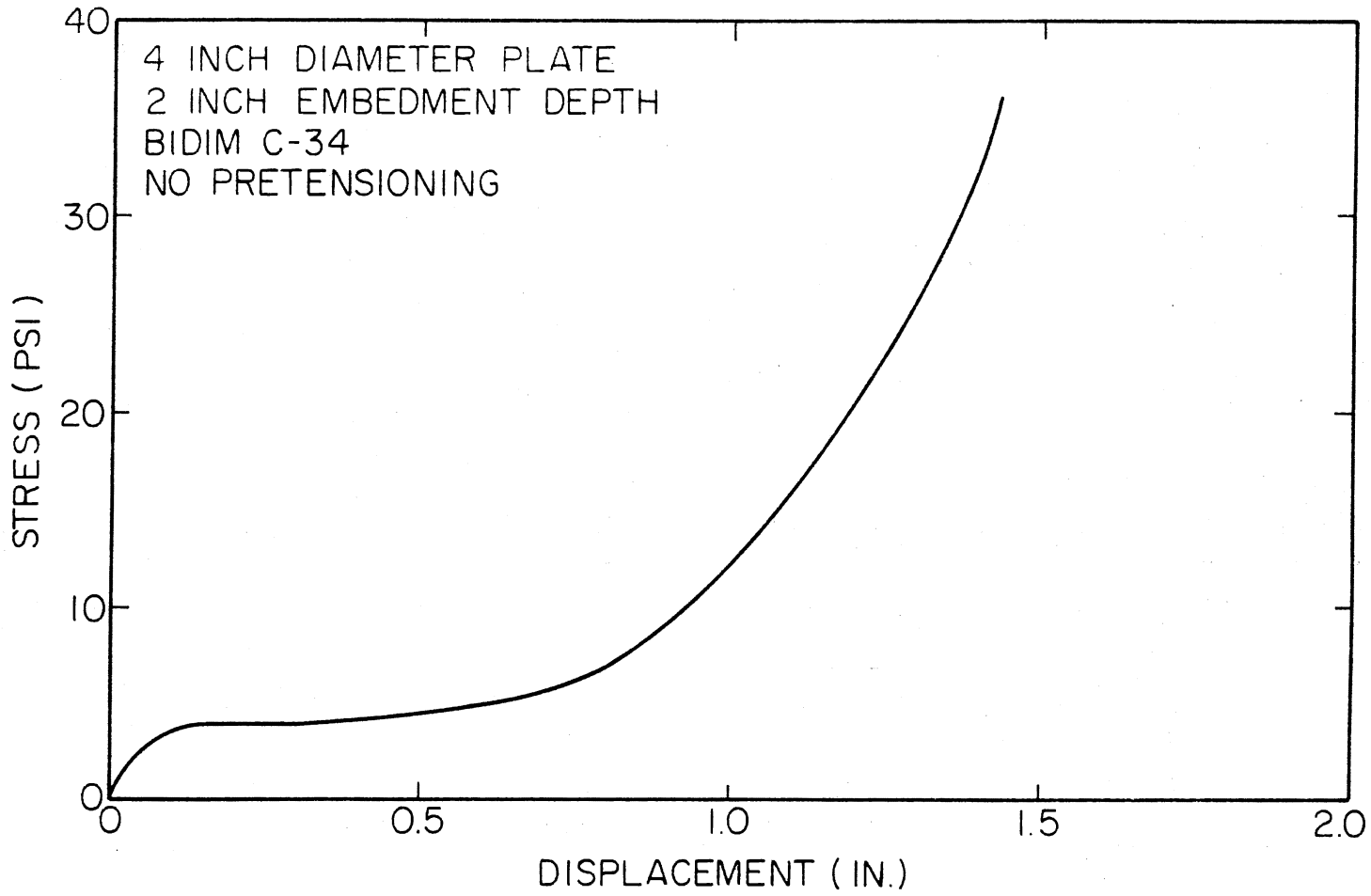

Figure 79. Load Bearing Test Data for Bidim C-34 Loaded with a Plate of Diameter B Equal to 4 in., at an Initial Embedment Depth of 2 in. (0.50B)-No Pretensioning

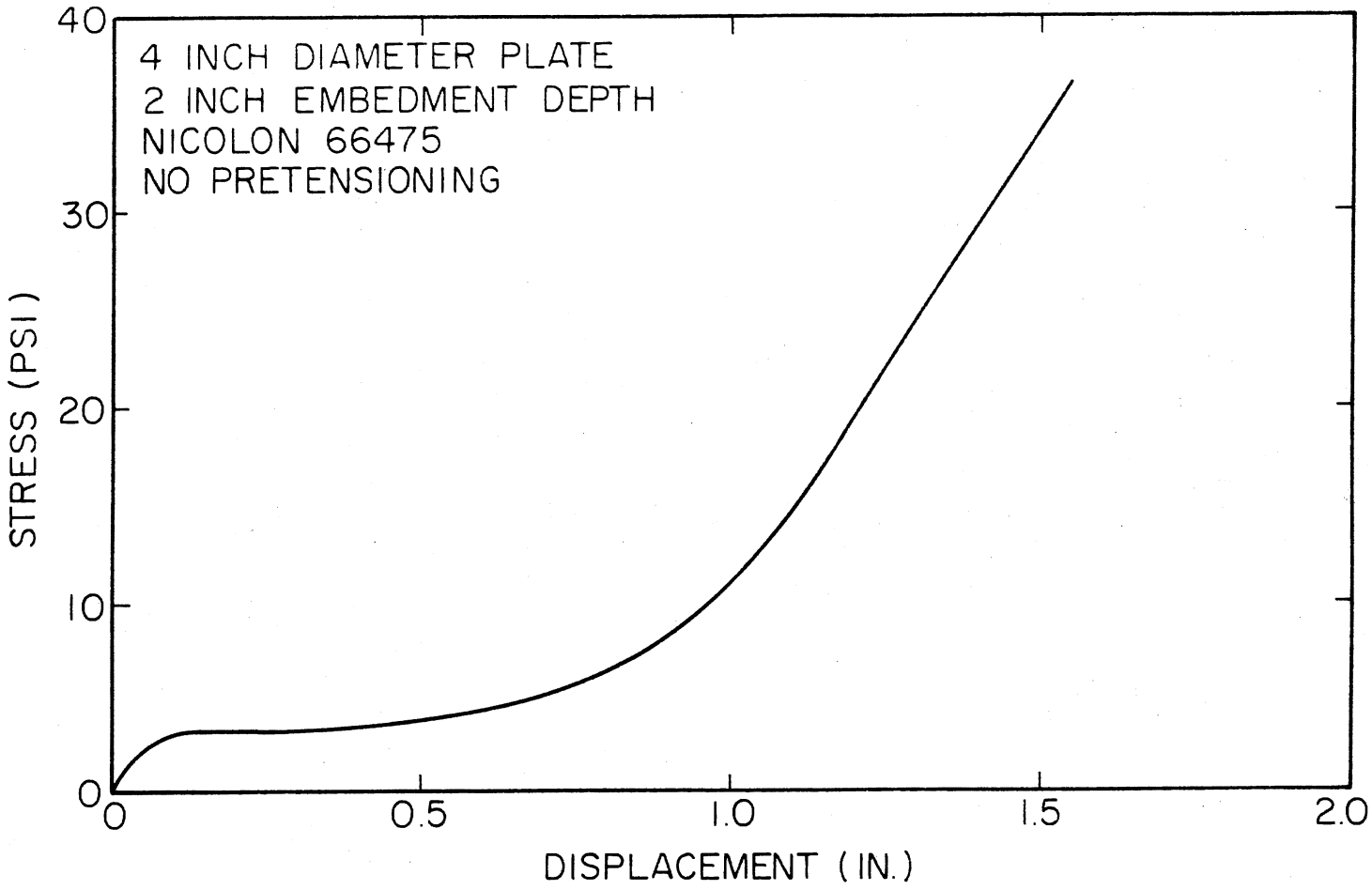

Figure 80. Load Bearing Test Data for Nicolon 66475 Loaded with a Plate of Diameter B Equal to 4 in., at an Initial Embedment Depth of 2 in. (0.50B)-No Pretensioning

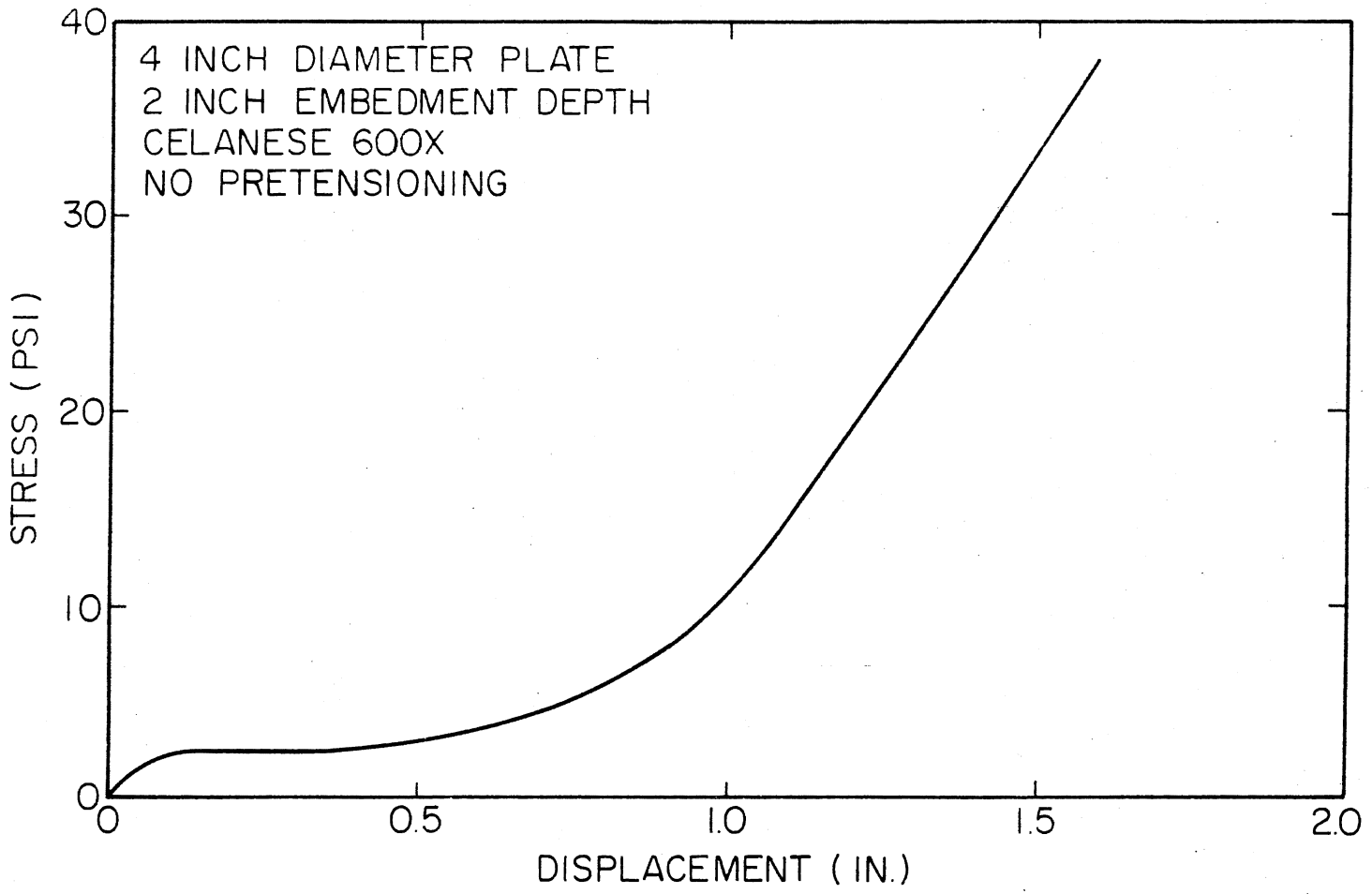

Figure 81. Load Bearing Test Data for Celanese 600X Loaded with a Plate of Diameter B Equal to 4 in., at an Initial Embedment Depth of 2 in. (0.50B)-No Pretensioning

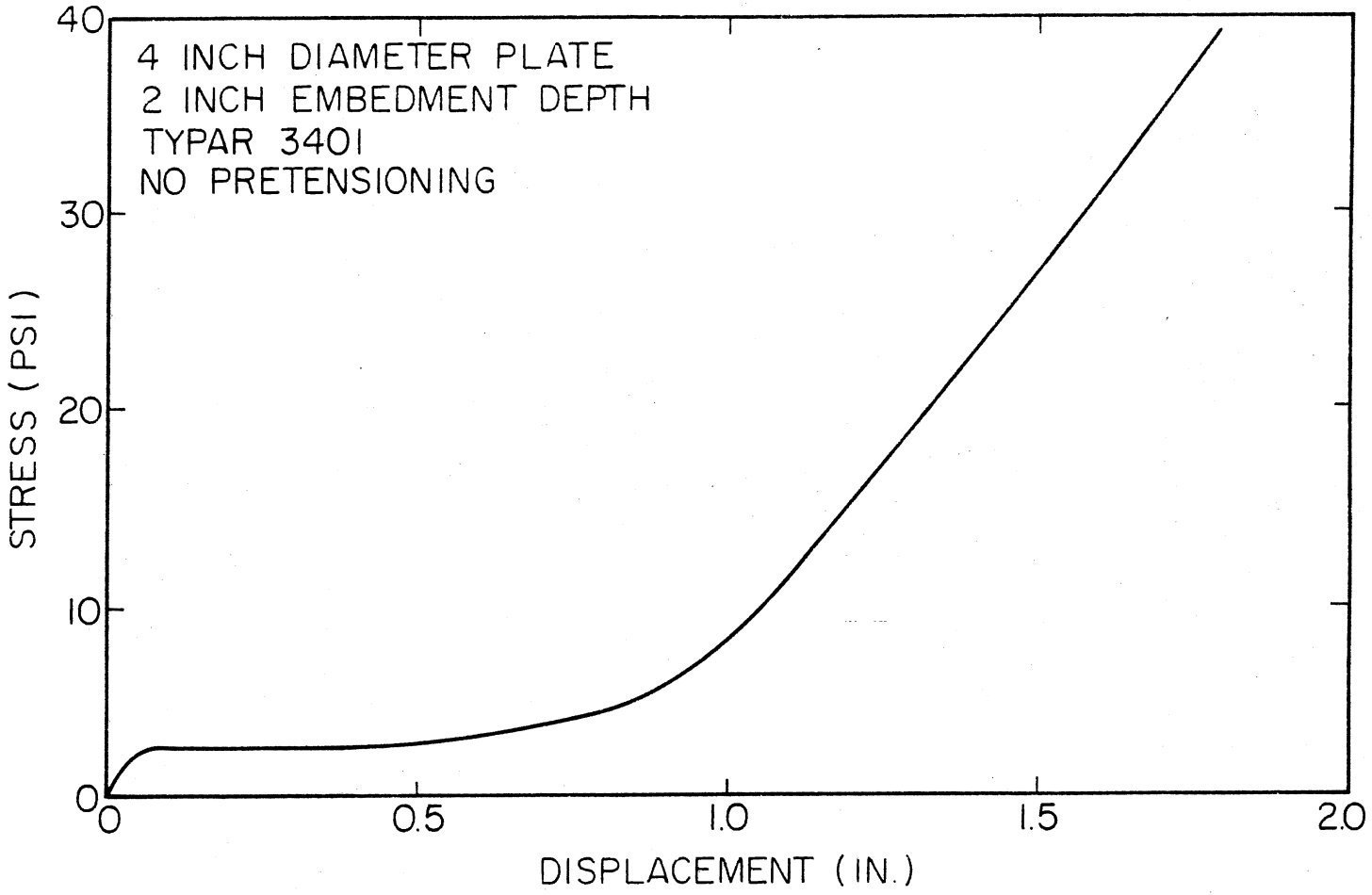

Figure 82. Load Bearing Test Data for Typar 3401 Loaded with a Plate of Diameter B Equal to 4 in., at an Initial Embedment Depth of 2 in. (0.50B)-No Pretensioning

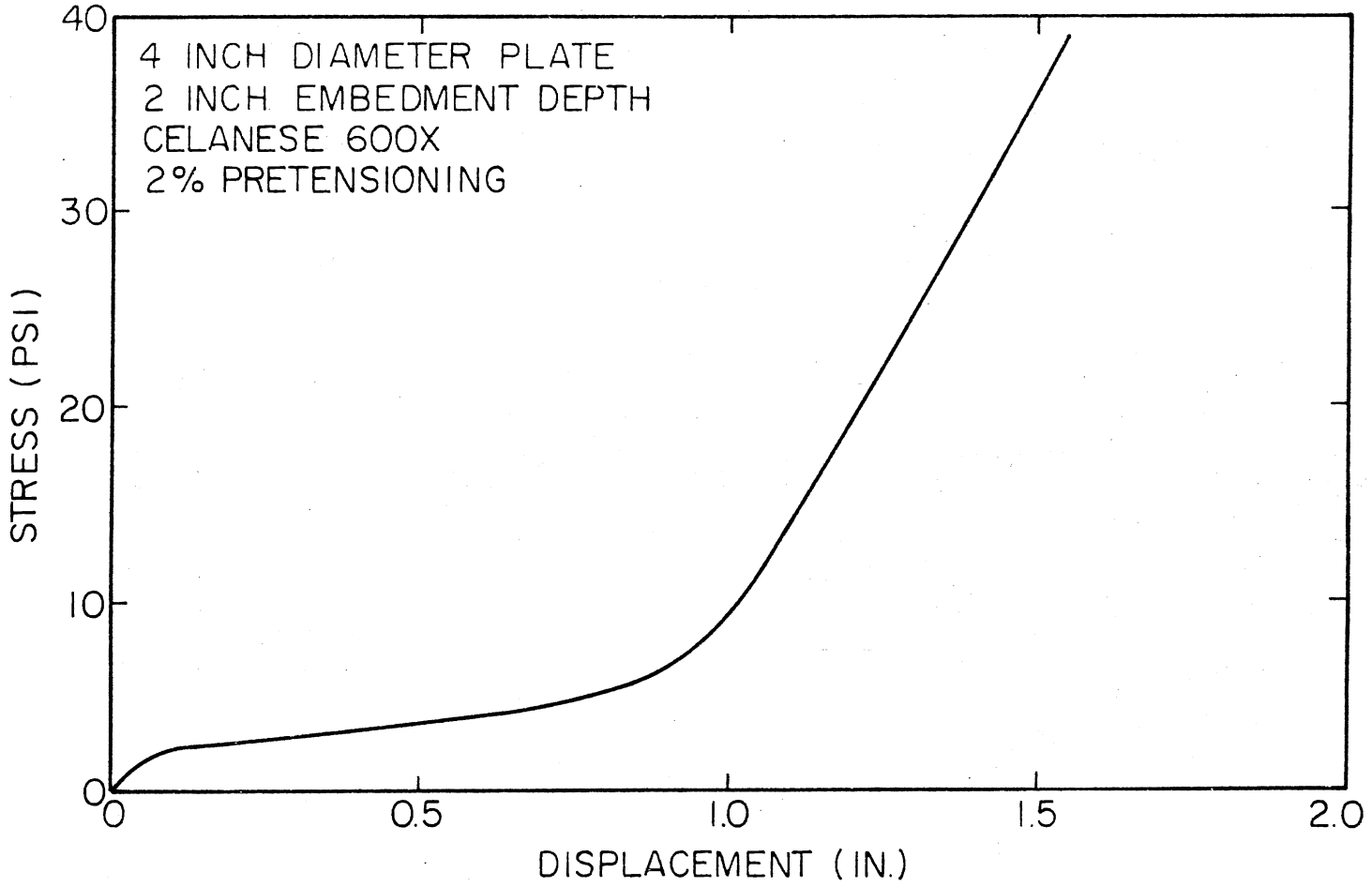

Figure 83. Load Bearing Test Data for Celanese 600X Loaded with a Plate of Diameter B Equal to 4 in., at an Initial Embedment Depth of 2 in. (0.50B)-2 Percent Pretensioning

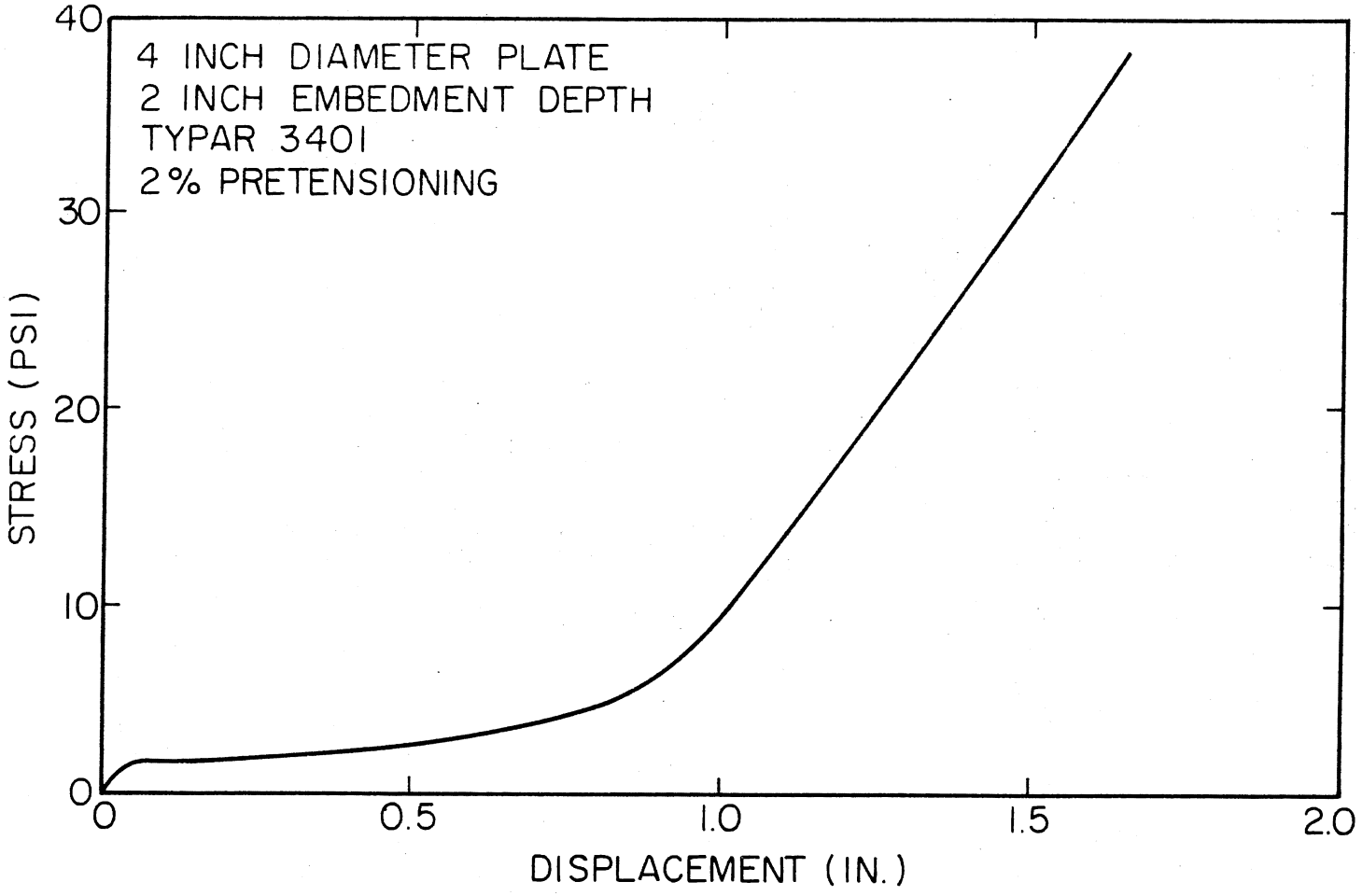

Figure 84. Load Bearing Test Data for Typar 3401 Loaded with a Plate of Diameter B Equal to 4 in., at an Initial Embedment Depth of 2 in. (0.50B)-2 Percent Pretensioning

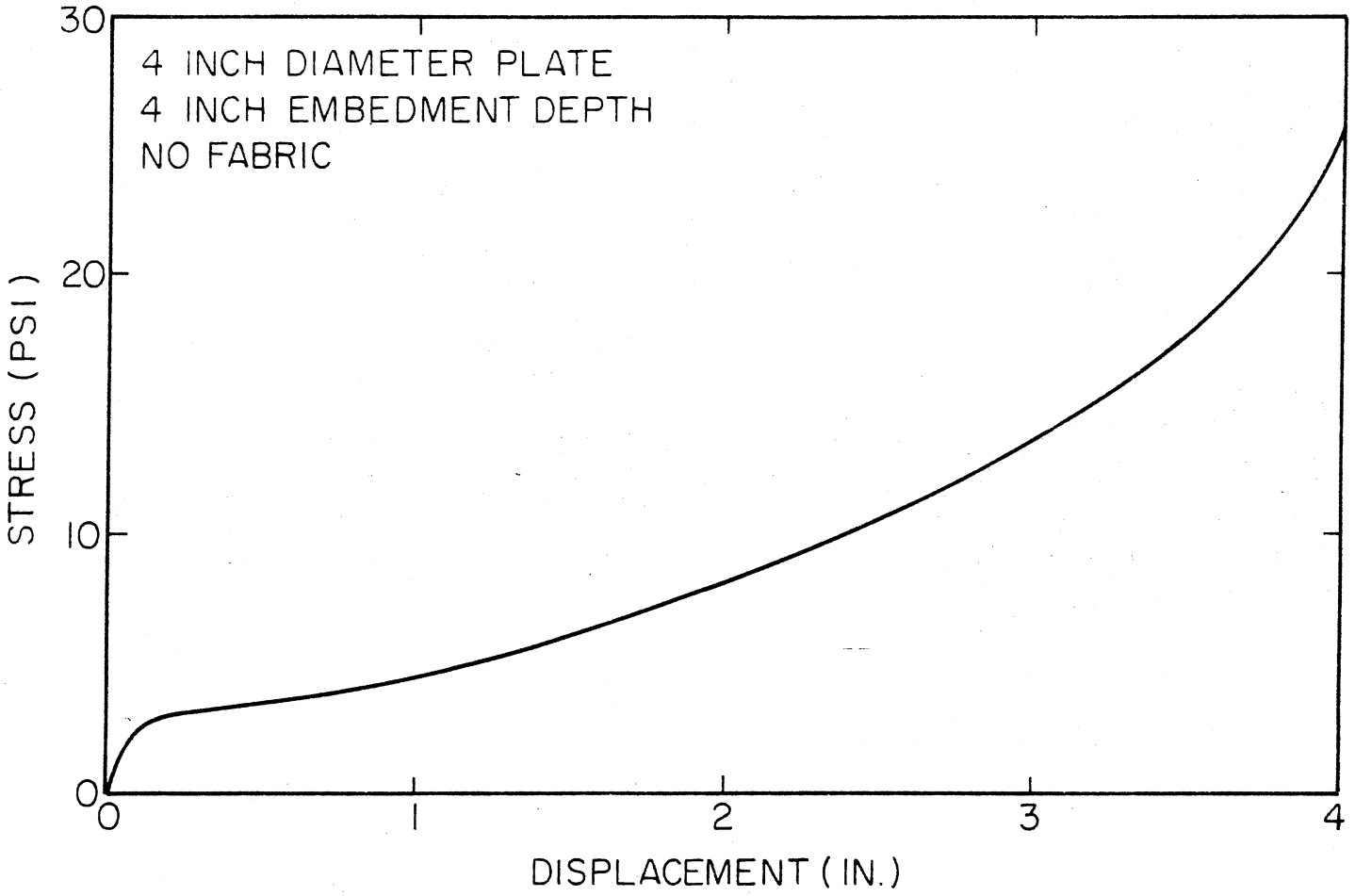

Figure 85. Load Bearing Test Data for a "No-Fabric" System Loaded with a Plate of Diameter B Equal to 4 in., with a 4 in. (1.00B) Thick Top Layer of Sand

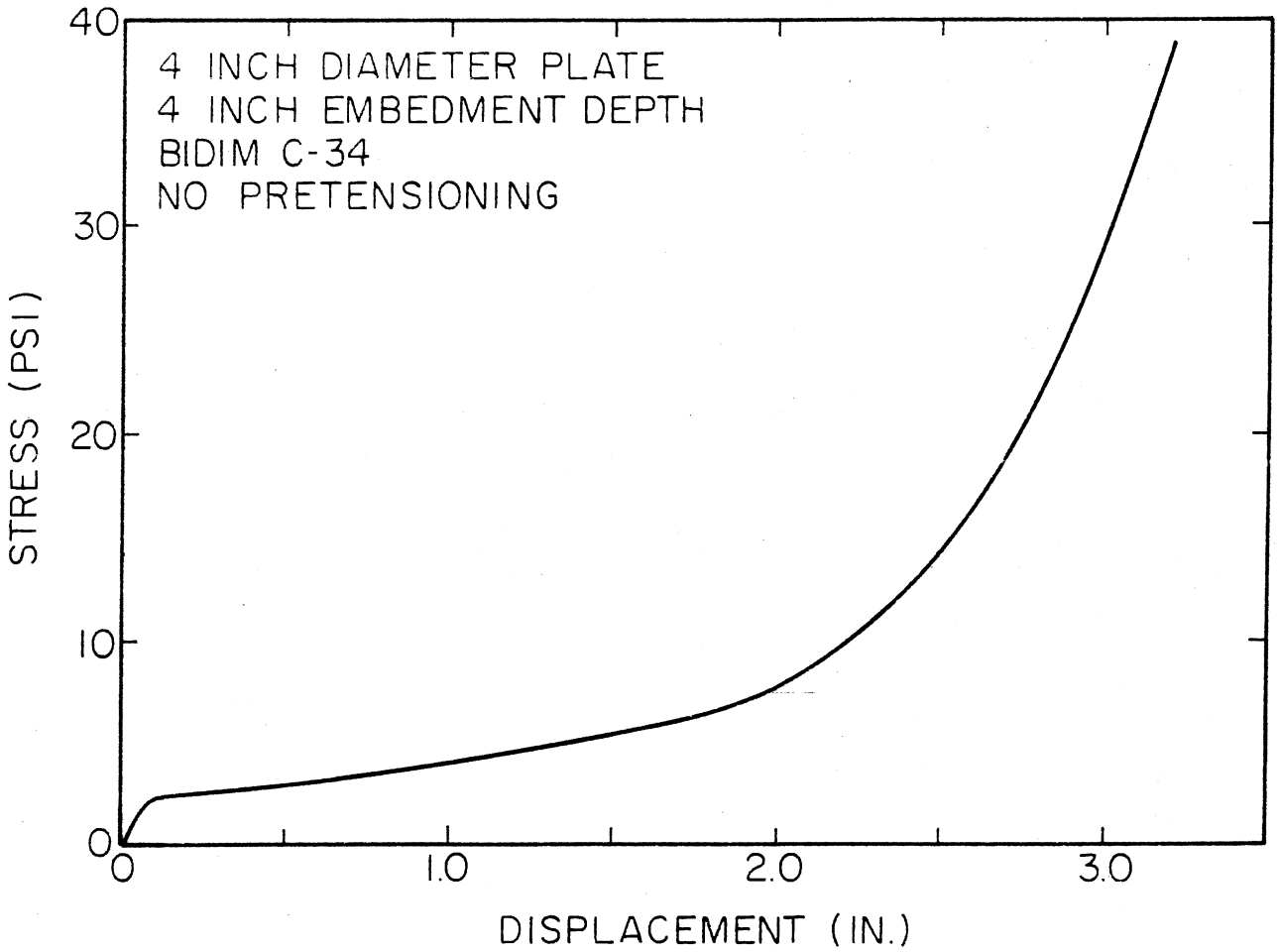

Figure 86. Load Bearing Test Data for Bidim C-34 Loaded with a Plate of Diameter B Equal to 4 in., at an Initial Embedment Depth of 4 in. (1.00B)-No Pretensioning

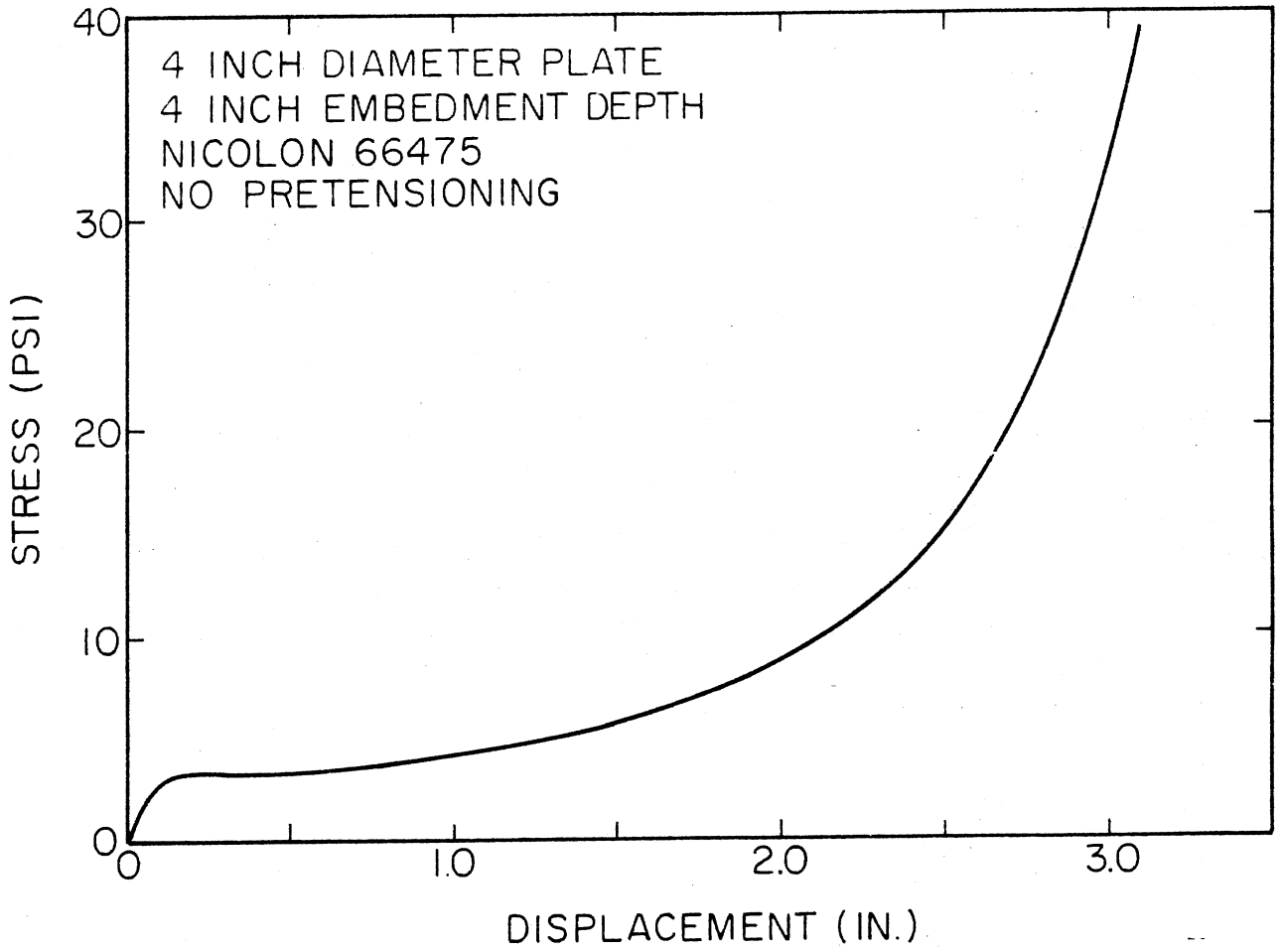

Figure 87. Load Bearing Test Data for Nicolon 66475 Loaded with a Plate of Diameter B Equal to 4 in., at an Initial Embedment Depth of 4 in. (1.00B)-No Pretensioning

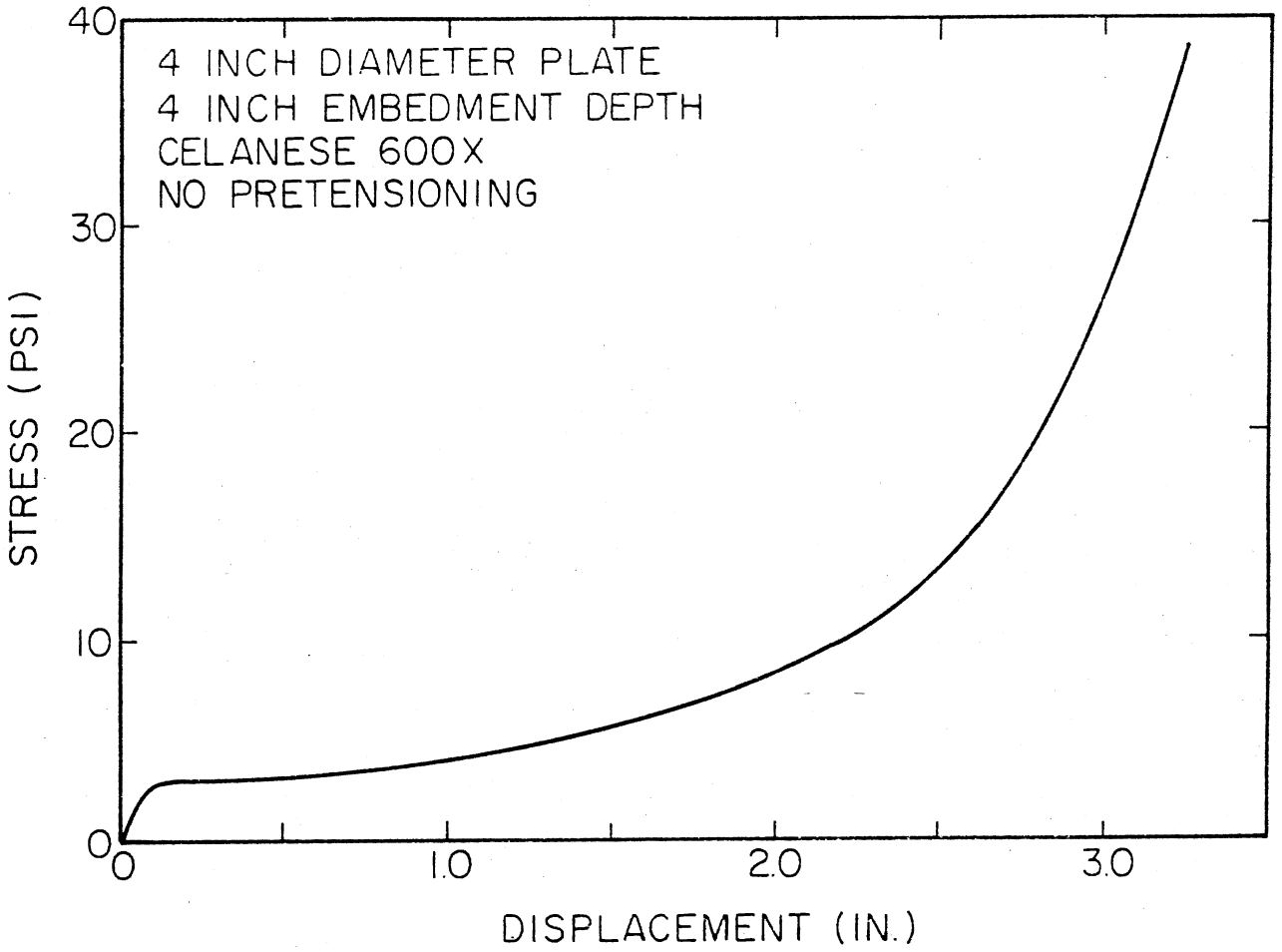

Figure 88. Load Bearing Test Data for Celanese 600X Loaded with a Plate of Diameter B Equal to 4 in., at an Initial Embedment Depth of 4 in. (1.00B)-No Pretensioning

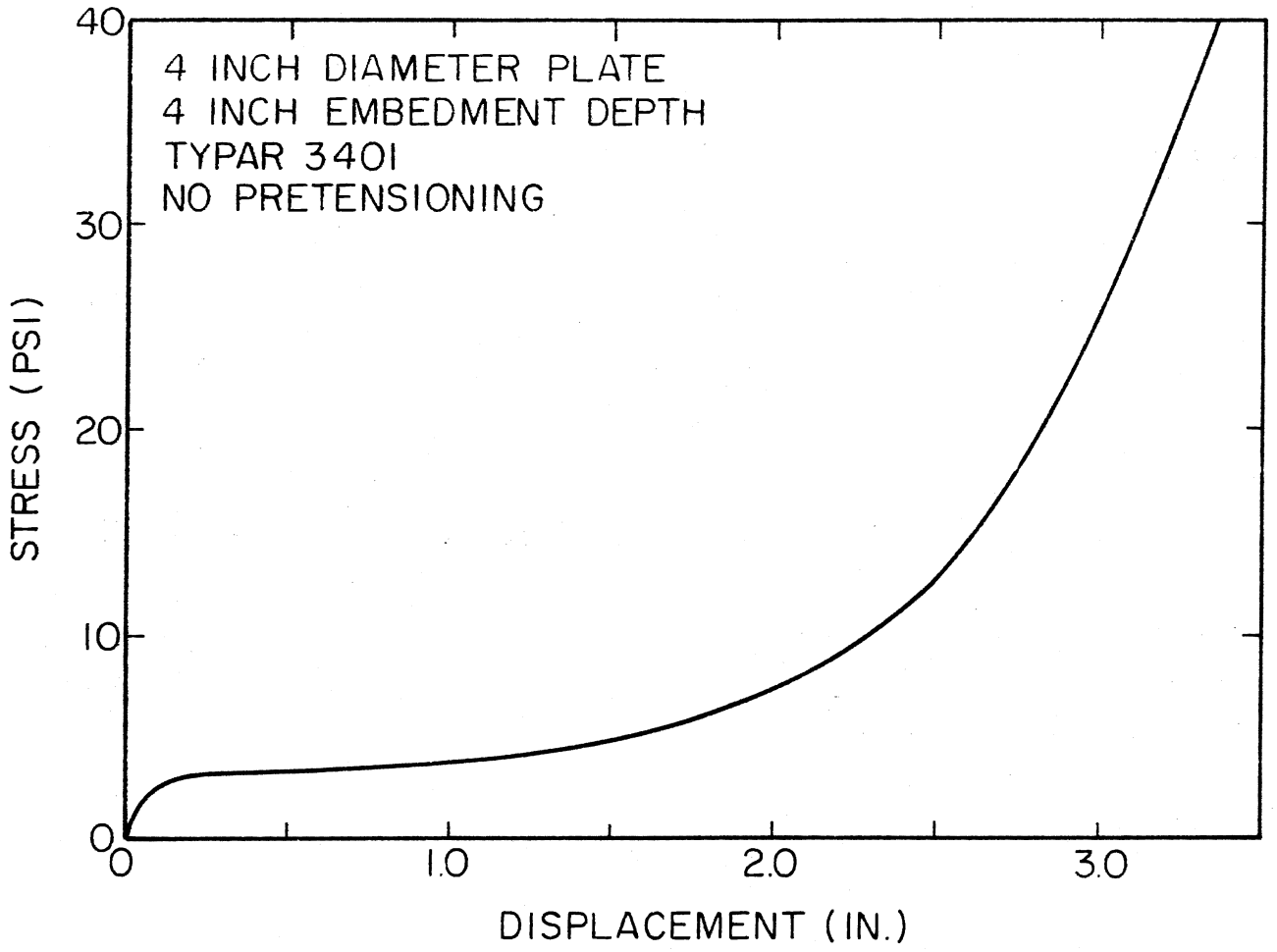

Figure 89. Load Bearing Test Data for Typar 3401 Loaded with a Plate of Diameter B Equal to 4 in., at an **Initial** Embedment Depth of 4 in. (1.00B)-No Pretensioning

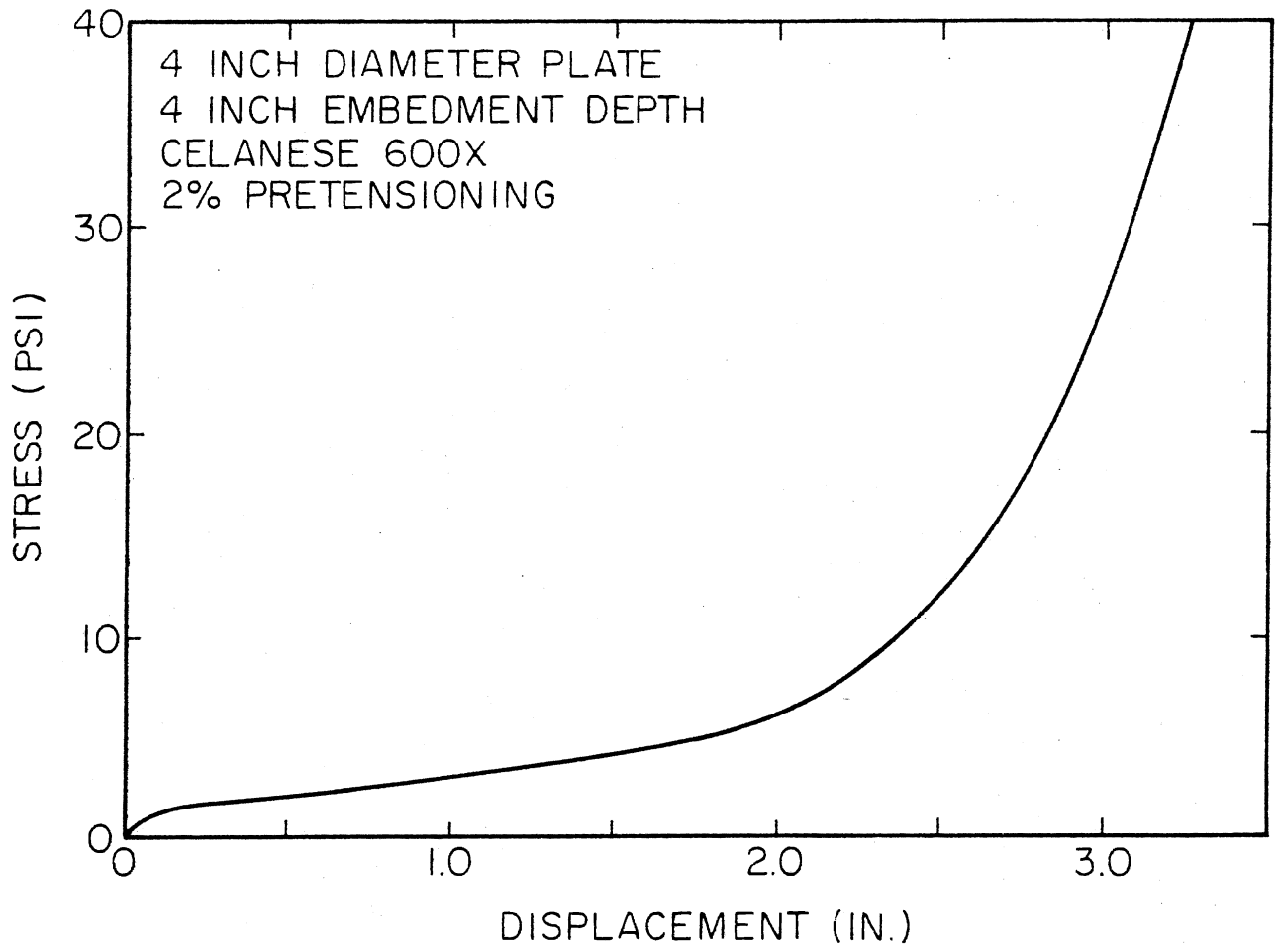

Figure 90. Load Bearing Test Data for Celanese 600X Loaded with a Plate of Diameter B Equal to 4 in., at an Initial Embedment Depth of 4 in. (1.00B)-2 Percent Pretensioning

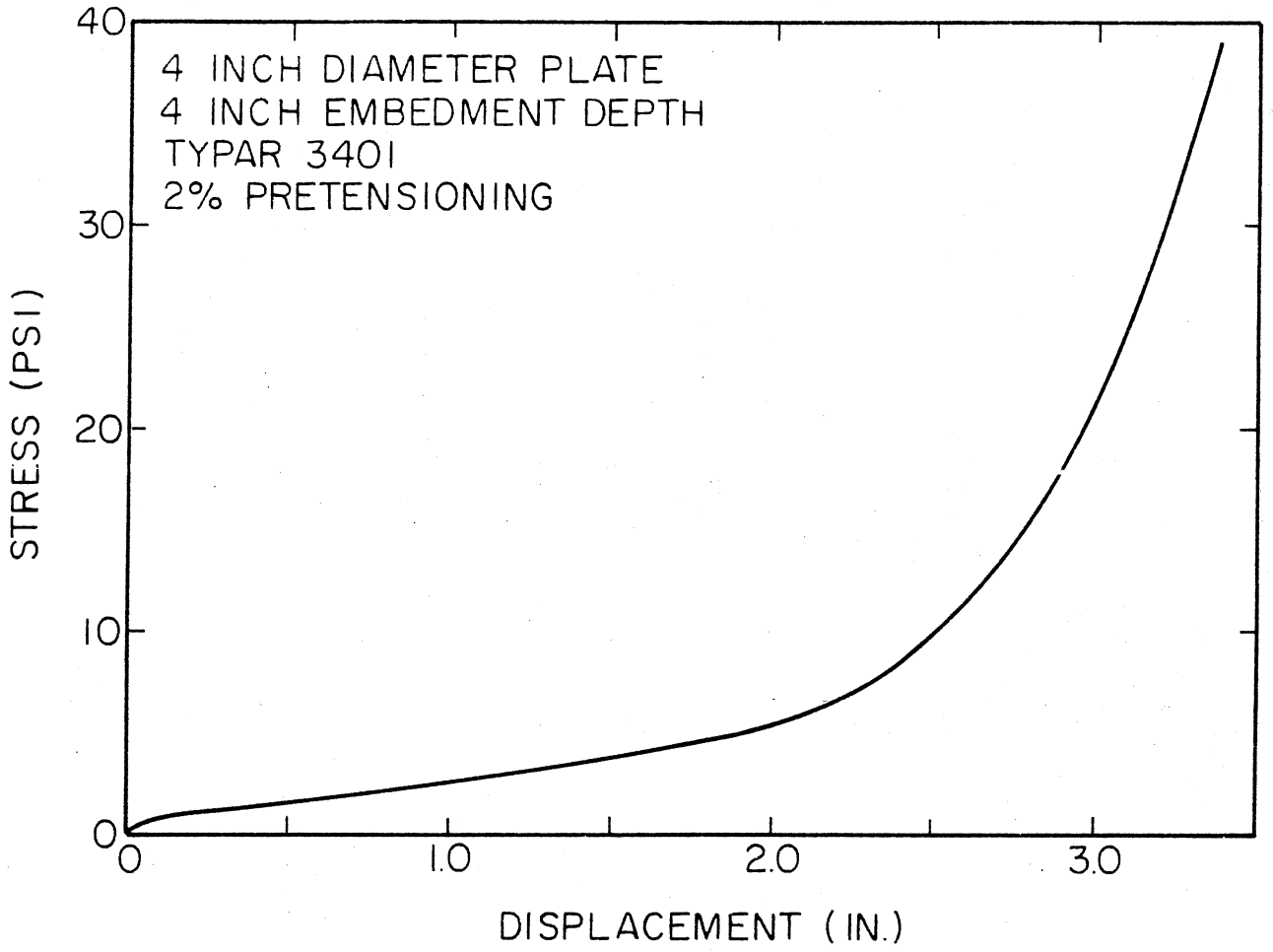

Figure 91. Load Bearing Test Data for Typar 3401 Loaded with a Plate of Diameter B Equal to 4 in., at an Initial Embedment Depth of 4 in. (1.00B)-2 Percent Pretensioning

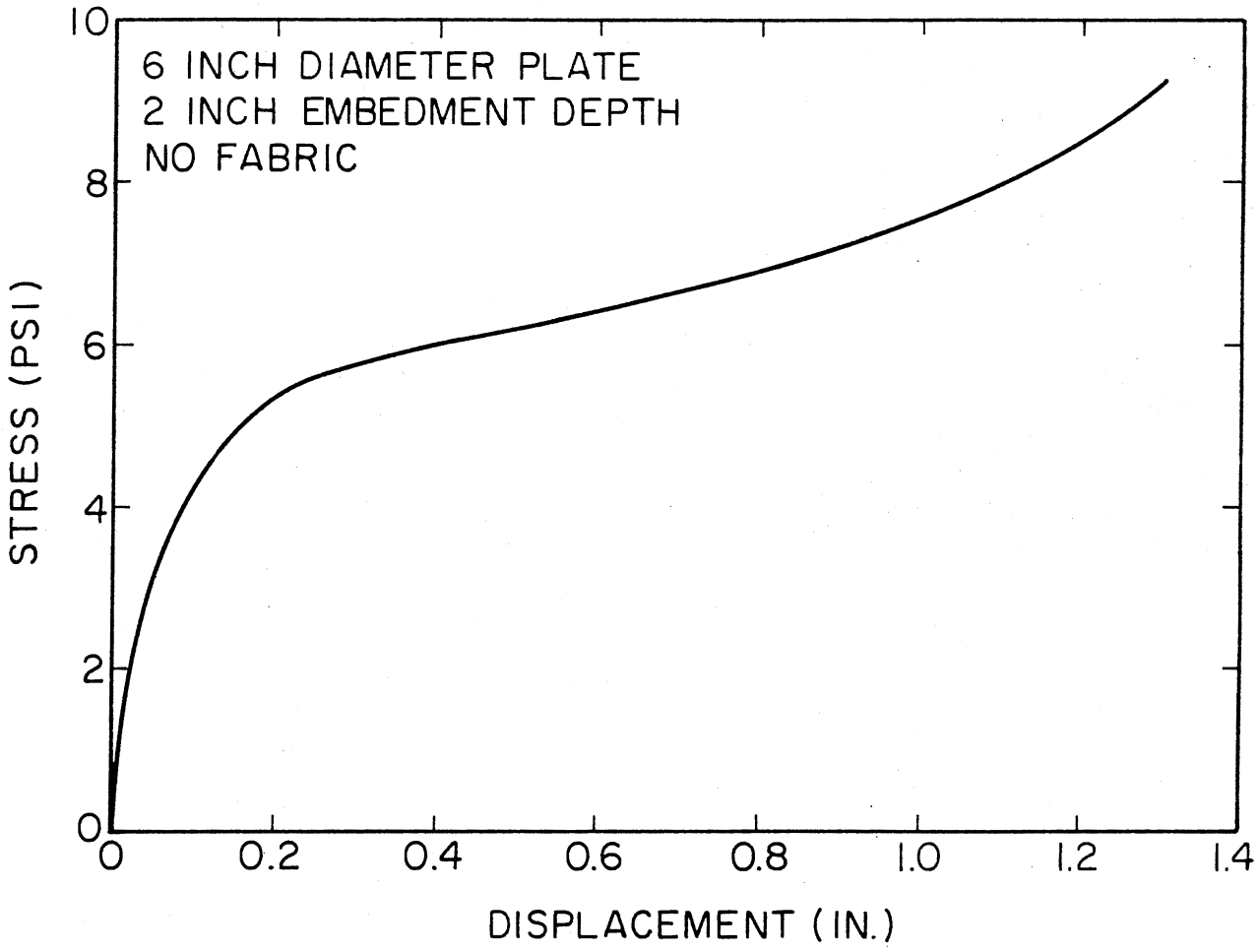

Figure 92. Load Bearing Test Data for a "No-Fabric" System Loaded with a Plate of Diameter B Equal to 6 in., with a 2 in. (0.33B) Thick Top Layer of Sand

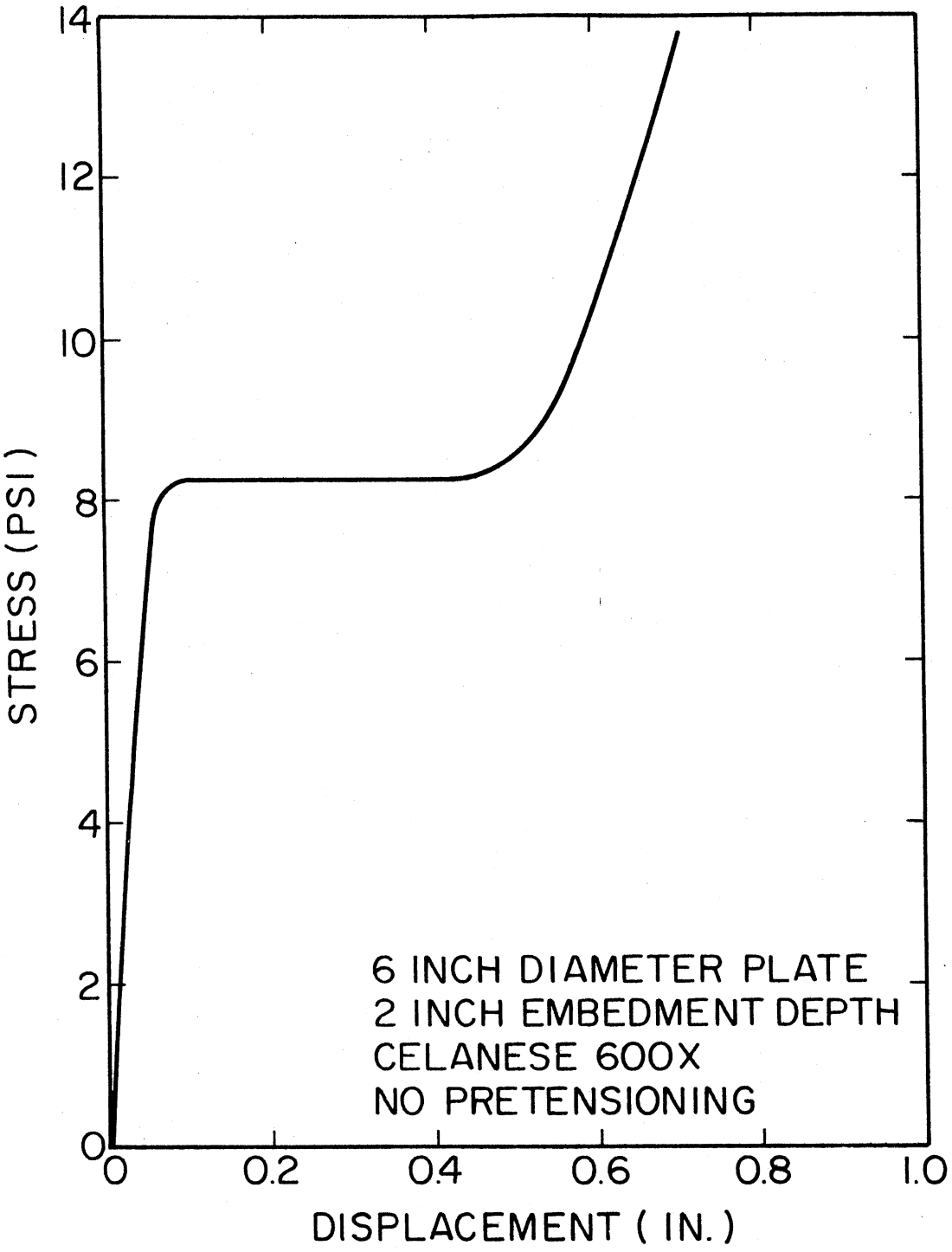

Figure 93. Load Bearing Test Data for Celanese 600X Loaded with a Plate of Diameter B Equal to 6 in., at an Initial Embedment Depth of 2 in. (0.33B)-No Pretensioning

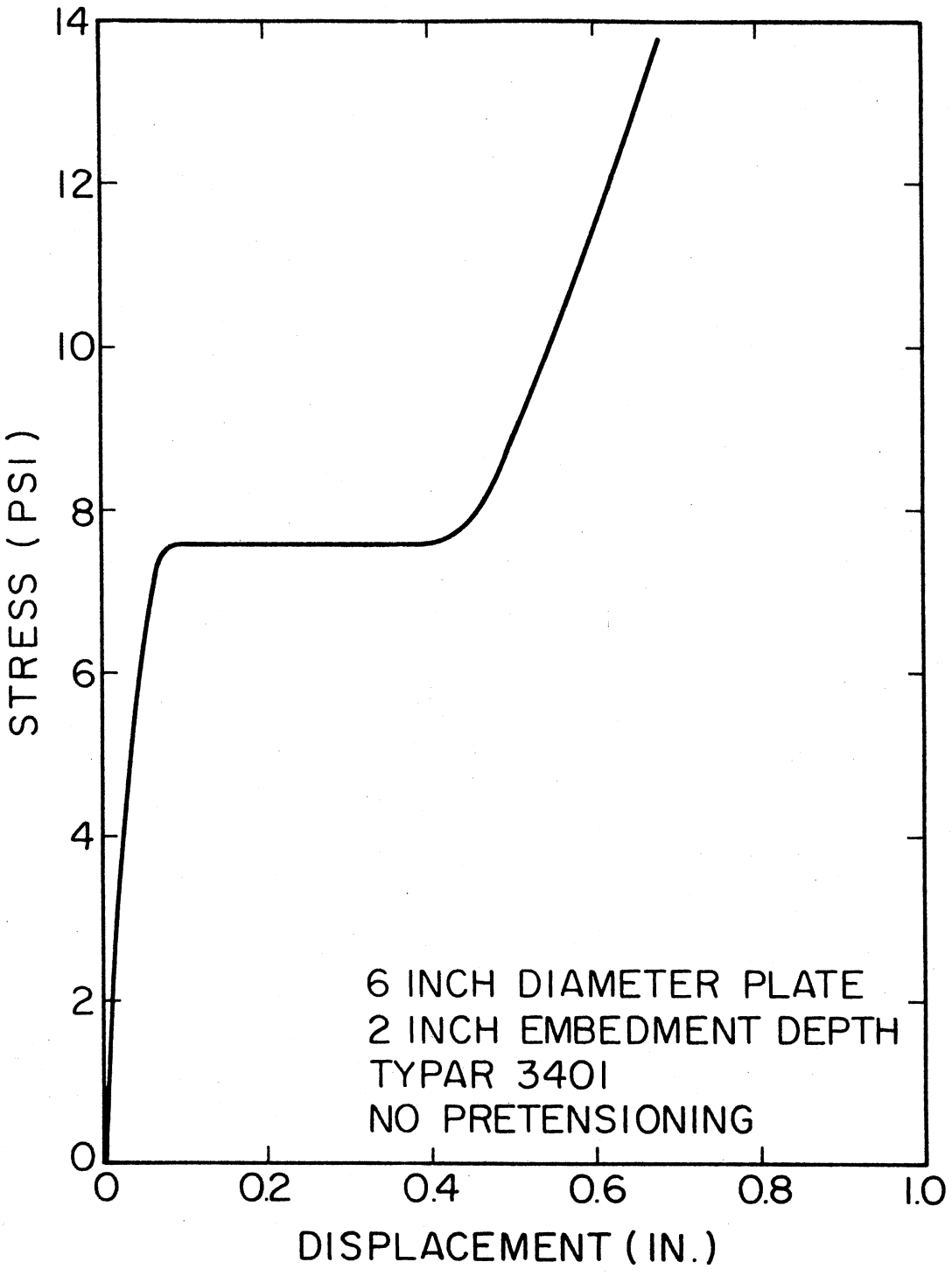

Figure 94. Load Bearing Test Data for Typar 3401 Loaded with a Plate of Diameter B Equal to 6 in., at an Initial Embedment Depth of 2 in. (0.33B)-No Pretensioning

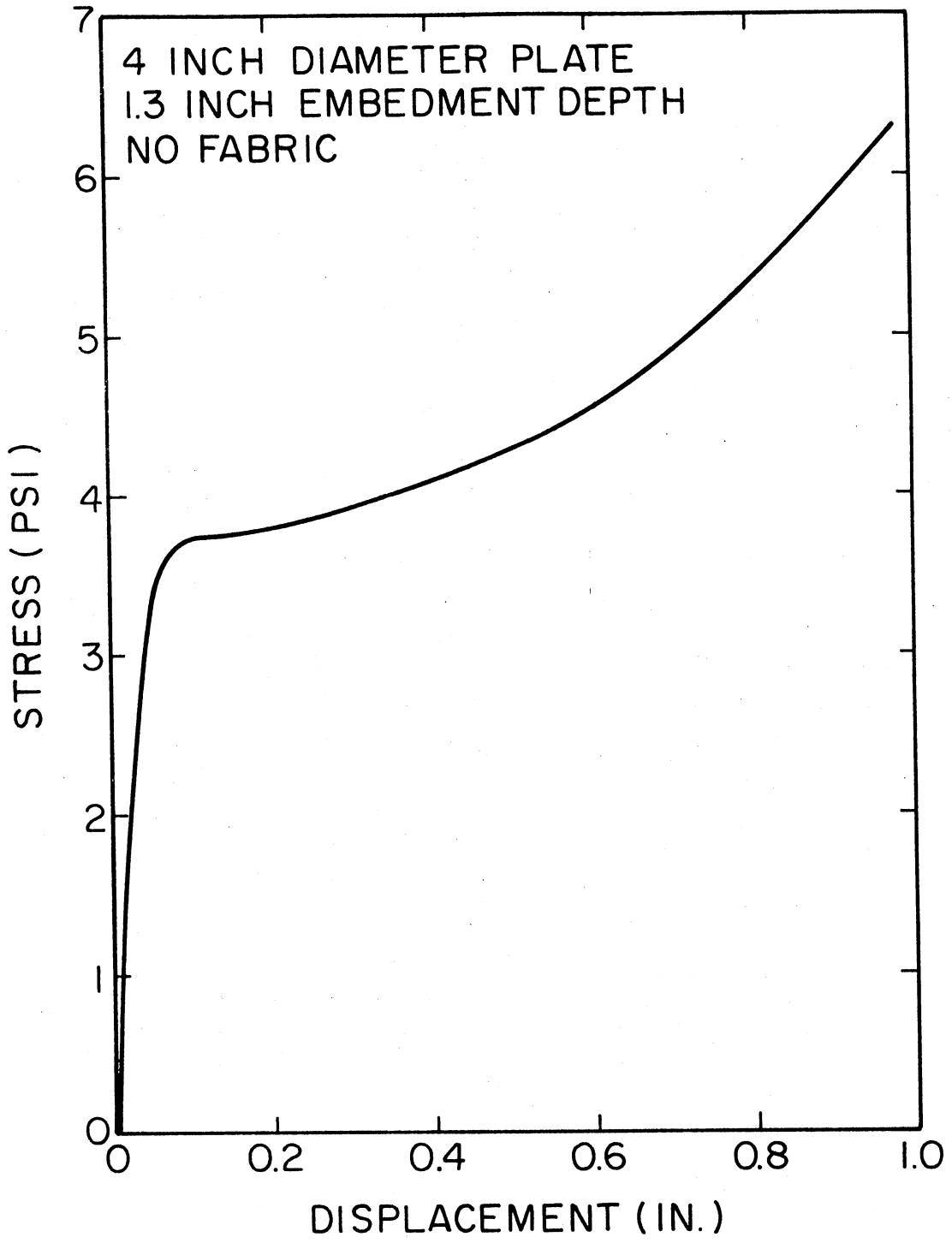

Figure 95. Load Bearing Test Data for a "No-Fabric" System Loaded with a Plate of Diameter B Equal to 4 in., with a 1.33 in. (0.33B) Thick Top Layer of Sand

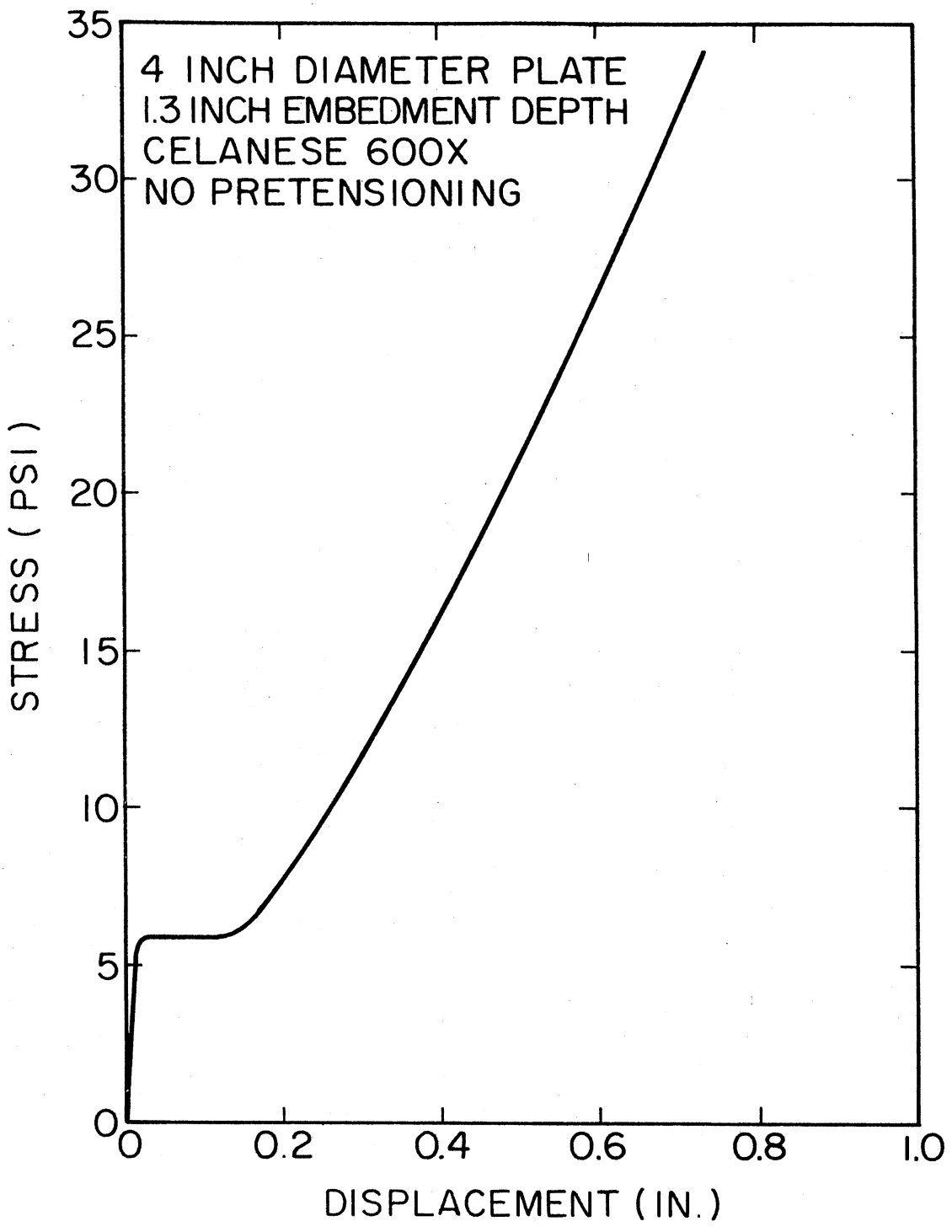

Figure 96. Load Bearing Test Data for Celanese 600X Loaded with a Plate of Diameter B Equal to 4 in., at an Initial Embedment Depth of 1.33 in. (0.33B)-No Pretensioning

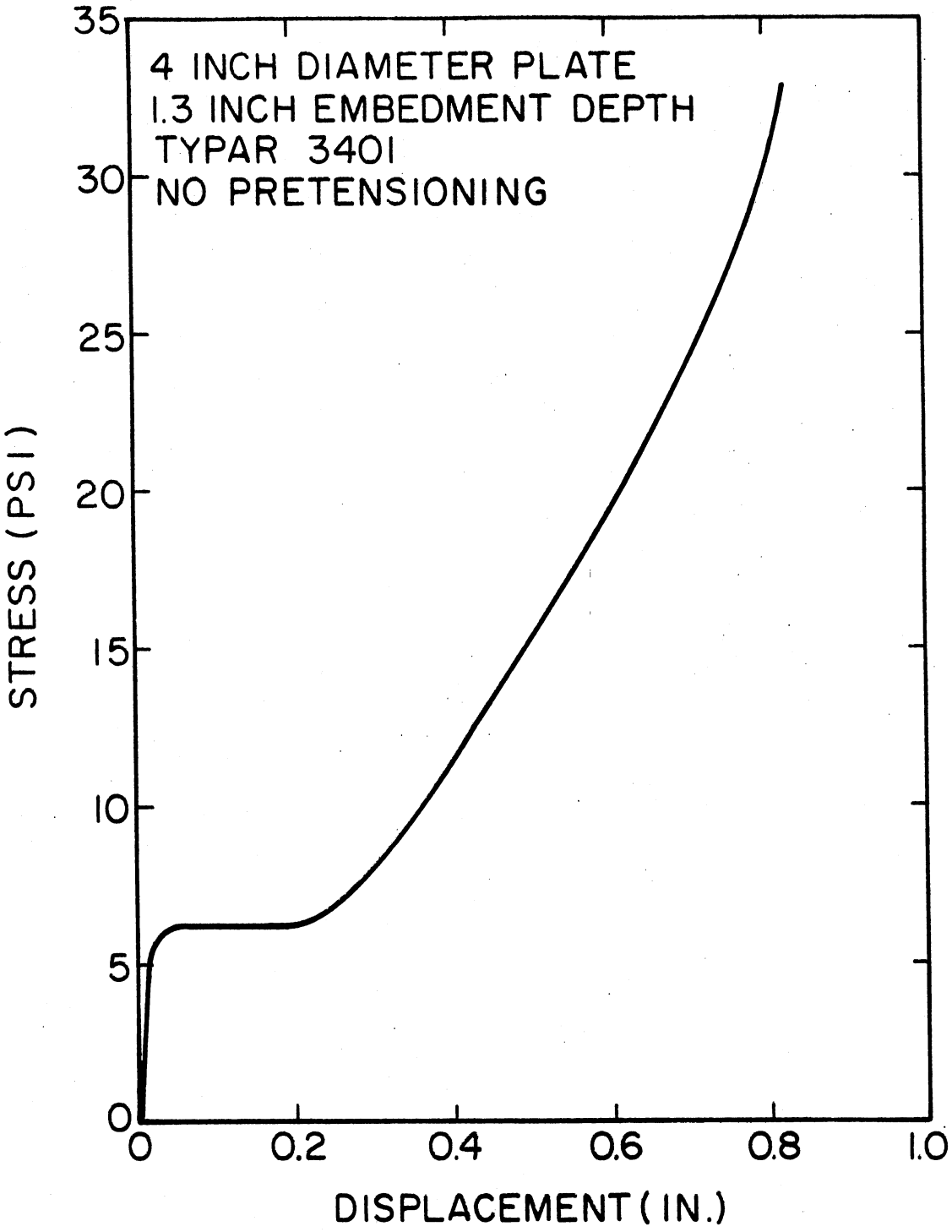

Figure 97. Load Bearing Test Data for Typar 3401 Loaded with a Plate of Diameter B Equal to 4 in., at an Initial Embedment Depth of 1.33 In. (0.33B)-No Pretensioning

VITA

Jack D. Lawmaster

Candidate for the Degree of

Master of Science

Thesis: A LABORATORY STUDY OF THE ROLE OF GEOTECHNICAL FABRIC AS A REINFORCING MEDIUM IN A SOIL-FABRIC SYSTEM

Major Field: Civil Engineering

Biographical:

Personal Data: Born in Sapulpa, Oklahoma, May 21, 1954, the son of Mr and Mrs. Roger E. Lawmaster.

Education: Graduated from Mounds High School, Mounds, Oklahoma, in May, 1972; received Bachelor of Science in Civil Engineering degree from Oklahoma State University in December, 1978; enrolled in Graduate Program at Texas Agricultural and Mechanical University from January, 1979 to May, 1979; completed requirements for Master of Science degree in Civil Engineering at Oklahoma State University in December, 1980.

Professional Experience: Undergraduate Research Assistant, Civil Engineering, Oklahoma State University, January, 1978 to May, 1978; Undergraduate Teaching Assistant, Civil Engineering, Oklahoma State University, August, 1978 to December 1978; Graduate Research Assistant, Civil Engineering, Texas A&M University, January, 1979 to May, 1979; Graduate Research Assistant, Civil Engineering, Oklahoma State University, June, 1979 to June, 1980; part time Civil Engineer, June, 1979 to May, 1980 and full time Civil Engineer, starting September, 1980, Haliburton Associates, Engineering Consultants, Stillwater, Oklahoma.

Professional Organizations: Student Member of American Society of Civil Engineers; Associate Member of Oklahoma Society of Professional Engineers; Member of Chi Epsilon.